


# Second Buckingham-effect virial coefficients of non-dipolar molecules

by

**Verlan Moodley**



*Submitted in partial fulfilment of the  
requirements for the degree of  
Master of Science in Physics in the  
School of Chemistry and Physics,  
University of KwaZulu-Natal.*

School of Chemistry and Physics  
University of KwaZulu-Natal  
Private Bag X01, Pietermaritzburg  
Scottsville 3209, South Africa

Supervisor: Dr V W Couling

**2019**

# Abstract

A molecular-tensor theory of the second electric-field-gradient-induced birefringence (EFGIB) virial coefficient  $B_Q$ , which describes the effects of molecular pair interactions on the molar Buckingham constant  ${}_mQ$ , is developed for non-dipolar molecules with axial and higher symmetry.

The resulting expressions for contributions to  $B_Q$  are evaluated numerically for the molecules  $\text{CO}_2$ ,  $\text{C}_2\text{H}_4$  and  $\text{C}_2\text{H}_6$ . These molecules were chosen since previously developed molecular-tensor theories of the second light-scattering virial coefficient  $B_\rho$  and the second Kerr-effect virial coefficient  $B_K$  have yielded calculated values for these species which are in close agreement with the available measured data.

The  $B_Q$  values calculated for  $\text{CO}_2$ ,  $\text{C}_2\text{H}_4$  and  $\text{C}_2\text{H}_6$  reveal that, for the fluids behaving as gases, the pair-interaction contributions to  ${}_mQ$  are generally at or below the threshold of resolution of the EFGIB apparatus, so that the measured  ${}_mQ$  values reported in the literature have not been contaminated by pair-interaction effects. In addition, it is seen that if the precision of measured  ${}_mQ$  data can be increased by around an order of magnitude, it should in principle become possible to resolve  $B_Q$  contributions, particularly for higher gas densities.

# Declaration

I, Verlan Moodley, declare that

1. The research reported in this thesis, except where otherwise indicated, is my original research.
2. This thesis has not been submitted for any degree or examination at any other university.
3. This thesis does not contain other persons' data, pictures, graphs or other information, unless specifically acknowledged as being sourced from other persons.
4. This thesis does not contain any other persons' writing, unless specifically acknowledged as being sourced from other researchers. Where other written sources have been quoted, then:
  - (a) their words have been rewritten but the general information attributed to them has been referenced;
  - (b) where their exact words have been used, their writing has been placed inside quotation marks, and referenced.

5. This thesis does not contain text, graphics or tables copied and pasted from the internet, unless specifically acknowledged, and the source being detailed in the thesis and in the References sections.

Signed .....

I hereby certify that this statement is correct.

Signed .....

V W Couling  
Supervisor

# Dedication

I dedicate this thesis to my late father, Yagumburam Moodley who sadly passed in January of 2016, shortly before I had decided to proceed with this research. He raised me with kindness and taught me patience and humility. He supported and advised me in all my decisions, never uttering a discouraging word. He always told me that I am solely in charge of my future but the key to a great future begins with educating one's self, by this he didn't just mean a traditional university degree, but more than that, he wished for his children to educate themselves about life, the world, and people. His greatest attribute was the kindness he had for people. I will forever thank him for teaching me that there is more to life than material wealth, it is more important to be wealthy in love, kindness, compassion and health. Though he may no longer be in my life, the morals and values he instilled in me will remain forever. Rest well Dad.

# Acknowledgements

I wish to take this opportunity to thank all the people who have assisted and motivated me throughout this undertaking, without your support and kindness this would have been a much tougher experience. I would especially like to thank the following people and organisations:

My supervisor, Dr V W Couling, for his exceptional guidance and wisdom. The countless hours spent working on this project not only showed his knowledge and dedication to the field, but also the kindness he possesses. Thank you for encouraging me to pursue my Masters Degree.

The staff of the physics department who are always willing to lend a helping hand, in particular the technical staff, Mr K Penzhorn (who has since retired) and Mr R Sivraman both of whom were very helpful in solving all nature of problems and assisting in any way they could.

My mother Asothie, your support through all these years of study mean the world to me, thank you for your patience, guidance and most importantly for always being there to talk with. My two brothers, Dhesendren and Mergan, your support has always been important to me, without your encouragement and strength I would not be the person I am today. My sister, Nirika thank you for always believing in me and pushing me to do my best.

I would also like to thank my friends Billu, Derish, Gee, Shiv, Pershen, Shnowy and Ted for always being there to help and support me through the stress and motivating me to always give 100 percent in everything I do.

The financial assistance of the National Research Foundation (NRF) towards this research is hereby acknowledged. Opinions expressed and conclusions arrived at, are those of the author and are not necessarily to be attributed to the NRF.



# Contents

<b>1</b>	<b>Review and Introduction</b>	<b>1</b>
1.1	Review . . . . .	1
1.1.1	The multipole expansion . . . . .	1
1.1.2	Direct experimental determination of molecular electric quadrupole moments . . . . .	5
1.2	The EFGIB of interacting molecules . . . . .	7
1.3	The aim of this project . . . . .	10
1.3.1	The relevance of molecular electric quadrupole moments . . . . .	10
1.3.2	Accounting for pair-interaction contributions to EFGIB . . . . .	11
<b>2</b>	<b>The Theory of the Buckingham Effect</b>	<b>13</b>
2.1	Non-interacting molecules . . . . .	13
2.2	Non-dipolar interacting molecules . . . . .	25
<b>3</b>	<b>Results</b>	<b>50</b>
3.1	Carbon Dioxide . . . . .	50
3.2	Ethene . . . . .	59
3.3	Ethane . . . . .	65
3.4	Concluding Remarks . . . . .	71
<b>A</b>		<b>73</b>
A.1	Fortran Program to calculate the $\Theta_1\alpha_3$ contribution to $B_Q$ . . . . .	73

**Bibliography**

**88**

# List of Tables

3.1	The molecular properties of CO <sub>2</sub> used in the calculation of $B_Q$ . . . . .	51
3.2	The relative magnitudes of the contributions to $B_Q$ for CO <sub>2</sub> at $T = 250\text{K}$	52
3.3	The relative magnitudes of the contributions to $B_Q$ for CO <sub>2</sub> at $T = 300\text{K}$	52
3.4	The relative magnitudes of the contributions to $B_Q$ for CO <sub>2</sub> at $T = 400\text{K}$	53
3.5	The relative magnitudes of the contributions to $B_Q$ for CO <sub>2</sub> at $T = 500\text{K}$	53
3.6	A summary of the calculated $B_Q$ values for CO <sub>2</sub> . . . . .	54
3.7	Densities (inverse molar volumes) for gaseous CO <sub>2</sub> at relevant temperatures and pressures . . . . .	57
3.8	Calculated $B_Q/V_m$ contributions to ${}_mQ$ for CO <sub>2</sub> at the temperatures and pressures in Table 3.7 . . . . .	57
3.9	The molecular properties of C <sub>2</sub> H <sub>4</sub> used in the calculation of $B_Q$ . . . . .	60
3.10	The relative magnitudes of the contributions to $B_Q$ for C <sub>2</sub> H <sub>4</sub> at $T = 250\text{K}$ . . . . .	61
3.11	The relative magnitudes of the contributions to $B_Q$ for C <sub>2</sub> H <sub>4</sub> at $T = 300\text{K}$ . . . . .	61
3.12	The relative magnitudes of the contributions to $B_Q$ for C <sub>2</sub> H <sub>4</sub> at $T = 400\text{K}$ . . . . .	62
3.13	The relative magnitudes of the contributions to $B_Q$ for C <sub>2</sub> H <sub>4</sub> at $T = 500\text{K}$ . . . . .	62
3.14	A summary of the calculated $B_Q$ values for C <sub>2</sub> H <sub>4</sub> . . . . .	63

3.15	Densities (inverse molar volumes) for gaseous $C_2H_4$ at relevant temperatures and pressures . . . . .	63
3.16	Calculated $B_Q/V_m$ contributions to ${}_mQ$ for $C_2H_4$ at the temperatures and pressures in Table 3.15 . . . . .	64
3.17	The molecular properties of $C_2H_6$ used in the calculation of $B_Q$ . . . . .	66
3.18	The relative magnitudes of the contributions to $B_Q$ for $C_2H_6$ at $T = 250K$ . . . . .	67
3.19	The relative magnitudes of the contributions to $B_Q$ for $C_2H_6$ at $T = 300K$ . . . . .	67
3.20	The relative magnitudes of the contributions to $B_Q$ for $C_2H_6$ at $T = 400K$ . . . . .	68
3.21	The relative magnitudes of the contributions to $B_Q$ for $C_2H_6$ at $T = 500K$ . . . . .	68
3.22	A summary of the calculated $B_Q$ values for $C_2H_6$ . . . . .	69
3.23	Densities (inverse molar volumes) for gaseous $C_2H_6$ at relevant temperatures and pressures . . . . .	69
3.24	Calculated $B_Q/V_m$ contributions to ${}_mQ$ for $C_2H_6$ at the temperatures and pressures in Table 3.23 . . . . .	70

# Chapter 1

## Review and Introduction

### 1.1 Review

The permanent multipole moments of a molecule, such as its electric dipole, quadrupole and octopole moments, are fundamental properties which describe the molecular charge distribution [1–3]. For molecules which are far apart compared to the molecular dimensions, it is these permanent electric moments which determine the intermolecular energy of interaction, called the electrostatic energy. The polarizabilities describe the distortion of the molecular charge distribution either by external applied fields or the fields arising from the permanent moments of the neighbouring molecules. Accurate and precise knowledge of the permanent multipole moments and polarizabilities is necessary for a detailed understanding of molecular structure and intermolecular forces.

#### 1.1.1 The multipole expansion

A full description of two interacting molecules is a many-body problem, requiring consideration of the dynamic interaction of all charges on each other. Such a description is not readily tractable, and simplifications become necessary. Ignoring the

internal motion of the molecule's electrons as well as the motion of the molecule as a whole allows for the application of electrostatic theory. If the separation of the molecules is sufficiently large, it becomes possible to expand the electrostatic potential of a molecule about an arbitrarily chosen origin which is close to the charges. This gives rise to a series of moments of charge, knowledge of which allows for useful characterization of the molecule.

Consider a distribution of charges  $q_i$  in a vacuum. Let the charges have displacement vectors  $\mathbf{r}_i$  from an arbitrary origin  $O$  which is close to, or within, the distribution. The electrostatic potential  $\phi$  produced by this distribution at some arbitrary point  $P$  with displacement vector  $\mathbf{R}$  from the origin, where  $R > r_i$ , is given by

$$\phi(\mathbf{R}) = \frac{1}{4\pi\epsilon_0} \sum_i \frac{q_i}{|\mathbf{R} - \mathbf{r}_i|}. \quad (1.1)$$

Invoking the binomial theorem to expand the denominator of this summation yields

$$\phi(\mathbf{R}) = \frac{1}{4\pi\epsilon_0} \left[ \frac{1}{R} \sum_i q_i + \frac{R_\alpha}{R^3} \sum_i q_i r_{i\alpha} + \frac{3R_\alpha R_\beta - R^2 \delta_{\alpha\beta}}{2R^5} \sum_i q_i r_{i\alpha} r_{i\beta} + \dots \right]. \quad (1.2)$$

The Greek subscripts  $\alpha, \beta, \dots$ , denote tensor components (a vector being a first-rank tensor), and can be equal to the Cartesian components  $x, y$  or  $z$ . Using the Einstein summation convention, a repeated Greek subscript denotes a summation over all three Cartesian components.  $\delta_{\alpha\beta}$  is the Kronecker delta tensor,  $\delta_{\alpha\beta} = 1$  if  $\alpha = \beta$ ,  $\delta_{\alpha\beta} = 0$  if  $\alpha \neq \beta$ . The various moments of electric charge of the distribution are as follows:

the total charge

$$q = \sum_i q_i , \quad (1.3)$$

the electric dipole moment

$$\mu_\alpha = \sum_i q_i r_{i\alpha} , \quad (1.4)$$

and the (primitive) electric quadrupole moment

$$Q_{\alpha\beta} = \sum_i q_i r_{i\alpha} r_{i\beta} . \quad (1.5)$$

The higher-order moments are the octopole, hexadecapole,  $\dots$ , however, since their contributions to the electrostatic potential of molecules which have a permanent electric quadrupole moment are successively smaller, they will not be considered in this work. The definition of the electric quadrupole moment in equation (1.5) is known as the primitive, or traced, quadrupole moment. An alternative, and often more useful, definition is the traceless quadrupole moment, which describes the departure from spherical symmetry of the charge distribution, and is given by [4]

$$\Theta_{\alpha\beta} = \frac{1}{2} (3Q_{\alpha\beta} - Q_{\gamma\gamma} \delta_{\alpha\beta}) = \frac{1}{2} \sum_i q_i (3r_{i\alpha} r_{i\beta} - r_i^2 \delta_{\alpha\beta}) . \quad (1.6)$$

The name “traceless” arises because  $\Theta_{\alpha\alpha} = 0$ .

The electrostatic potential of the charge distribution can be recast in terms of the moments of charge, namely

$$\phi(\mathbf{R}) = \frac{1}{4\pi\epsilon_0} \left[ \frac{1}{R} q + \frac{R_\alpha}{R^3} \mu_\alpha + \frac{3R_\alpha R_\beta - R^2 \delta_{\alpha\beta}}{3R^5} \Theta_{\alpha\beta} + \dots \right] . \quad (1.7)$$

Here, the contributions arising from terms for successively higher multipole mo-

ments are successively diminished by a factor of the order  $\frac{1}{R}$ . Hence, the leading non-vanishing moment provides a reasonably accurate description of the electrostatic potential  $\phi$  at point  $P$  provided the distance  $R$  is sufficiently large. Since the contribution to the expanded property arising from each of the multipole moments depends only on the displacement  $\mathbf{R}$  of point  $P$  from  $O$ , the multipole moments are considered to be located at the origin  $O$ .

If an electrostatic field  $\mathbf{E}$  is applied to the charge distribution, the distribution will experience a net force  $\mathbf{F}$  given by

$$F_\alpha = \sum_i q_i E_{i\alpha} = q(E_\alpha)_0 + \mu_\beta (\nabla_\beta E_\alpha)_0 + \frac{1}{3} \Theta_{\beta\gamma} (\nabla_\gamma \nabla_\beta E_\alpha)_0 + \dots \quad (1.8)$$

Here, the field and its derivatives are determined at the origin  $O$  about which the Taylor expansion of the field has been taken. From equation (1.8), it can be shown that a quadrupolar charge distribution will experience a torque in a region of uniform field gradient. Equation (1.8) can be used to determine the potential energy  $U$  of the charge distribution in the presence of the applied field [3, 5]:

$$U = - \int_{r_1(\mathbf{E}=0)}^{r_2(\mathbf{E}=\mathbf{E})} F_\alpha dr_\alpha = q\phi - \int_0^{\mathbf{E}} \mu_\alpha dE_\alpha - \frac{1}{3} \int_0^{\mathbf{E}} \Theta_{\alpha\beta} d(\nabla_\beta E_\alpha) - \dots \quad (1.9)$$

For a rigid charge distribution, it is only the permanent multipole moments which will contribute to equation (1.9), giving

$$U = q\phi - \mu_\alpha^{(0)} E_\alpha - \frac{1}{3} \Theta_{\alpha\beta}^{(0)} \nabla_\beta E_\alpha - \dots \quad (1.10)$$

where the permanent multipole moments have the superscript  $(0)$ .

For an axially symmetric charge distribution, each multipole moment is determined by a single scalar quantity, namely  $q, \mu, \Theta, \dots$ ; for example, the quadrupole moment



$\Theta_{\alpha\beta}$  has principal components  $\Theta_{zz} = \Theta$ ,  $\Theta_{xx} = \Theta_{yy} = -\frac{1}{2}\Theta$ .

The effect of a change of origin on a quadrupole moment can be established by moving  $O$  by  $\mathbf{r}'$  to  $O'$ . The quadrupole moment  $\Theta'$  relative to the new origin  $O'$  is

$$\Theta'_{\alpha\beta} = \frac{1}{2} \sum_i q_i (3r'_{i\alpha}r'_{i\beta} - (r'_i)^2\delta_{\alpha\beta}) \quad (1.11)$$

which becomes

$$\Theta'_{\alpha\beta} = \Theta_{\alpha\beta} - \frac{3}{2}\mu_\alpha r'_\beta - \frac{3}{2}\mu_\beta r'_\alpha + \mu_\gamma r'_\gamma \delta_{\alpha\beta} + \frac{1}{2}q \{3r'_\alpha r'_\beta - (r')^2\delta_{\alpha\beta}\} . \quad (1.12)$$

The quadrupole moment is seen to be independent of the choice of origin if and only if both  $q$  and  $\mu_\alpha$  are zero. Indeed, it can be shown that in general, only the leading non-zero electric multipole moment is independent of the choice of origin. For a dipolar molecule, the quadrupole moment will depend on the location of the origin. In this work, only non-dipolar molecules will be considered.

### 1.1.2 Direct experimental determination of molecular electric quadrupole moments

As described in the preceding section, a non-uniform electric field will exert a torque on a quadrupolar molecule. In a gas of such molecules, the electric field will result in partial alignment of the molecules, causing the gas to become anisotropic and hence birefringent. This electric-field-gradient-induced birefringence (EFGIB), now known as the Buckingham effect, when described by a suitable molecular-tensor theory, yields a direct means for the determination of the electric quadrupole moment of a molecule. This method was first proposed by Buckingham in 1959 [6], and the experiment was first successfully demonstrated by Buckingham and Disch on

the CO<sub>2</sub> molecule in 1963 [7]. Since then, a number of researchers have performed EFGIB experiments on a range of non-dipolar as well as dipolar molecules, as described in two recent review articles [8, 9].

Buckingham's initial theory [6] is applicable only to non-dipolar molecules. The quadrupole moment of a dipolar molecule will depend on the origin to which these moments are referred. Hence, in 1968, Buckingham and Longuet-Higgins developed a new theory of EFGIB for dipolar molecules based upon the forward scattering of light-wave radiation by the molecules when in the presence of an applied non-uniform electric field [10].

In 1991, Imrie and Raab published a new theory of EFGIB using eigenvalue theory of wave propagation, based on Maxwell's equations [11]. Their theory used the primitive electric quadrupole moment, and their derived expression for the induced birefringence was shown to be origin independent, as required. However, when using the traceless quadrupole moment in their theory, they obtained an origin-dependent result for the birefringence of dipolar molecules which differed from the Buckingham Longuet-Higgins theory. In an attempt to resolve this discrepancy, accurate *ab initio* calculations of the dipolar molecules CO, N<sub>2</sub>O and OCS were undertaken by Rizzo, Coriani, Halkier and co-workers [12, 13], whose results favoured the Longuet-Higgins theory. Raab and de Lange eventually brought a definitive resolution to the controversy through a revision of the Imrie-Raab theory, re-obtaining exactly the original Buckingham and Longuet-Higgins result [3, 14, 15].

Experimental measurement of EFGIB has been used to determine the electric quadrupole moments of a range of small molecules including H<sub>2</sub>, O<sub>2</sub>, N<sub>2</sub>, Cl<sub>2</sub>, CO<sub>2</sub>, CS<sub>2</sub>, C<sub>2</sub>H<sub>4</sub>, C<sub>2</sub>H<sub>6</sub>, C<sub>3</sub>H<sub>4</sub>, C<sub>3</sub>H<sub>6</sub>, C<sub>4</sub>H<sub>6</sub>, C<sub>6</sub>H<sub>6</sub>, C<sub>6</sub>F<sub>6</sub>, CO, OCS, N<sub>2</sub>O and CH<sub>3</sub>F [7, 16–30]. In all of these experiments it has been assumed that the contribution to the EFGIB

arising from molecular pair interactions is negligible.

There exists a range of alternative methods for measuring the electric quadrupole moments of molecules, these methods often relying on the study of molecular interactions, such as through collision-induced absorption in far-infrared spectra [4]. Most of these methods are indirect, and are dependent on the model used to describe the intermolecular interaction potential. Consequently, these data are not considered to be particularly reliable [4].

*Ab initio* quantum mechanical calculations of molecular properties such as the molecular electric quadrupole moment are becoming increasingly sophisticated and accurate. A good review of present state-of-the-art techniques is available [31]. To attain highly accurate *ab initio* calculations of the electric quadrupole moment is a non-trivial task, and requires the use of large basis sets and the inclusion of electron correlation effects and vibrational averaging, making the calculations computationally intensive. Accurate experimental determinations of quadrupole moments provide the quantum computationalists with useful benchmarks against which to assess the effects arising from refinements in their high-level *ab initio* methods.

## 1.2 The EFGIB of interacting molecules

A number of electromagnetic properties of gases are proportional to the number density of the constituent molecules, and for ideal gases, this proportionality is exact since each molecule is treated as an independent system, there being no interactions between the molecules. For real gases, in which molecules do interact with their neighbours, the electromagnetic properties will display a non-linear dependence on the number density of the molecules.

In 1956, Buckingham and Pople demonstrated how these intermolecular interaction effects can be accounted for through the use of a virial-type expansion [32]. In general, they represented any measurable molecular-optic property of a real gas by the parameter  $Q$ , and provided as examples of particular properties the refractive index, the dielectric constant, the Kerr effect and the Cotton-Mouton effect. The molecular-optic property which is the subject of this investigation is the Buckingham effect, for which the property  $Q$  is the molar Buckingham constant  ${}_mQ$ .  $Q$  can be expressed as a virial expansion in inverse powers of the molar volume  $V_m$  as follows:

$$Q = A_Q + \frac{B_Q}{V_m} + \frac{C_Q}{V_m^2} + \dots , \quad (1.13)$$

where the first virial coefficient  $A_Q$  provides the ideal gas contribution to  $Q$ , while  $B_Q$  is the second virial coefficient describing the contribution to  $Q$  arising from the interaction of molecular pairs, and  $C_Q$  is the third virial coefficient, accounting for the contribution arising from interacting triplets. These virial coefficients are functions of the temperature alone, or for optical phenomena, of temperature and optical frequency alone [32].

If  $Q$  is a macroscopic property of a mole of ideal-gas molecules, and  $q$  is the microscopic contribution to this property arising from a single molecule, then  $Q$  will be the sum of the  $N_A$  mean contributions  $\bar{q}$  of the individual isolated molecules, namely

$$Q = A_Q = N_A \bar{q} . \quad (1.14)$$

For higher gas densities, there are times when a representative molecule 1 is interacting with a neighbouring molecule 2, their relative configuration being described by the collective symbol  $\tau$ , and their contribution to  $Q$  at any given instant being  $q_{12}(\tau)$ . (The interaction configuration  $\tau$  is described in detail following equation (2.48)). Molecule 1 must be treated as half of an interacting pair, so that its contribution to

$Q$  at a given instant is  $\frac{1}{2}q_{12}(\tau)$ . Neglecting any triplet or higher-order interactions,  $Q$  becomes [32]

$$Q = N_A \left\{ \bar{q} + \int_{\tau} \left[ \frac{1}{2}q_{12}(\tau) - \bar{q} \right] P(\tau) d\tau \right\} , \quad (1.15)$$

where  $P(\tau) d\tau$  is the probability that molecule 1 has a neighbour in the range  $(\tau, \tau + d\tau)$ . The relationship between the intermolecular potential energy  $U_{12}(\tau)$  and the probability function is provided by

$$P(\tau) = \frac{N_A}{\Omega V_m} e^{-U_{12}(\tau)/kT} , \quad (1.16)$$

where  $\Omega = V_m^{-1} \int_{\tau} d\tau$ . From equation (1.13),

$$B_Q = \lim_{V_m \rightarrow \infty} (Q - A_Q) V_m , \quad (1.17)$$

which combined with equations (1.14) to (1.16) yields

$$B_Q = \frac{N_A^2}{V_m} \int_{\tau} \left[ \frac{1}{2}q_{12}(\tau) - \bar{q} \right] e^{-U_{12}(\tau)/kT} d\tau . \quad (1.18)$$

This general expression for  $B_Q$  can be applied to the particular molecular-optic property  $Q$  under consideration. In this work, it will be applied to EFGIB for interacting pairs of non-dipolar molecules.

In 2003, Marchesan, Coriani and Rizzo published a paper presenting a computational *ab initio* investigation of the density dependence of EFGIB for gases of the noble atoms helium, neon and argon [33]. The second EFGIB virial coefficient was computed for each of these gases over a range of temperature. These atoms do not possess permanent quadrupole moments, being spherically symmetric. For interacting pairs, the dimers do however exhibit a small quadrupole moment. By computing

the internuclear dependence of the molecular quadrupole moment and the dipole-dipole-quadrupole and dipole-magnetic dipole-dipole hyperpolarizabilities of the van der Waals dimers, they were able to successfully determine the second EFGIB virial coefficients for these species. The pair-interaction contributions to the EFGIB were found to be of the order of a few tens of parts per million for helium and neon, and of the order of a few parts per thousands for argon at standard experimental conditions, and hence would not be detectable with the presently available experimental apparatus.

We are not aware of any other theoretical studies of the density dependence of EFGIB in the literature.

## **1.3 The aim of this project**

### **1.3.1 The relevance of molecular electric quadrupole moments**

Multipole theory in electrostatics, magnetostatics and electrodynamics has often been very successful in relating various macroscopic electromagnetic phenomena in matter to the microscopic structure of individual molecules (for gases) or of unit cells (for crystals) [1–3]. For molecules which have no permanent electric dipole moment, and for which the electric quadrupole moment is the leading moment of charge, accurate and precise knowledge of the quadrupole becomes essential to the description of a range of thermodynamic, structural and spectral properties.

Take  $\text{CO}_2$  for example.  $\text{CO}_2$  is a greenhouse gas, and its release into the atmosphere via the burning of fossil fuels is contributing to global climate change. Post-combustion capture of this molecule is presently an extremely active field of research. The quadrupole moment of  $\text{CO}_2$  is relatively large, and this can be exploited since

the molecule can bind preferentially to adsorbents compared to the nitrogen and oxygen in the atmosphere, these molecules both having comparatively rather small quadrupole moments [34–38]. The quadrupole moment of  $\text{CO}_2$  is also relevant to atmospheric and space physics, such as in the measurement and modelling of radiative transfer in planetary atmospheres, which includes significant effects from collision-induced absorption involving  $\text{CO}_2$  and other molecules. [39]

For those dipolar molecules which have relatively small dipole moments, such as  $\text{CO}$ ,  $\text{N}_2\text{O}$  and  $\text{OCS}$ , their quadrupole moments can play a significant role in various phenomena.  $\text{N}_2\text{O}$  is also a major greenhouse gas as well as an ozone-depleting gas, and the quadrupole moment is essential to understanding, for example, its adsorption and desorption as a means to suppressing its emission from soil [40].  $\text{CO}$  is an important biological gas, and knowledge of its molecular quadrupole moment has proven useful in, for example, the modelling of the migration of the  $\text{CO}$  molecule in myoglobin via molecular dynamics simulations [41].  $\text{CO}$  is also the second most abundant gas-phase molecule in the interstellar medium. It is present in the solid phase in dense molecular clouds, and recent quantum-mechanical simulations of solid  $\text{CO}$  show how the quadrupolar character of the molecule accounts for the energetics of the  $\text{CO}$ - $\text{H}_2\text{O}$  ice interaction [42].

### 1.3.2 Accounting for pair-interaction contributions to EFGIB

Measurement of EFGIB in gases is clearly a very useful route to determining molecular electric quadrupole moments. What is assumed in these experiments is that contributions arising from molecular pair interactions are sufficiently small at typical experimental pressures and temperatures that they can be ignored. The essential aim of this project is to develop a molecular-tensor theory of second Buckingham-

effect virial coefficients  $B_Q$ , and to use it to calculate  $B_Q$  for some typical small molecules. This will allow for a quantitative assessment of the relative contributions of pair-interaction effects to the measured EFGIB for a range of gases. Such knowledge can guide experimentalists in future attempts to measure  $B_Q$ , since the gas densities at which pair interactions should become discernible using present EFGIB apparatus will be known. Knowledge of  $B_Q$  will also reveal the extent to which the measured EFGIB data in the literature have been contaminated by pair-interaction contributions.

Section 2.1 of Chapter 2 reviews the theory of the Buckingham effect in ideal gases, while Section 2.2 presents the new molecular-tensor theory for the Buckingham effect accounting for pair-interaction contributions in dense gases comprised of non-dipolar molecules. Chapter 3 presents the calculated second EFGIB virial coefficients for gases of pure  $\text{CO}_2$ ,  $\text{C}_2\text{H}_4$  and  $\text{C}_2\text{H}_6$ , and includes comprehensive discussion of the implications of the results, both for existing measured EFGIB data and for any future experimental determinations of EFGIB data.



# Chapter 2

## The Theory of the Buckingham Effect

### 2.1 Non-interacting molecules

The approach initially adopted by Buckingham to derive a theory of the EFGIB effect, or Buckingham effect, for the special case of non-dipolar molecules [6] is similar to that used by Buckingham and Pople to obtain theories of the Kerr electro-optic effect [43] and the Cotton-Mouton magneto-optic effect [44].

Consider a neutral molecule in the presence of an external electrostatic field  $\mathbf{E}$  and field gradient  $\nabla\mathbf{E}$ . The orientation and position of the molecule is given by the variable  $\tau$ . For all but the lightest of molecules at typical experimental temperatures (*ca.* 300 K to 500 K) the rotational energy levels are sufficiently close together that the orientation may be considered to vary continuously, and hence be treated classically rather than quantum mechanically.

The electric field  $\mathbf{E}$  can be written in tensor notation as  $E_\alpha$ , while the field gradient  $\nabla\mathbf{E}$  can be written as  $\nabla_\beta E_\alpha$ , or as  $E_{\alpha\beta}$ . Buckingham's EFGIB apparatus comprises

a gas cell which is a conducting metal cylinder down the length of which run two thin parallel wires, which are separated by a small distance and which are equidistant from the cylinder's axis [7]. The cylinder is earthed, while the wires are held at the same potential relative to the cylinder, such that the axis experiences zero electric field but a high field gradient. If the space-fixed laboratory frame  $O(x, y, z)$  is fixed in the quadrupole cell such that  $z$  is along the axis of the cylinder and in the direction of propagation of the light beam (which is parallel to, and centred on, the cell's axis), while the wires lie in the  $yz$ -plane, then the electric field-gradient tensor in the region between the wires is given by [6, 7]

$$\nabla_{\beta} E_{\alpha} = E_{\alpha\beta} = \begin{pmatrix} E_{xx} & 0 & 0 \\ 0 & E_{yy} = -E_{xx} & 0 \\ 0 & 0 & 0 \end{pmatrix}. \quad (2.1)$$

Here, the Greek subscripts pertain to the laboratory frame.

For a fixed position and orientation  $\tau$ , the energy of a molecule in the field is  $U(\tau, \mathbf{E}, \nabla \mathbf{E})$ . This energy can be written as a power-series expansion [1]

$$\begin{aligned} U(\tau, \mathbf{E}, \nabla \mathbf{E}) = & U^{(0)} - \mu_i^{(0)} E_i - \frac{1}{2} \alpha_{ij}^{(0)} E_i E_j - \frac{1}{6} \beta_{ijk}^{(0)} E_i E_j E_k \\ & - \frac{1}{24} \gamma_{ijkl}^{(0)} E_i E_j E_k E_l - \frac{1}{3} \Theta_{ij}^{(0)} E_{ij} - \frac{1}{3} A_{ijk}^{(0)} E_i E_j E_k \\ & - \frac{1}{6} B_{ijkl}^{(0)} E_i E_j E_k E_l - \frac{1}{6} C_{ijkl}^{(0)} E_{ij} E_{kl} + \dots, \end{aligned} \quad (2.2)$$

where the terms  $\mu_i^{(0)}$  and  $\Theta_{ij}^{(0)}$  are the permanent electric dipole and quadrupole moments respectively, while the second-rank tensor  $\alpha_{ij}^{(0)}$  is the static polarizability and

the third- and fourth-rank tensors  $\beta_{ijk}^{(0)}$  and  $\gamma_{ijkl}^{(0)}$  are the first- and second-order static hyperpolarizabilities of the molecule. These (hyper)polarizability tensors, together with the static polarizability tensors  $A_{ijk}^{(0)}$ ,  $B_{ijkl}^{(0)}$  and  $C_{ijkl}^{(0)}$ , arise from the distortion of the charge distribution of the molecule by the applied field  $E_\alpha$  and field gradient  $E_{\alpha\beta}$ . Each of these polarizability tensors is unique, resulting from a particular combination of applied electric field and/or field gradient. Note that all tensors with Roman subscripts refer to the molecule-fixed axes  $O(1, 2, 3)$ .

For a gas of non-dipolar molecules, which is the focus of this project, the energy reduces to

$$\begin{aligned}
 U(\tau, \mathbf{E}, \nabla \mathbf{E}) &= U^{(0)} - \frac{1}{2} \alpha_{ij}^{(0)} E_i E_j - \frac{1}{24} \gamma_{ijkl}^{(0)} E_i E_j E_k E_l \\
 &\quad - \frac{1}{3} \Theta_{ij}^{(0)} E_{ij} - \frac{1}{6} B_{ijkl}^{(0)} E_i E_j E_{kl} - \frac{1}{6} C_{ijkl}^{(0)} E_{ij} E_{kl} + \dots .
 \end{aligned} \tag{2.3}$$

For a dilute gas, the oscillating dipole moment  $\mu_i$  of a molecule arises solely due to the polarizing action of the oscillating electric field  $\mathcal{E}_i$  of the light wave, and it is this oscillating dipole which primarily determines the refractive index. The optical-frequency polarizability tensor  $\alpha_{ij}$  is modified by the applied non-uniform field so that the induced dipole moment for a non-dipolar diamagnetic molecule becomes [1]

$$\mu_i = \alpha_{ij} \mathcal{E}_j + \frac{1}{3} B_{ijkl} \mathcal{E}_j E_{kl} + \dots . \tag{2.4}$$

The differential polarizability  $\pi_{ij}$  is defined as [1]

$$\pi_{ij} = \frac{\partial \mu_i}{\partial \mathcal{E}_j} = \alpha_{ij} + \frac{1}{3} B_{ijkl} E_{kl} + \dots . \tag{2.5}$$

Buckingham's method to measure the molecular electric quadrupole moment of a gas molecule [6, 7] uses a technique whereby the gas sample is placed in the presence

of an applied non-uniform electric field, which partially orients the molecules. The resulting anisotropy in the refractive index, induced by the applied field and field gradient, is then measured ellipsometrically. This difference between the refractive indices of the gas for light travelling along the  $z$ -axis with electric vectors in the  $x$  and  $y$  directions,  $n_x - n_y$ , is given as [1]

$$n_x - n_y = \frac{2\pi N_A}{(4\pi\epsilon_0)V_m} \bar{\pi} . \quad (2.6)$$

Here  $N_A$  is Avogadro's number,  $\epsilon_0$  is the permittivity of free space,  $V_m$  is the molar volume of the gas sample, and  $\bar{\pi}$  is the orientational average of  $\pi$ , where  $\pi$  is the difference between the differential polarizabilities for a specific molecular configuration  $\tau$ , namely

$$\pi = \pi(\tau, \mathbf{E}, \nabla\mathbf{E}) = \pi_{xx} - \pi_{yy} = \pi_{ij} (a_i^x a_j^x - a_i^y a_j^y) . \quad (2.7)$$

Here,  $a_i^x$  is the direction cosine between the  $x$  space-fixed and  $i$  molecule-fixed axes, while  $a_i^y$  is the direction cosine between the  $y$  space-fixed and  $i$  molecule-fixed axes.

Since the molecule is tumbling in space, the overbar in  $\bar{\pi}$  denotes the orientational average of  $\pi$  over all configurations in the presence of the biasing influence of the applied non-uniform electric field. To proceed, it is assumed that the rapidly oscillating field of the incident light wave is sufficiently weak that it does not affect the orientation of the molecule, that the orientational variable  $\tau$  is continuous, and that a Boltzmann-type weighting factor can be used to determine the orientational average required [3].  $\bar{\pi}$  can then be written as

$$\bar{\pi} = \frac{\int \pi(\tau, \mathbf{E}, \nabla\mathbf{E}) e^{-U(\tau, \mathbf{E}, \nabla\mathbf{E})/kT} d\tau}{\int e^{-U(\tau, \mathbf{E}, \nabla\mathbf{E})/kT} d\tau} . \quad (2.8)$$

The biased average in equation (2.8) can be converted into isotropic averages, i.e. the much more straightforward orientational averages for zero field and field gradient. This is achieved through a Taylor-series expansion of  $\bar{\pi}$  in powers of both the field and field gradient, which yields

$$\bar{\pi} = AE_{xx} + BE_x^2 + CE_{xx}^3 + \dots \quad (2.9)$$

where

$$A = \left( \frac{\partial \bar{\pi}}{\partial E_{xx}} \right)_{E_x=E_{xx}=0}, \quad B = \frac{1}{2} \left( \frac{\partial^2 \bar{\pi}}{\partial E_x^2} \right)_{E_x=E_{xx}=0}, \quad C = \frac{1}{3!} \left( \frac{\partial^3 \bar{\pi}}{\partial E_{xx}^3} \right)_{E_x=E_{xx}=0}. \quad (2.10)$$

$\bar{\pi}$  is seen to be an even function of the electric field and an odd one in the electric field gradient. It can be shown that for molecules in the presence of a typical experimental electric field gradient of  $E_{xx} < 10^9 \text{ V m}^{-2}$ ,  $\bar{\pi}$  can be reduced to the first term in equation (2.9) as the subsequent terms are negligible when working in the dipole approximation [45]. Therefore

$$\bar{\pi} = AE_{xx} = \left( \frac{\partial \bar{\pi}}{\partial E_{xx}} \right)_{E_x=E_{xx}=0} E_{xx} \quad (2.11)$$

where  $\left( \frac{\partial \bar{\pi}}{\partial E_{xx}} \right)_{E_x=E_{xx}=0}$  is evaluated with both the field and the field gradient being zero. Differentiating equation (2.8) yields

$$\left( \frac{\partial \bar{\pi}}{\partial E_{xx}} \right)_{E_x=E_{xx}=0} = \left\langle \frac{\partial \pi}{\partial E_{xx}} \right\rangle - \frac{1}{kT} \left\langle \pi \left( \frac{\partial U}{\partial E_{xx}} \right) \right\rangle. \quad (2.12)$$

The angular brackets in (2.12) denote an isotropic average over all possible orientations  $\tau$  of the molecule. For molecular property  $X$ ,

$$\langle X \rangle = \frac{\int X(\tau, 0) e^{-U(\tau, 0)/kT} d\tau}{\int e^{-U(\tau, 0)/kT} d\tau}. \quad (2.13)$$

Substituting equation (2.12) back into equation (2.11) gives an expression for  $\bar{\pi}$  as

$$\bar{\pi} = \left\{ \left\langle \frac{\partial \pi}{\partial E_{xx}} \right\rangle - \frac{1}{kT} \left\langle \pi \left( \frac{\partial U}{\partial E_{xx}} \right) \right\rangle \right\} E_{xx} . \quad (2.14)$$

To solve for  $\bar{\pi}$  in equation (2.14), two expressions need to be evaluated, namely  $\left( \frac{\partial \pi}{\partial E_{xx}} \right)$  and  $\left( \pi \frac{\partial U}{\partial E_{xx}} \right)$ .

It is useful to first obtain the transformation of the electric field gradient from the laboratory frame of space-fixed axes into molecule-fixed axes. This is achieved by means of the direction cosines, so that

$$E_{ij} = a_{\alpha}^i a_{\beta}^j E_{\alpha\beta} . \quad (2.15)$$

Since the electric field gradient  $E_{\alpha\beta}$  has only two non-zero components, namely  $E_{xx}$  and  $E_{yy} = -E_{xx}$  (see equation (2.1)),  $E_{ij}$  becomes

$$E_{ij} = a_x^i a_x^j E_{xx} + a_y^i a_y^j E_{yy} = (a_x^i a_x^j - a_y^i a_y^j) E_{xx} , \quad (2.16)$$

which is equivalent to

$$E_{ij} = (a_i^x a_j^x - a_i^y a_j^y) E_{xx} . \quad (2.17)$$

In order to obtain  $\pi(\tau, \mathbf{E}, \nabla \mathbf{E})$ , the term  $\left( \frac{\partial \pi}{\partial E_{xx}} \right)$  needs to be evaluated. From equation (2.7),

$$\left( \frac{\partial \pi}{\partial E_{xx}} \right)_{E_x = E_{xx} = 0} = \frac{\partial}{\partial E_{xx}} \left[ \pi_{ij} (a_i^x a_j^x - a_i^y a_j^y) \right]_{E_x = E_{xx} = 0} . \quad (2.18)$$

Therefore, by differentiating equation (2.5) with respect to the field gradient com-

ponent  $E_{xx}$ , the following is obtained

$$\left( \frac{\partial \pi}{\partial E_{xx}} \right)_{E_x = E_{xx} = 0} = \left[ \frac{\partial}{\partial E_{xx}} \left( \alpha_{ij} + \frac{1}{3} B_{ijkl} E_{kl} + \dots \right) (a_i^x a_j^x - a_i^y a_j^y) \right]. \quad (2.19)$$

Making use of the result in equation (2.17) yields

$$\left( \frac{\partial \pi}{\partial E_{xx}} \right)_{E_x = E_{xx} = 0} = \left[ \frac{\partial}{\partial E_{xx}} \left( \alpha_{ij} + \frac{1}{3} B_{ijkl} (a_k^x a_l^x - a_k^y a_l^y) E_{xx} + \dots \right) (a_i^x a_j^x - a_i^y a_j^y) \right]. \quad (2.20)$$

Hence,

$$\left\langle \frac{\partial \pi}{\partial E_{xx}} \right\rangle = \frac{1}{3} B_{ijkl} \left\langle (a_i^x a_j^x - a_i^y a_j^y) (a_k^x a_l^x - a_k^y a_l^y) \right\rangle. \quad (2.21)$$

This expands to

$$\left\langle \frac{\partial \pi}{\partial E_{xx}} \right\rangle = \frac{1}{3} B_{ijkl} \left\langle a_i^x a_j^x a_k^x a_l^x - a_i^x a_j^x a_k^y a_l^y - a_i^y a_j^y a_k^x a_l^x + a_i^y a_j^y a_k^y a_l^y \right\rangle. \quad (2.22)$$

The isotropic averages of direction cosines are discussed in detail in [2], which provides the relationships

$$\left\langle a_i^x a_j^x a_k^x a_l^x \right\rangle = \left\langle a_i^y a_j^y a_k^y a_l^y \right\rangle, \quad (2.23)$$

$$\left\langle a_i^x a_j^x a_k^y a_l^y \right\rangle = \left\langle a_i^y a_j^y a_k^x a_l^x \right\rangle. \quad (2.24)$$

Substituting these results into equation (2.22) yields

$$\left\langle \frac{\partial \pi}{\partial E_{xx}} \right\rangle = \frac{2}{3} B_{ijkl} \left\langle a_i^x a_j^x a_k^x a_l^x - a_i^x a_j^x a_k^y a_l^y \right\rangle. \quad (2.25)$$

The terms in equation (2.25) are evaluated by invoking the following standard results

of isotropic averages [2, 43]:

$$\left\langle a_i^x a_j^x a_k^x a_l^x \right\rangle = \frac{1}{15} (\delta_{ij} \delta_{kl} + \delta_{ik} \delta_{jl} + \delta_{il} \delta_{jk}) , \quad (2.26)$$

$$\left\langle a_i^x a_j^x a_k^y a_l^y \right\rangle = \frac{1}{30} (4\delta_{ij} \delta_{kl} - \delta_{ik} \delta_{jl} - \delta_{il} \delta_{jk}) . \quad (2.27)$$

Substituting the results in equations (2.26) and (2.27) into equation (2.25) yields

$$\left\langle \frac{\partial \pi}{\partial E_{xx}} \right\rangle = \frac{1}{45} B_{ijkl} \left[ -2\delta_{ij} \delta_{kl} + 3\delta_{ik} \delta_{jl} + 3\delta_{il} \delta_{jk} \right] , \quad (2.28)$$

while contracting over the subscripts yields

$$\left\langle \frac{\partial \pi}{\partial E_{xx}} \right\rangle = \frac{1}{45} \left[ -2B_{iijj} + 3B_{ijij} + 3B_{ijji} \right] . \quad (2.29)$$

Equation (2.29) can be further reduced since the  $B$ -tensor is traceless [1], so that  $B_{iijj} = 0$ . Together with the result  $B_{ijij} = B_{ijji}$  [1], equation (2.29) can be written as

$$\left\langle \frac{\partial \pi}{\partial E_{xx}} \right\rangle = \frac{1}{45} \left[ 6B_{ijij} \right] = \frac{6}{45} B_{ijij} . \quad (2.30)$$

The second term in equation (2.14) still needs to be evaluated. This expression,  $\left( \pi \frac{\partial U}{\partial E_{xx}} \right)$ , is evaluated with the field and the field gradient being zero. By using equations (2.5) and (2.7) this term becomes

$$\left( \pi \frac{\partial U}{\partial E_{xx}} \right)_{E_x=E_{xx}=0} = \alpha_{ij} (a_i^x a_j^x - a_i^y a_j^y) \left( \frac{\partial U}{\partial E_{xx}} \right)_{E_x=E_{xx}=0} . \quad (2.31)$$

The term  $\left( \frac{\partial U}{\partial E_{xx}} \right)_{E_x=E_{xx}=0}$  is obtained through differentiation of equation (2.2) with



respect to the  $E_{xx}$  component of the electric field gradient, which yields

$$\left( \frac{\partial U}{\partial E_{xx}} \right)_{E_x=E_{xx}=0} = -\frac{1}{3} \Theta_{ij}^{(0)} (a_i^x a_j^x - a_i^y a_j^y) . \quad (2.32)$$

Hence,

$$\begin{aligned} \left\langle \pi \frac{\partial U}{\partial E_{xx}} \right\rangle &= -\frac{1}{3} \alpha_{ij} \Theta_{kl}^{(0)} \left\langle (a_i^x a_j^x - a_i^y a_j^y) (a_k^x a_l^x - a_k^y a_l^y) \right\rangle \\ &= -\frac{1}{3} \alpha_{ij} \Theta_{kl}^{(0)} \left\langle a_i^x a_j^x a_k^x a_l^x - a_i^x a_j^x a_k^y a_l^y - a_i^y a_j^y a_k^x a_l^x + a_i^y a_j^y a_k^y a_l^y \right\rangle . \end{aligned} \quad (2.33)$$

As before, use is made of the results for isotropic averages contained in equations (2.23) and (2.24), which leads to

$$\left\langle \pi \frac{\partial U}{\partial E_{xx}} \right\rangle = -\frac{2}{3} \alpha_{ij} \Theta_{kl}^{(0)} \left\langle a_i^x a_j^x a_k^x a_l^x - a_i^x a_j^x a_k^y a_l^y \right\rangle . \quad (2.34)$$

This can be further simplified by substitution of the results from equations (2.26) and (2.27), yielding

$$\left\langle \pi \frac{\partial U}{\partial E_{xx}} \right\rangle = -\frac{1}{45} \alpha_{ij} \Theta_{kl}^{(0)} \left\langle -2\delta_{ij}\delta_{kl} + 3\delta_{ik}\delta_{jl} + 3\delta_{il}\delta_{jk} \right\rangle . \quad (2.35)$$

Contracting over the subscripts yields

$$\begin{aligned} \left\langle \pi \frac{\partial U}{\partial E_{xx}} \right\rangle &= -\frac{1}{45} \left[ -2\alpha_{ii} \Theta_{kk}^{(0)} + 3\alpha_{ij} \Theta_{ij}^{(0)} + 3\alpha_{ij} \Theta_{ji}^{(0)} \right] \\ &= -\frac{1}{45} \left[ -2\alpha_{ii} \Theta_{kk}^{(0)} + 6\alpha_{ij} \Theta_{ij}^{(0)} \right] . \end{aligned} \quad (2.36)$$

The quadrupole tensor  $\Theta_{ij}^{(0)}$  is traceless, that is the components along the diagonal

sum to zero, therefore  $\Theta_{kk}^{(0)} = 0$ . Consequently, equation (2.36) reduces to

$$\left\langle \pi \frac{\partial U}{\partial E_{xx}} \right\rangle = -\frac{6}{45} \alpha_{ij} \Theta_{ij}^{(0)}. \quad (2.37)$$

The two terms required in equation (2.14) have been evaluated, and the expression for  $\bar{\pi}$  becomes

$$\bar{\pi} = \frac{6}{45} \left[ B_{ijij} + \frac{\alpha_{ij} \Theta_{ij}^{(0)}}{kT} \right] E_{xx}. \quad (2.38)$$

Equation (2.38) can then be substituted into equation (2.6) to give

$$\begin{aligned} n_x - n_y &= \frac{2\pi N_A}{(4\pi\epsilon_0)V_m} \bar{\pi} \\ &= \frac{2\pi N_A}{(4\pi\epsilon_0)V_m} \cdot \frac{6}{45} \left[ B_{ijij} + \frac{\alpha_{ij} \Theta_{ij}^{(0)}}{kT} \right] E_{xx} \\ &= \frac{N_A E_{xx}}{15\epsilon_0 V_m} \left[ B_{ijij} + \frac{\alpha_{ij} \Theta_{ij}^{(0)}}{kT} \right]. \end{aligned} \quad (2.39)$$

Equation (2.39) is an expression for the birefringence induced in the gas by the applied inhomogeneous electric field expressed in terms of the microscopic molecular properties of an individual molecule. The molar Buckingham constant  ${}_m Q$  is defined to be [6, 46]

$${}_m Q = \frac{6n(3\epsilon_r + 2)}{5\epsilon_r(n^2 + 2)^2} \lim_{E_{xx} \rightarrow 0} \left( \frac{n_x - n_y}{E_{xx}} \right) V_m. \quad (2.40)$$

Substituting equation (2.39) into equation (2.40) gives an expression for the molar Buckingham constant in the limit of infinite dilution as

$${}_m Q = \frac{2N_A}{45\epsilon_0} \left[ B_{ijij} + \frac{\alpha_{ij} \Theta_{ij}^{(0)}}{kT} \right]. \quad (2.41)$$

In the EFGIB experiment, a monochromatic beam of linearly-polarized laser light travels along the  $z$ -axis, which is chosen to coincide with the axis of the gas cell. The long, fine, parallel wires used to establish the inhomogeneous electric field define the  $yz$  plane, and the laser beam is polarized at  $45^\circ$  to this plane so that as it enters the cell, it may be resolved into two components with orthogonal electric vectors  $\mathcal{E}_x$  and  $\mathcal{E}_y$  which will experience different refractive indices  $n_x$  and  $n_y$  as they travel through the birefringent medium. The beam will emerge from the cell elliptically polarized, since the two components will now have a relative phase difference  $\delta$  of

$$\delta = \frac{2\pi l}{\lambda} (n_x - n_y) , \quad (2.42)$$

where  $l$  is the pathlength of the medium, and  $\lambda$  is the wavelength of the light. The azimuth of this elliptically-polarized beam will still be  $45^\circ$  to the  $yz$  plane, and passing it through a quarter-wave plate with fast axis set at an azimuth of  $45^\circ$ , the light will emerge linearly polarized but rotated from the initial  $45^\circ$  plane of polarization by an angle  $\delta/2$  radians. The optical retardation  $\delta$  is the observable property in the experiment, and from equation (2.42) it yields  $(n_x - n_y)$ , which together with knowledge of the refractive index and relative permittivity of the gas, its temperature and density, and the strength of the applied electric field gradient, allows for the calculation of  ${}_mQ$  via equation (2.40).

Although this project focuses on non-dipolar molecules, there is an important consequence of the Buckingham-Longuet Higgins (BLH) theory of dipolar molecules [10] for non-dipolar species, which is now examined. The BLH theory of EFGIB for dipolar molecules is based on the forward scattering of radiation by the molecules in the birefringent medium. Unlike equation (2.4), which is to electric dipole order, the BLH theory is applied to electric quadrupole-magnetic dipole order, so that the moments induced in a non-dipolar molecule in the presence of the incident light-wave

fields  $\mathcal{E}_i$  and  $\mathcal{B}_i$  are [3, 10, 14]

$$\mu_i = \alpha_{ij}\mathcal{E}_j + \frac{1}{3}B_{ijkl}\mathcal{E}_j\nabla_l E_k + \frac{1}{3}\mathcal{B}_{iljk}(\nabla_k\mathcal{E}_j)E_l + \frac{1}{\omega}J'_{ijk}\dot{\mathcal{B}}_j E_k, \quad (2.43)$$

$$\Theta_{ij} = \mathcal{B}_{kl ij}\mathcal{E}_k E_l, \quad (2.44)$$

and

$$m_i = -\frac{1}{\omega}J'_{jik}\dot{\mathcal{E}}_j E_k, \quad (2.45)$$

where  $\omega$  is the frequency of the radiation. The BLH forward-scattering theory of EFGIB has been presented in thorough detail by Raab and de Lange [3, 14], and will not be reproduced here, it being sufficient for present purposes to simply provide the end result, namely

$${}_m Q = \frac{2N_A}{45\varepsilon_0} \left[ \frac{15}{2}b + \frac{\alpha_{ij}\Theta_{ij}^{(0)}}{kT} \right]. \quad (2.46)$$

In equation (2.41),  $\frac{15}{2}b = B_{ijij}$ , but in equation (2.46),

$$\frac{15}{2}b = B_{ijij} - \mathcal{B}_{ijij} - 5\omega^{-1}\varepsilon_{ijk}J'_{ijk}, \quad (2.47)$$

where  $\varepsilon_{ijk}$  is the Levi-Civita tensor. Equation (2.46) has two terms, indicating that in EFGIB, the anisotropy in the refractive index of the fluid arises from two distinct contributions. The source of the temperature-independent term is the distortion of the molecular charge distribution by the applied field gradient, while that of the temperature-dependent term is the orientational effect of the electric field gradient on the molecular quadrupole moments. Nearly all of the earlier EFGIB experiments were performed at a single (ambient) temperature, hence avoiding the challenges in recording measurements at higher temperatures. The temperature-independent

term was then assumed to make a negligible contribution to  ${}_mQ$ , so that setting  $\frac{15}{2}b = 0$  in equation (2.46) allowed for the quadrupole moment to be extracted provided the polarizability tensor  $\alpha_{ij}$  was known. Since 1997, there have been several temperature-dependent investigations of EFGIB for smaller molecules, and these have revealed the extent to which the electronic-distortion term contributes to the induced birefringence: 3% for CO<sub>2</sub> [22, 27], -5% for CS<sub>2</sub> [22], -9% for C<sub>6</sub>H<sub>6</sub> [25], 7% for C<sub>6</sub>F<sub>6</sub> [25], 10% for N<sub>2</sub> [26], 5% for N<sub>2</sub>O [28] and 7% for CO [29]. These contributions, though often small, are clearly not negligible, especially since the aim of the EFGIB experiment is to extract precise and accurate values of the molecular quadrupole moments, with combined experimental uncertainties typically around 2 to 3%.

For the purposes of the present investigation, the contribution of the electronic-distortion tensors in equation (2.47) to the second EFGIB virial coefficient  $B_Q$  will be ignored. The reasons for this are twofold. Firstly, the individual tensor components for these polarizabilities are not known (either experimentally or computationally) even for small molecules, and so at present it is not feasible to calculate their contribution to  $B_Q$ , and secondly it seems reasonable to expect that their contribution to  $B_Q$  will be of the same order as for  $A_Q$ , namely around 10% or lower.

The new molecular-tensor theory for  $B_Q$  of non-dipolar molecules is now presented. It follows the formalism of Buckingham's original theory of EFGIB for non-interacting molecules [6] as has been presented in this section.

## 2.2 Non-dipolar interacting molecules

For higher gas densities, the methodology of Buckingham and Pople [32] for the treatment of intermolecular interaction effects via a virial expansion, as outlined in

general in Section 1.2 of Chapter 1, is followed.

Recall from equation (2.6) that in the limit of infinite dilution, the refractive index difference  $n_x - n_y$  of a gas in the presence of an applied non-uniform electric field is

$$n_x - n_y = \frac{2\pi N_A}{(4\pi\epsilon_0)V_m} \bar{\pi} \quad (2.48)$$

where  $\bar{\pi}$  is the average over all configurations  $\tau$  of the quantity  $\pi_{ij}(a_i^x a_j^x - a_i^y a_j^y)$  of a representative *isolated* molecule in the presence of the biasing influence of the applied non-uniform electric field.

For higher gas densities, the contribution of a representative molecule 1 to  $n_x - n_y$  is not always given by equation (2.48), since there are times when molecule 1 has to be treated as half of an interacting pair. When molecule 1 is in the presence of a neighbouring molecule 2, the relative configuration of which is specified by  $\tau$ , then the instantaneous contribution of molecule 1 to the induced birefringence becomes

$$\frac{1}{2} \left\{ \frac{2\pi N_A}{(4\pi\epsilon_0)V_m} \pi^{(12)}(\tau, \mathbf{E}, \nabla\mathbf{E}) \right\} \quad (2.49)$$

where

$$\pi^{(12)}(\tau, \mathbf{E}, \nabla\mathbf{E}) = \pi^{(12)} = \pi_{ij}^{(12)}(a_i^x a_j^x - a_i^y a_j^y) . \quad (2.50)$$

Here,  $\pi_{ij}^{(12)}$  is the differential polarizability of the interacting pair, an expression for which will need to be derived explicitly. To obtain the biased orientational average  $\overline{\pi^{(12)}(\tau, \mathbf{E}, \nabla\mathbf{E})}$ , the molecular pair is allowed to rotate as a rigid whole (in the fixed configuration  $\tau$ ) in the presence of the biasing influence of the field and field gradient,  $E_\alpha$  and  $\nabla_\beta E_\alpha$  respectively. This biased average can then be converted into isotropic averages through a Taylor expansion in powers of  $\mathbf{E}$  and  $\nabla\mathbf{E}$ . Just as in the analysis

of an isolated molecule provided in equations (2.9) to (2.11), the leading term is

$$\overline{\pi^{(12)}(\tau, \mathbf{E}, \nabla \mathbf{E})} = \left( \frac{\overline{\partial \pi^{(12)}(\tau, \mathbf{E}, \nabla \mathbf{E})}}{\partial E_{xx}} \right)_{E_x = E_{xx} = 0} E_{xx} \quad (2.51)$$

where

$$\left( \frac{\overline{\partial \pi^{(12)}(\tau, \mathbf{E}, \nabla \mathbf{E})}}{\partial E_{xx}} \right)_{E_x = E_{xx} = 0} = \left\langle \frac{\partial \pi^{(12)}}{\partial E_{xx}} \right\rangle - \frac{1}{kT} \left\langle \pi^{(12)} \frac{\partial U^{(12)}}{\partial E_{xx}} \right\rangle, \quad (2.52)$$

yielding

$$\overline{\pi^{(12)}(\tau, \mathbf{E}, \nabla \mathbf{E})} = \left\{ \left\langle \frac{\partial \pi^{(12)}}{\partial E_{xx}} \right\rangle - \frac{1}{kT} \left\langle \pi^{(12)} \frac{\partial U^{(12)}}{\partial E_{xx}} \right\rangle \right\} E_{xx}. \quad (2.53)$$

Here,  $U^{(12)} = U^{(12)}(\tau, 0, 0)$ , the potential energy of the interacting pair of molecules in the absence of the applied field and field gradient. The quantities inside the angular brackets are initially referred to the molecule-fixed axes  $O(1, 2, 3)$ . The tensor product in  $O(1, 2, 3)$  is fixed for a given interaction configuration  $\tau$ . As the pair rotates as a rigid whole in the laboratory frame  $O(x, y, z)$ , the average projection of the pair properties, referred to  $O(1, 2, 3)$ , is averaged into  $O(x, y, z)$  over all orientations. Averaging over the pair-interaction parameters  $\tau$  can then be performed.

The density dependence of the molar Buckingham constant  ${}_m Q$  can be expressed as the virial expansion

$${}_m Q = A_Q + \frac{B_Q}{V_m} + \frac{C_Q}{V_m^2} + \dots, \quad (2.54)$$

where  $A_Q$ ,  $B_Q$  and  $C_Q$  are the first, second and third Buckingham-effect virial coefficients. From equation (2.40), the molar Buckingham constant  ${}_m Q$  in the limit of

infinite dilution is

$$\begin{aligned}
 A_Q &= \lim_{V_m \rightarrow \infty} ({}_m Q) = \lim_{V_m \rightarrow \infty} \left\{ \frac{6n(3\varepsilon_r + 2)(n_x - n_y)V_m}{5\varepsilon_r(n^2 + 2)^2 E_{xx}} \right\}_{E_{xx} \rightarrow 0} \\
 &= \frac{2}{3} \cdot \frac{2\pi N_A}{(4\pi\varepsilon_0)} \left( \frac{\partial \bar{\pi}}{\partial E_{xx}} \right)_{E_x = E_{xx} = 0} .
 \end{aligned} \tag{2.55}$$

Extrapolating this expression to higher densities yields

$${}_m Q = A_Q + \int_{\tau} \frac{4\pi N_A}{3(4\pi\varepsilon_0)} \left\{ \frac{1}{2} \left( \frac{\partial \bar{\pi}^{(12)}}{\partial E_{xx}} \right)_{E_x = E_{xx} = 0} - \left( \frac{\partial \bar{\pi}}{\partial E_{xx}} \right)_{E_x = E_{xx} = 0} \right\} P(\tau) d\tau , \tag{2.56}$$

where  $P(\tau)d\tau$  is the probability of molecule 1 having a neighbour in the range  $(\tau, \tau + d\tau)$ , with  $P(\tau)$  given in equation (1.16). Comparing equation (2.56) with equation (2.54),  $B_Q$  is seen to be

$$B_Q = \frac{4\pi N_A^2}{3\Omega(4\pi\varepsilon_0)} \int_{\tau} \left\{ \frac{1}{2} \left( \frac{\partial \bar{\pi}^{(12)}}{\partial E_{xx}} \right)_{E_x = E_{xx} = 0} - \left( \frac{\partial \bar{\pi}}{\partial E_{xx}} \right)_{E_x = E_{xx} = 0} \right\} e^{-\frac{U_{12}(\tau)}{kT}} d\tau . \tag{2.57}$$

The relative configuration  $\tau$  of two molecules of general symmetry may be expressed by seven variables, namely the separation  $R$  of the two molecular centres, the Euler angles  $\alpha_1, \beta_1$  and  $\gamma_1$  used to define the direction cosines  $a_i^\alpha$  between the laboratory frame  $O(x, y, z)$  (referred to by  $\alpha, \beta, \gamma \dots$ ) and the molecule-fixed axes  $O(1, 2, 3)$  of molecule 1 (referred to by  $i, j, k \dots$ ), and the Euler angles  $\alpha_2, \beta_2$  and  $\gamma_2$  defining the direction cosines  $a_i^\alpha$  between the laboratory frame and the molecule-fixed axes  $O(1', 2', 3')$  of molecule 2 (referred to by  $i', j', k' \dots$ ). These variables are described in full by Couling and Graham [47, 48], together with the evaluation of the normalization constant, which is  $\Omega = (8\pi^2)^2$ . The explicit expressions for the direction cosine tensors are



$$\begin{aligned}
a_i^\alpha &= \begin{bmatrix} \cos\gamma_1 & \sin\gamma_1 & 0 \\ -\sin\gamma_1 & \cos\gamma_1 & 0 \\ 0 & 0 & 1 \end{bmatrix} \begin{bmatrix} \cos\beta_1 & 0 & -\sin\beta_1 \\ 0 & 1 & 0 \\ \sin\beta_1 & 0 & \cos\beta_1 \end{bmatrix} \begin{bmatrix} \cos\alpha_1 & \sin\alpha_1 & 0 \\ -\sin\alpha_1 & \cos\alpha_1 & 0 \\ 0 & 0 & 1 \end{bmatrix} \\
&= \begin{bmatrix} \cos\alpha_1\cos\beta_1\cos\gamma_1 - \sin\alpha_1\sin\gamma_1 & \sin\alpha_1\cos\beta_1\cos\gamma_1 + \cos\alpha_1\sin\gamma_1 & -\sin\beta_1\cos\gamma_1 \\ -\cos\alpha_1\cos\beta_1\sin\gamma_1 - \sin\alpha_1\cos\gamma_1 & -\sin\alpha_1\cos\beta_1\sin\gamma_1 + \cos\alpha_1\cos\gamma_1 & \sin\beta_1\sin\gamma_1 \\ \cos\alpha_1\sin\beta_1 & \sin\alpha_1\sin\beta_1 & \cos\beta_1 \end{bmatrix}, \tag{2.58}
\end{aligned}$$

and

$$\begin{aligned}
a_{i'}^\alpha &= \begin{bmatrix} \cos\alpha_2\cos\beta_2\cos\gamma_2 - \sin\alpha_2\sin\gamma_2 & \sin\alpha_2\cos\beta_2\cos\gamma_2 + \cos\alpha_2\sin\gamma_2 & -\sin\beta_2\cos\gamma_2 \\ -\cos\alpha_2\cos\beta_2\sin\gamma_2 - \sin\alpha_2\cos\gamma_2 & -\sin\alpha_2\cos\beta_2\sin\gamma_2 + \cos\alpha_2\cos\gamma_2 & \sin\beta_2\sin\gamma_2 \\ \cos\alpha_2\sin\beta_2 & \sin\alpha_2\sin\beta_2 & \cos\beta_2 \end{bmatrix}. \tag{2.59}
\end{aligned}$$

Equation (2.57) becomes

$$\begin{aligned}
B_Q &= \frac{2N_A^2}{24\pi^2(4\pi\epsilon_0)} \int_{R=0}^{\infty} \int_{\alpha_1=0}^{2\pi} \int_{\beta_1=0}^{\pi} \int_{\gamma_1=0}^{2\pi} \int_{\alpha_2=0}^{2\pi} \int_{\beta_2=0}^{\pi} \int_{\gamma_2=0}^{2\pi} \\
&\quad \times \left\{ \frac{1}{2} \left( \frac{\partial \overline{\pi^{(12)}}}{\partial E_{xx}} \right)_{E_x=E_{xx}=0} - \left( \frac{\partial \bar{\pi}}{\partial E_{xx}} \right)_{E_x=E_{xx}=0} \right\} \exp(-U_{12}(\tau)/kT) \tag{2.60}
\end{aligned}$$

$$\times R^2 \sin\beta_1 \sin\beta_2 dR d\alpha_1 d\beta_1 d\gamma_1 d\alpha_2 d\beta_2 d\gamma_2 .$$

Evaluation of  $B_Q$  by integrating over the pair interaction coordinates in equation (2.60) requires the intermolecular potential  $U_{12}(\tau)$ . In addition, the expression

$\frac{1}{2} \left( \frac{\partial \overline{\pi^{(12)}}}{\partial E_{xx}} \right)_{E_x=E_{xx}=0}$  needs to be evaluated, which requires the differential polarizabil-

ity  $\pi_{iw}^{(12)}$  for interacting molecular pairs:

$$\pi_{iw}^{(12)} = \frac{\partial \mu_i^{(12)}}{\partial \mathcal{E}_w} \quad (2.61)$$

where  $\mu_i^{(12)}(\mathcal{E}_w)$  is the total oscillating dipole moment induced on the interacting pair by the incident light-wave field  $\mathcal{E}_w$ . In order to proceed it becomes necessary to make an assumption about the molecules, namely that they always retain their separate identities. While this will hold true in the long-range limit, at very short ranges, the charge distributions of the molecules will begin to overlap, a situation which will require high-level *ab initio* calculations for definitive description. Such calculations are extremely demanding and computationally intensive even for interacting atoms, but especially so for interacting molecules. Treating the molecules as if they retain their separate identities even in the region of overlap has proven profitable in the explication of molecular interactions for Rayleigh light-scattering [47, 49–51] and the Kerr effect [48, 52–54], where agreement between measured and calculated second virial coefficients can be achieved to within 10% or better, providing a measure of justification for the simplifying assumption, which allows equation (2.61) to be written as

$$\pi_{iw}^{(12)} = \frac{\partial(\mu_i^{(1)} + \mu_i^{(2)})}{\partial \mathcal{E}_w} . \quad (2.62)$$

Substituting this into equation (2.50), the difference between the differential polarizabilities of an interacting pair in a specific configuration  $\tau$  in the presence of the

applied field and field gradient is found to be

$$\begin{aligned}
\pi^{(12)}(\tau, \mathbf{E}, \nabla \mathbf{E}) &= \pi_{iw}^{(12)}(a_i^x a_w^x - a_i^y a_w^y) \\
&= \left( \frac{\partial \mu_i^{(1)}}{\partial \mathcal{E}_w} + \frac{\partial \mu_i^{(2)}}{\partial \mathcal{E}_w} \right) (a_i^x a_w^x - a_i^y a_w^y) \\
&= \left( \pi_{iw}^{(1)} + \pi_{iw}^{(2)} \right) (a_i^x a_w^x - a_i^y a_w^y) \\
&= \pi^{(1)}(\tau, \mathbf{E}, \nabla \mathbf{E}) + \pi^{(2)}(\tau, \mathbf{E}, \nabla \mathbf{E}) .
\end{aligned} \tag{2.63}$$

Now the dipole moment of molecule 1,  $\mu_i^{(1)}$ , is induced not exclusively by the oscillating light-wave field  $\mathcal{E}_j$ , but also partly by the field  $\mathcal{F}_j^{(1)}$  which arises at molecule 1 due to the oscillating moments on molecule 2, so that

$$\mu_i^{(1)}(\mathcal{E}_j) = \left( \alpha_{ij}^{(1)} + \frac{1}{3} B_{ijkl}^{(1)} E_{kl} + \dots \right) \left( \mathcal{E}_j + \mathcal{F}_j^{(1)} \right) . \tag{2.64}$$

With the aid of the second-rank  $T$ -tensor [1],  $\mathcal{F}_j^{(1)}$  has the form

$$\mathcal{F}_j^{(1)} = T_{jm}^{(1)} \mu_m^{(2)} \tag{2.65}$$

where

$$\mu_m^{(2)}(\mathcal{E}_n) = \left( \alpha_{mn}^{(2)} + \frac{1}{3} B_{mnab}^{(2)} E_{ab} + \dots \right) \left( \mathcal{E}_n + \mathcal{F}_n^{(2)} \right) , \tag{2.66}$$

where, in turn,

$$\mathcal{F}_n^{(2)} = T_{np}^{(2)} \mu_p^{(1)} . \tag{2.67}$$

Note that

$$T^{(1)} = (-1)^n T^{(2)} , \quad (2.68)$$

where  $n$  is the rank of the  $T$ -tensor [1]. If equations (2.66) and (2.67) are substituted into equation (2.65), followed by successive substitutions of  $\mathcal{F}_j^{(1)}$  and  $\mathcal{F}_n^{(2)}$ , a series of terms contributing to the net field  $\mathcal{F}_j^{(1)}$  in equation (2.65) is obtained, which, when substituted into equation (2.64), yields the required expression for the total oscillating dipole moment induced on molecule 1 by the light-wave field in the presence of the neighbouring molecule 2:

$$\begin{aligned} \mu_i^{(1)}(\mathcal{E}_w) = & \alpha_{iw}^{(1)} \mathcal{E}_w + \alpha_{ij}^{(1)} T_{jk} \alpha_{kw}^{(2)} \mathcal{E}_w + \alpha_{ij}^{(1)} T_{jk} \alpha_{kl}^{(2)} T_{lm} \alpha_{mw}^{(1)} \mathcal{E}_w \\ & + \alpha_{ij}^{(1)} T_{jk} \alpha_{kl}^{(2)} T_{lm} \alpha_{mn}^{(1)} T_{np} \alpha_{pw}^{(2)} \mathcal{E}_w + \alpha_{ij}^{(1)} T_{jk} \alpha_{kl}^{(2)} T_{lm} \alpha_{mn}^{(1)} T_{np} \alpha_{pq}^{(2)} T_{qr} \alpha_{rw}^{(1)} \mathcal{E}_w \\ & + \alpha_{ij}^{(1)} T_{jk} \alpha_{kl}^{(2)} T_{lm} \alpha_{mn}^{(1)} T_{np} \alpha_{pq}^{(2)} T_{qr} \alpha_{rs}^{(1)} T_{st} \alpha_{tw}^{(2)} \mathcal{E}_w + \dots \\ & + \frac{1}{3} B_{i w k l}^{(1)} E_{kl} \mathcal{E}_w + \frac{1}{3} \alpha_{ij}^{(1)} T_{jk} B_{k w m n}^{(2)} E_{mn} \mathcal{E}_w + \frac{1}{3} B_{i j k l}^{(1)} E_{kl} T_{jm} \alpha_{mw}^{(2)} \mathcal{E}_w \\ & + \frac{1}{3} \alpha_{ij}^{(1)} T_{jk} \alpha_{kl}^{(2)} T_{lm} B_{m w p q}^{(1)} E_{pq} \mathcal{E}_w + \frac{1}{3} \alpha_{ij}^{(1)} T_{jk} B_{k l m n}^{(2)} E_{mn} T_{lp} \alpha_{pw}^{(1)} \mathcal{E}_w \\ & + \frac{1}{3} B_{i j k l}^{(1)} E_{kl} T_{jm} \alpha_{mn}^{(2)} T_{np} \alpha_{pw}^{(1)} \mathcal{E}_w + \dots . \end{aligned} \quad (2.69)$$

Performing the operation  $\frac{\partial}{\partial \mathcal{E}_w}$  on equation (2.69) yields the expression for the polarizability of molecule 1 in the presence of both the applied inhomogeneous field and a neighbouring molecule 2 in a specific relative configuration  $\tau$ :

$$\begin{aligned}
\pi_{iw}^{(1)} &= \frac{\partial \mu_i^{(1)}}{\partial \mathcal{E}_w} = \alpha_{iw}^{(1)} + \alpha_{ij}^{(1)} T_{jk} \alpha_{kw}^{(2)} + \alpha_{ij}^{(1)} T_{jk} \alpha_{kl}^{(2)} T_{lm} \alpha_{mw}^{(1)} \\
&+ \alpha_{ij}^{(1)} T_{jk} \alpha_{kl}^{(2)} T_{lm} \alpha_{mn}^{(1)} T_{np} \alpha_{pw}^{(2)} + \alpha_{ij}^{(1)} T_{jk} \alpha_{kl}^{(2)} T_{lm} \alpha_{mn}^{(1)} T_{np} \alpha_{pq}^{(2)} T_{qr} \alpha_{rw}^{(1)} \\
&+ \alpha_{ij}^{(1)} T_{jk} \alpha_{kl}^{(2)} T_{lm} \alpha_{mn}^{(1)} T_{np} \alpha_{pq}^{(2)} T_{qr} \alpha_{rs}^{(1)} T_{st} \alpha_{tw}^{(2)} + \dots \\
&+ \frac{1}{3} B_{i w k l}^{(1)} E_{kl} + \frac{1}{3} \alpha_{ij}^{(1)} T_{jk} B_{k w m n}^{(2)} E_{mn} + \frac{1}{3} B_{i j k l}^{(1)} E_{kl} T_{j m} \alpha_{m w}^{(2)} \\
&+ \frac{1}{3} \alpha_{ij}^{(1)} T_{jk} \alpha_{kl}^{(2)} T_{lm} B_{m w p q}^{(1)} E_{pq} + \frac{1}{3} \alpha_{ij}^{(1)} T_{jk} B_{k l m n}^{(2)} E_{mn} T_{l p} \alpha_{p w}^{(1)} \\
&+ \frac{1}{3} B_{i j k l}^{(1)} E_{kl} T_{j m} \alpha_{m n}^{(2)} T_{n p} \alpha_{p w}^{(1)} + \dots .
\end{aligned} \tag{2.70}$$

This equation can be generalized to a differential polarizability  $\pi_{iw}^{(p)}$  of a molecule  $p$  in the presence of the non-uniform field and a neighbouring molecule  $q$ . In addition, use of equation (2.19) allows the field gradient  $E_{ij}$  to be expressed as  $E_{ij} = E_{xx}(a_i^x a_j^x - a_i^y a_j^y)$ . The result is

$$\begin{aligned}
\pi_{iw}^{(p)} &= \alpha_{iw}^{(p)} + \alpha_{ij}^{(p)} T_{jk} \alpha_{kw}^{(q)} + \alpha_{ij}^{(p)} T_{jk} \alpha_{kl}^{(q)} T_{lm} \alpha_{mw}^{(p)} \\
&+ \alpha_{ij}^{(p)} T_{jk} \alpha_{kl}^{(q)} T_{lm} \alpha_{mn}^{(p)} T_{np} \alpha_{pw}^{(q)} + \alpha_{ij}^{(p)} T_{jk} \alpha_{kl}^{(q)} T_{lm} \alpha_{mn}^{(p)} T_{np} \alpha_{pq}^{(q)} T_{qr} \alpha_{rw}^{(p)} \\
&+ \alpha_{ij}^{(p)} T_{jk} \alpha_{kl}^{(q)} T_{lm} \alpha_{mn}^{(p)} T_{np} \alpha_{pq}^{(q)} T_{qr} \alpha_{rs}^{(p)} T_{st} \alpha_{tw}^{(q)} + \dots \\
&+ \frac{1}{3} B_{i w k l}^{(p)} E_{xx} (a_k^x a_l^x - a_k^y a_l^y) + \frac{1}{3} \alpha_{ij}^{(p)} T_{jk} B_{k w m n}^{(q)} E_{xx} (a_m^x a_n^x - a_m^y a_n^y) \\
&+ \frac{1}{3} B_{i j k l}^{(p)} T_{j m} \alpha_{m w}^{(q)} E_{xx} (a_k^x a_l^x - a_k^y a_l^y) \\
&+ \frac{1}{3} \alpha_{ij}^{(p)} T_{jk} \alpha_{kl}^{(q)} T_{lm} B_{m w p q}^{(p)} E_{xx} (a_p^x a_q^x - a_p^y a_q^y) \\
&+ \frac{1}{3} \alpha_{ij}^{(p)} T_{jk} B_{k l m n}^{(q)} T_{lp} \alpha_{pw}^{(p)} E_{xx} (a_m^x a_n^x - a_m^y a_n^y) \\
&+ \frac{1}{3} B_{i j k l}^{(p)} T_{j m} \alpha_{m n}^{(q)} T_{np} \alpha_{pw}^{(p)} E_{xx} (a_k^x a_l^x - a_k^y a_l^y) + \dots .
\end{aligned} \tag{2.71}$$

The potential of the interacting pair of molecules in the presence of the static applied inhomogeneous field is defined to be [3, 6]

$$\begin{aligned}
U^{(12)}(\tau, \mathbf{E}, \nabla \mathbf{E}) &= U^{(12)}(\tau, 0, 0) - \int_0^{E_i} \mu_i^{(12)}(\tau, \mathbf{E}, \nabla \mathbf{E}) dE_i \\
&- \frac{1}{3} \int_0^{\nabla_j E_i} \Theta_{ij}^{(12)}(\tau, \mathbf{E}, \nabla \mathbf{E}) d(\nabla_j E_i) .
\end{aligned} \tag{2.72}$$

The Kerr-effect terms from  $\int_0^{E_x} \mu_i^{(12)}(\tau, \mathbf{E}, \nabla \mathbf{E}) a_i^x dE_x$  disappear when the potential

is differentiated with respect to the field gradient in equation (2.53). Since this is the only term in equation (2.53) which contains the potential, for our purposes it suffices to write the potential  $U^{(12)}$  as

$$U^{(12)}(\tau, \mathbf{E}, \nabla \mathbf{E}) = U^{(12)}(\tau, 0, 0) - \frac{1}{3} \int_0^{E_{xx}} \Theta_{ij}^{(12)}(\tau, \mathbf{E}, \nabla E) (a_i^x a_j^x - a_i^y a_j^y) dE_{xx} , \quad (2.73)$$

where, from equation (2.17),  $\nabla_j E_i = E_{ij}$  has been written as  $(a_i^x a_j^x - a_i^y a_j^y) E_{xx}$ , and where  $\Theta_{ij}^{(12)}$  is the total quadrupole moment of the pair in the presence of  $E_{xx}$ . As was argued for the dipole moment of the interacting pair, the quadrupole moment of each molecule is assumed to always retain its separate identity such that

$$\Theta_{ij}^{(12)} = \Theta_{ij}^{(1)} + \Theta_{ij}^{(2)} . \quad (2.74)$$

The potential becomes

$$U^{(12)}(\tau, \mathbf{E}, \nabla \mathbf{E}) = U^{(12)}(\tau, 0) + U^{(1)}(\tau, E_{xx}) + U^{(2)}(\tau, E_{xx}) . \quad (2.75)$$

$\Theta_{ij}^{(p)}$  is the total quadrupole moment (permanent and induced) of molecule  $p$  in the presence of the field and field gradient of a neighbouring molecule  $q$ , which can be written as [1]

$$\Theta_{ij}^{(p)} = \Theta_{0ij}^{(p)} + A_{0ijk}^{(p)} (E_k + F_k^{(p)}) + C_{0ijkl}^{(p)} (E_{kl} + F_{kl}^{(p)}) + \dots . \quad (2.76)$$

Here,  $\Theta_{0ij}^{(p)}$  is the permanent quadrupole moment of the molecule (now identified by the subscript zero),  $A_{0ijk}^{(p)}$  and  $C_{0ijkl}^{(p)}$  are static polarizability tensors (also denoted by the subscript zero), while  $F_k^{(p)}$  and  $F_{kl}^{(p)}$  are the static field and field gradient, respectively, arising at molecule  $p$  due to the permanent and induced multipole

moments of the neighbouring molecule  $q$ , which can be written as [1]

$$F_k^{(p)} = -\frac{1}{3}T_{klm}^{(p)}\Theta_{lm}^{(q)} \quad (2.77)$$

and

$$F_{kl}^{(p)} = -\frac{1}{3}T_{klmn}^{(p)}\Theta_{mn}^{(q)} . \quad (2.78)$$

For the non-dipolar molecules of this investigation, the static tensor  $A_{0ijk}^{(p)}$  in equation (2.76) is equal to zero, so that the quadrupole moment for molecule  $p$  simplifies to

$$\Theta_{ij}^{(p)} = \Theta_{0ij}^{(p)} + C_{0ijkl}^{(p)}(E_{kl} + F_{kl}^{(p)}) . \quad (2.79)$$

Now,

$$F_{kl}^{(p)} = -\frac{1}{3}T_{klmn}^{(p)}\Theta_{mn}^{(q)} \quad (2.80)$$

requires

$$\Theta_{mn}^{(q)} = \Theta_{0mn}^{(q)} + C_{0mnpq}^{(q)}(E_{pq} + F_{pq}^{(q)}) , \quad (2.81)$$

where

$$F_{pq}^{(q)} = -\frac{1}{3}T_{pqrs}^{(q)}\Theta_{rs}^{(p)} . \quad (2.82)$$

Successive substitutions of  $F_{kl}^{(p)}$  and  $F_{pq}^{(q)}$  into equation (2.79) provide the series of



terms contributing to the total static quadrupole moment of molecule  $p$ :

$$\Theta_{ij}^{(p)} = \Theta_{0ij}^{(p)} + C_{0ijkl}^{(p)} E_{kl} - \frac{1}{3} C_{0ijkl}^{(p)} T_{klmn} \Theta_{0mn}^{(q)} + \frac{1}{9} C_{0ijkl}^{(p)} T_{klmn} C_{0mnpq}^{(q)} T_{pqrs} \Theta_{0rs}^{(p)} + \dots \quad (2.83)$$

Substituting equation (2.83) into equation (2.73), and bearing in mind equation (2.75), the expression for the potential energy of molecule  $p$  becomes

$$U^{(p)}(\tau, E_{xx}) = \left[ -\frac{1}{3} \Theta_{0ij}^{(p)} + \frac{1}{9} C_{0ijkl}^{(p)} T_{klmn} \Theta_{0mn}^{(q)} + \dots \right] (a_i^x a_j^x - a_i^y a_j^y) E_{xx} \quad (2.84)$$

Armed with the explicit expressions for  $\pi_{iw}^{(p)}$  in equation (2.71) and  $U^{(p)}$  in equation (2.84), it is now possible to evaluate the term  $\frac{1}{2} \left( \frac{\partial \pi^{(12)}}{\partial E_{xx}} \right)_{E_x=E_{xx}=0}$  in the expression for  $B_Q$  in equation (2.60). Recall equation (2.52):

$$\left( \frac{\partial \pi^{(12)}(\tau, \mathbf{E}, \nabla \mathbf{E})}{E_{xx}} \right)_{E_x=E_{xx}=0} = \left\langle \frac{\partial \pi^{(12)}}{\partial E_{xx}} \right\rangle - \frac{1}{kT} \left\langle \pi^{(12)} \frac{\partial U^{(12)}}{\partial E_{xx}} \right\rangle \quad (2.85)$$

Equation (2.63) yields

$$\left\langle \frac{\partial \pi^{(12)}}{\partial E_{xx}} \right\rangle = \left\langle \frac{\partial \pi^{(1)}}{\partial E_{xx}} \right\rangle + \left\langle \frac{\partial \pi^{(2)}}{\partial E_{xx}} \right\rangle, \quad (2.86)$$

and since molecules 1 and 2 are identical, the isotropic averages of their molecular properties must be the same, so that

$$\left\langle \frac{\partial \pi^{(12)}}{\partial E_{xx}} \right\rangle = 2 \left\langle \frac{\partial \pi^{(1)}}{\partial E_{xx}} \right\rangle \quad (2.87)$$

Similarly, and with the additional use of equation (2.75),

$$\left\langle \pi^{(12)} \frac{\partial U^{(12)}}{\partial E_{xx}} \right\rangle = \left\langle (\pi^{(1)} + \pi^{(2)}) \left( \frac{\partial U^{(1)}}{\partial E_{xx}} + \frac{\partial U^{(2)}}{\partial E_{xx}} \right) \right\rangle, \quad (2.88)$$

which expands to

$$\left\langle \pi^{(12)} \frac{\partial U^{(12)}}{\partial E_{xx}} \right\rangle = \left\langle \pi^{(1)} \frac{\partial U^{(1)}}{\partial E_{xx}} \right\rangle + \left\langle \pi^{(1)} \frac{\partial U^{(2)}}{\partial E_{xx}} \right\rangle + \left\langle \pi^{(2)} \frac{\partial U^{(1)}}{\partial E_{xx}} \right\rangle + \left\langle \pi^{(2)} \frac{\partial U^{(2)}}{\partial E_{xx}} \right\rangle \quad (2.89)$$

and, in turn, simplifies to

$$\left\langle \pi^{(12)} \frac{\partial U^{(12)}}{\partial E_{xx}} \right\rangle = 2 \left\langle \pi^{(1)} \frac{\partial U^{(1)}}{\partial E_{xx}} \right\rangle + 2 \left\langle \pi^{(1)} \frac{\partial U^{(2)}}{\partial E_{xx}} \right\rangle. \quad (2.90)$$

Hence,

$$\frac{1}{2} \left( \frac{\partial \overline{\pi^{(12)}(\tau, \mathbf{E}, \nabla \mathbf{E})}}{\partial E_{xx}} \right)_{E_x = E_{xx} = 0} = \left\langle \frac{\partial \pi^{(1)}}{\partial E_{xx}} \right\rangle - \frac{1}{kT} \left[ \left\langle \pi^{(1)} \frac{\partial U^{(1)}}{\partial E_{xx}} \right\rangle + \left\langle \pi^{(1)} \frac{\partial U^{(2)}}{\partial E_{xx}} \right\rangle \right]. \quad (2.91)$$

The isotropic averages in equation (2.91) are now evaluated, beginning with  $\left\langle \frac{\partial \pi^{(1)}}{\partial E_{xx}} \right\rangle$ . Differentiating equation (2.71) with respect to the field gradient  $E_{xx}$  and setting the field gradient to zero yields

$$\begin{aligned} \left( \frac{\partial \pi_{iw}^{(1)}}{\partial E_{xx}} \right)_{E_x = E_{xx} = 0} &= \left[ \frac{1}{3} B_{iwnp}^{(1)} + \frac{1}{3} \alpha_{ij}^{(1)} T_{jk} B_{kwnp}^{(2)} \right. \\ &\quad + \frac{1}{3} B_{ijnp}^{(1)} T_{jm} \alpha_{mw}^{(2)} \\ &\quad + \frac{1}{3} \alpha_{ij}^{(1)} T_{jk} \alpha_{kl}^{(2)} T_{lm} B_{mwnp}^{(1)} \\ &\quad + \frac{1}{3} \alpha_{ij}^{(1)} T_{jk} B_{klnp}^{(2)} T_{lm} \alpha_{mw}^{(1)} \\ &\quad \left. + \frac{1}{3} B_{ijnp}^{(1)} T_{jk} \alpha_{kl}^{(2)} T_{lm} \alpha_{mw}^{(2)} + \dots \right] (a_n^x a_p^x - a_n^y a_p^y). \end{aligned} \quad (2.92)$$

From equation (2.63),

$$\pi^{(1)} = \pi_{iw}^{(1)}(a_i^x a_w^x - a_i^y a_w^y) \quad (2.93)$$

so that

$$\begin{aligned} \left( \frac{\partial \pi^{(1)}}{\partial E_{xx}} \right)_{E_x = E_{xx} = 0} &= \left[ \frac{1}{3} B_{iwnp}^{(1)} + \frac{1}{3} \alpha_{ij}^{(1)} T_{jk} B_{kwnp}^{(2)} \right. \\ &+ \frac{1}{3} B_{ijnp}^{(1)} T_{jm} \alpha_{mw}^{(2)} \\ &+ \frac{1}{3} \alpha_{ij}^{(1)} T_{jk} \alpha_{kl}^{(2)} T_{lm} B_{mwnp}^{(1)} \\ &+ \frac{1}{3} \alpha_{ij}^{(1)} T_{jk} B_{klmp}^{(2)} T_{lm} \alpha_{mw}^{(1)} \\ &\left. + \frac{1}{3} B_{ijnp}^{(1)} T_{jk} \alpha_{kl}^{(2)} T_{lm} \alpha_{mw}^{(2)} + \dots \right] (a_n^x a_p^x - a_n^y a_p^y)(a_i^x a_w^x - a_i^y a_w^y) . \end{aligned} \quad (2.94)$$

The isotropic average of equation (2.94) requires the isotropic average of the product of direction cosines, which has already been handled in equations (2.21) to (2.28). As already mentioned, there is a paucity of molecular  $B_{ijkl}$  tensor components in the literature, and so these terms will not be considered further. In any event, their expected contribution to  $B_Q$  is only a few percent. The BLH theory leads to additional interaction-induced contributions from  $\mathcal{B}_{ijkl}$  and  $J'_{ijk}$ , which would need to be derived within the BLH theory [3, 10, 14], and which is beyond the scope of this project, though these tensor components are also not available in the literature. Fortunately, the combined contribution of these terms to  $B_Q$  should only be a few percent, so that their omission is not of serious concern. PhD student Mr

Siyabonga Ntombela, who is undertaking a project on EFGIB in the BLH formalism, is currently evaluating these terms as part of his project, as a means to verify these assumptions. This will require *ab initio* computation of the  $B_{ijkl}$ ,  $\mathcal{B}_{ijkl}$  and  $J'_{ijk}$  optical-frequency tensor components.

The remaining two isotropic averages in equation (2.91) are now evaluated. Initially, equation (2.84) is differentiated with respect to the field gradient, giving

$$\left( \frac{\partial U^{(p)}}{\partial E_{xx}} \right)_{E_x=E_{xx}=0} = \left[ -\frac{1}{3}\Theta_{0ij}^{(p)} + \frac{1}{9}C_{ijkl}^{(p)}T_{klmn}\Theta_{0mn}^{(q)} + \dots \right] (a_i^x a_j^x - a_i^y a_j^y). \quad (2.95)$$

Then,  $(\pi^{(1)})_{E_x=E_{xx}=0}$  can be multiplied by the sum of the terms  $(\frac{\partial U^{(1)}}{\partial E_{xx}})_{E_x=E_{xx}=0}$  and  $(\frac{\partial U^{(2)}}{\partial E_{xx}})_{E_x=E_{xx}=0}$ , hence providing the dominant contributions to  $B_Q$ . From equation (2.71)

$$\begin{aligned} (\pi^{(1)})_{E_{xx}=E_x=0} &= \left[ \pi_{iw}^{(1)} (a_i^x a_w^x - a_i^y a_w^y) \right]_{E_x=E_{xx}=0} \\ &= (\alpha_{iw}^{(1)} + \alpha_{ij}^{(1)} T_{jk} \alpha_{kw}^{(2)} + \alpha_{ij}^{(1)} T_{jk} \alpha_{kl}^{(2)} T_{lm} \alpha_{mw}^{(1)} \\ &\quad + \alpha_{ij}^{(1)} T_{jk} \alpha_{kl}^{(2)} T_{lm} \alpha_{mn}^{(1)} T_{np} \alpha_{pw}^{(2)} + \alpha_{ij}^{(1)} T_{jk} \alpha_{kl}^{(2)} T_{lm} \alpha_{mn}^{(1)} T_{np} \alpha_{pq}^{(2)} T_{qr} \alpha_{rw}^{(1)} \\ &\quad + \alpha_{ij}^{(1)} T_{jk} \alpha_{kl}^{(2)} T_{lm} \alpha_{mn}^{(1)} T_{np} \alpha_{pq}^{(2)} T_{qr} \alpha_{rs}^{(1)} T_{st} \alpha_{tw}^{(2)} + \dots) (a_i^x a_w^x - a_i^y a_w^y), \end{aligned} \quad (2.96)$$

while from equation (2.84)

$$\left( \frac{\partial U^{(1)}}{\partial E_{xx}} \right)_{E_x=E_{xx}=0} = -\frac{1}{3}\Theta_{0ab}^{(1)} (a_a^x a_b^x - a_a^y a_b^y) \quad (2.97)$$

wherein the  $C$ -tensor terms, the contributions of which are expected to be negli-

ble, have been omitted. Thus  $\langle \pi^{(1)} \frac{\partial U^{(1)}}{\partial E_{xx}} \rangle$  becomes

$$\begin{aligned}
\left\langle \pi^{(1)} \frac{\partial U^{(1)}}{\partial E_{xx}} \right\rangle &= -\frac{1}{3} \left\{ \alpha_{iw}^{(1)} \Theta_{0ab}^{(1)} + \alpha_{ij}^{(1)} T_{jk} \alpha_{kw}^{(2)} \Theta_{0ab}^{(1)} + \alpha_{ij}^{(1)} T_{jk} \alpha_{kl}^{(2)} T_{lm} \alpha_{mw}^{(1)} \Theta_{0ab}^{(1)} \right. \\
&\quad + \alpha_{ij}^{(1)} T_{jk} \alpha_{kl}^{(2)} T_{lm} \alpha_{mn}^{(1)} T_{np} \alpha_{pw}^{(2)} \Theta_{0ab}^{(1)} \\
&\quad + \alpha_{ij}^{(1)} T_{jk} \alpha_{kl}^{(2)} T_{lm} \alpha_{mn}^{(1)} T_{np} \alpha_{pq}^{(2)} T_{qr} \alpha_{rw}^{(1)} \Theta_{0ab}^{(1)} \\
&\quad \left. + \alpha_{ij}^{(1)} T_{jk} \alpha_{kl}^{(2)} T_{lm} \alpha_{mn}^{(1)} T_{np} \alpha_{pq}^{(2)} T_{qr} \alpha_{rs}^{(1)} T_{st} \alpha_{tw}^{(2)} \Theta_{0ab}^{(1)} + \dots \right\} \\
&\quad \times \left\langle (a_i^x a_w^x - a_i^y a_w^y) (a_a^x a_b^x - a_a^y a_b^y) \right\rangle.
\end{aligned} \tag{2.98}$$

The relevant results for isotropic averages contained in equations (2.21) to (2.28) are summarized here for convenience:

$$\begin{aligned}
\left\langle (a_i^x a_w^x - a_i^y a_w^y) (a_a^x a_b^x - a_a^y a_b^y) \right\rangle &= 2 \left\langle a_i^x a_w^x a_a^x a_b^x - a_i^x a_w^x a_a^y a_b^y \right\rangle \\
&= \frac{1}{15} \left( -2\delta_{iw} \delta_{ab} + 3\delta_{ia} \delta_{wb} + 3\delta_{ib} \delta_{wa} \right).
\end{aligned} \tag{2.99}$$

Application of these results to equation (2.98) yields

$$\begin{aligned}
\left\langle \pi^{(1)} \frac{\partial U^{(1)}}{\partial E_{xx}} \right\rangle &= -\frac{1}{45} \left\{ \alpha_{iw}^{(1)} \Theta_{0ab}^{(1)} + \alpha_{ij}^{(1)} T_{jk} \alpha_{kw}^{(2)} \Theta_{0ab}^{(1)} + \alpha_{ij}^{(1)} T_{jk} \alpha_{kl}^{(2)} T_{lm} \alpha_{mw}^{(1)} \Theta_{0ab}^{(1)} \right. \\
&\quad + \alpha_{ij}^{(1)} T_{jk} \alpha_{kl}^{(2)} T_{lm} \alpha_{mn}^{(1)} T_{np} \alpha_{pw}^{(2)} \Theta_{0ab}^{(1)} \\
&\quad + \alpha_{ij}^{(1)} T_{jk} \alpha_{kl}^{(2)} T_{lm} \alpha_{mn}^{(1)} T_{np} \alpha_{pq}^{(2)} T_{qr} \alpha_{rw}^{(1)} \Theta_{0ab}^{(1)} \\
&\quad \left. + \alpha_{ij}^{(1)} T_{jk} \alpha_{kl}^{(2)} T_{lm} \alpha_{mn}^{(1)} T_{np} \alpha_{pq}^{(2)} T_{qr} \alpha_{rs}^{(1)} T_{st} \alpha_{tw}^{(2)} \Theta_{0ab}^{(1)} + \dots \right\} \\
&\quad \times \left( -2\delta_{iw} \delta_{ab} + 3\delta_{ia} \delta_{wb} + 3\delta_{ib} \delta_{wa} \right) .
\end{aligned} \tag{2.100}$$

Contracting over the subscripts gives

$$\begin{aligned}
\left\langle \Pi^{(1)} \frac{\partial U^{(1)}}{\partial E_{xx}} \right\rangle = & -\frac{1}{45} \left[ \left\{ -2\alpha_{ii}^{(1)} \Theta_{0aa}^{(1)} + 3\alpha_{iw}^{(1)} \Theta_{0iw}^{(1)} + 3\alpha_{iw}^{(1)} \Theta_{0wi}^{(1)} \right\} \right. \\
& + \left\{ -2\alpha_{ij}^{(1)} T_{jk} \alpha_{ki}^{(2)} \Theta_{0aa}^{(1)} + 3\alpha_{ij}^{(1)} T_{jk} \alpha_{kw}^{(2)} \Theta_{0iw}^{(1)} + 3\alpha_{ij}^{(1)} T_{jk} \alpha_{kw}^{(2)} \Theta_{0wi}^{(1)} \right\} \\
& + \left\{ -2\alpha_{ij}^{(1)} T_{jk} \alpha_{kl}^{(2)} T_{lm} \alpha_{mi}^{(1)} \Theta_{0aa}^{(1)} \right. \\
& + \left. 3\alpha_{ij}^{(1)} T_{jk} \alpha_{kl}^{(2)} T_{lm} \alpha_{mw}^{(1)} \Theta_{0iw}^{(1)} + 3\alpha_{ij}^{(1)} T_{jk} \alpha_{kl}^{(2)} T_{lm} \alpha_{mw}^{(1)} \Theta_{0wi}^{(1)} \right\} \\
& + \left\{ -2\alpha_{ij}^{(1)} T_{jk} \alpha_{kl}^{(2)} T_{lm} \alpha_{mn}^{(1)} T_{np} \alpha_{pi}^{(2)} \Theta_{0aa}^{(1)} \right. \\
& + \left. 3\alpha_{ij}^{(1)} T_{jk} \alpha_{kl}^{(2)} T_{lm} \alpha_{mn}^{(1)} T_{np} \alpha_{pw}^{(2)} \Theta_{0iw}^{(1)} + 3\alpha_{ij}^{(1)} T_{jk} \alpha_{kl}^{(2)} T_{lm} \alpha_{mn}^{(1)} T_{np} \alpha_{pw}^{(2)} \Theta_{0wi}^{(1)} \right\} \\
& + \left\{ -2\alpha_{ij}^{(1)} T_{jk} \alpha_{kl}^{(2)} T_{lm} \alpha_{mn}^{(1)} T_{np} \alpha_{pq}^{(2)} T_{qr} \alpha_{ri}^{(1)} \Theta_{0aa}^{(1)} \right. \\
& + \left. 3\alpha_{ij}^{(1)} T_{jk} \alpha_{kl}^{(2)} T_{lm} \alpha_{mn}^{(1)} T_{np} \alpha_{pq}^{(2)} T_{qr} \alpha_{rw}^{(1)} \Theta_{0iw}^{(1)} \right. \\
& + \left. 3\alpha_{ij}^{(1)} T_{jk} \alpha_{kl}^{(2)} T_{lm} \alpha_{mn}^{(1)} T_{np} \alpha_{pq}^{(2)} T_{qr} \alpha_{rw}^{(1)} \Theta_{0wi}^{(1)} \right\} \\
& + \left\{ -2\alpha_{ij}^{(1)} T_{jk} \alpha_{kl}^{(2)} T_{lm} \alpha_{mn}^{(1)} T_{np} \alpha_{pq}^{(2)} T_{qr} \alpha_{rs}^{(1)} T_{st} \alpha_{ti}^{(2)} \Theta_{0aa}^{(1)} \right. \\
& + \left. 3\alpha_{ij}^{(1)} T_{jk} \alpha_{kl}^{(2)} T_{lm} \alpha_{mn}^{(1)} T_{np} \alpha_{pq}^{(2)} T_{qr} \alpha_{rs}^{(1)} T_{st} \alpha_{tw}^{(2)} \Theta_{0iw}^{(1)} \right. \\
& + \left. 3\alpha_{ij}^{(1)} T_{jk} \alpha_{kl}^{(2)} T_{lm} \alpha_{mn}^{(1)} T_{np} \alpha_{pq}^{(2)} T_{qr} \alpha_{rs}^{(1)} T_{st} \alpha_{tw}^{(2)} \Theta_{0wi}^{(1)} \right\} + \dots \left. \right].
\end{aligned}
\tag{2.101}$$

Since the quadrupole moment is traceless, any quadrupole terms with a repeated subscript  $\Theta_{0aa}^{(p)}$  are equal to zero and are eliminated from the equation. Also, the quadrupole moment tensor is symmetric in its subscripts, so that  $\Theta_{0iw}^{(p)} = \Theta_{0wi}^{(p)}$ . Hence,

$$\begin{aligned} \left\langle \pi^{(1)} \frac{\partial U^{(1)}}{\partial E_{xx}} \right\rangle = & -\frac{6}{45} \left[ \alpha_{iw}^{(1)} \Theta_{0wi}^{(1)} + \alpha_{ij}^{(1)} T_{jk} \alpha_{kw}^{(2)} \Theta_{0wi}^{(1)} + \alpha_{ij}^{(1)} T_{jk} \alpha_{kl}^{(2)} T_{lm} \alpha_{mw}^{(1)} \Theta_{0wi}^{(1)} \right. \\ & + \alpha_{ij}^{(1)} T_{jk} \alpha_{kl}^{(2)} T_{lm} \alpha_{mn}^{(1)} T_{np} \alpha_{pw}^{(2)} \Theta_{0wi}^{(1)} \\ & + \alpha_{ij}^{(1)} T_{jk} \alpha_{kl}^{(2)} T_{lm} \alpha_{mn}^{(1)} T_{np} \alpha_{pq}^{(2)} T_{qr} \alpha_{rw}^{(1)} \Theta_{0wi}^{(1)} \\ & \left. + \alpha_{ij}^{(1)} T_{jk} \alpha_{kl}^{(2)} T_{lm} \alpha_{mn}^{(1)} T_{np} \alpha_{pq}^{(2)} T_{qr} \alpha_{rs}^{(1)} T_{st} \alpha_{tw}^{(2)} \Theta_{0wi}^{(1)} + \dots \right]. \end{aligned} \quad (2.102)$$

A similar analysis yields

$$\begin{aligned} \left\langle \pi^{(1)} \frac{\partial U^{(2)}}{\partial E_{xx}} \right\rangle = & -\frac{6}{45} \left[ \alpha_{iw}^{(1)} \Theta_{0wi}^{(2)} + \alpha_{ij}^{(1)} T_{jk} \alpha_{kw}^{(2)} \Theta_{0wi}^{(2)} + \alpha_{ij}^{(1)} T_{jk} \alpha_{kl}^{(2)} T_{lm} \alpha_{mw}^{(1)} \Theta_{0wi}^{(2)} \right. \\ & + \alpha_{ij}^{(1)} T_{jk} \alpha_{kl}^{(2)} T_{lm} \alpha_{mn}^{(1)} T_{np} \alpha_{pw}^{(2)} \Theta_{0wi}^{(2)} \\ & + \alpha_{ij}^{(1)} T_{jk} \alpha_{kl}^{(2)} T_{lm} \alpha_{mn}^{(1)} T_{np} \alpha_{pq}^{(2)} T_{qr} \alpha_{rw}^{(1)} \Theta_{0wi}^{(2)} \\ & \left. + \alpha_{ij}^{(1)} T_{jk} \alpha_{kl}^{(2)} T_{lm} \alpha_{mn}^{(1)} T_{np} \alpha_{pq}^{(2)} T_{qr} \alpha_{rs}^{(1)} T_{st} \alpha_{tw}^{(2)} \Theta_{0wi}^{(2)} + \dots \right]. \end{aligned} \quad (2.103)$$

The terms contributing to the integral for  $B_Q$  in equation (2.60) can be expressed



in condensed notation as

$$\begin{aligned}
& \left\{ \frac{1}{2} \left( \frac{\partial \overline{\pi^{(12)}}}{\partial E_{xx}} \right)_{E_x=E_{xx}=0} - \left( \frac{\partial \overline{\pi}}{\partial E_{xx}} \right)_{E_x=E_{xx}=0} \right\} \\
& = \Theta_1 \alpha_1 + \Theta_1 \alpha_2 + \Theta_1 \alpha_3 + \Theta_1 \alpha_4 + \Theta_1 \alpha_5 + \Theta_1 \alpha_6 + \cdots \\
& \quad + B_1 \alpha_1 + B_1 \alpha_2 + B_1 \alpha_3 + \cdots .
\end{aligned} \tag{2.104}$$

The explicit expressions for  $\Theta_1 \alpha_1$ ,  $\Theta_1 \alpha_2$ ,  $\cdots$  are

$$\Theta_1 \alpha_1 = \frac{2}{15kT} \left\{ \alpha_{iw}^{(1)} \Theta_{0wi}^{(2)} \right\}, \tag{2.105}$$

$$\Theta_1 \alpha_2 = \frac{2}{15kT} \left\{ \alpha_{ij}^{(1)} T_{jk} \alpha_{kw}^{(2)} \Theta_{0wi}^{(1)} + \alpha_{ij}^{(1)} T_{jk} \alpha_{kw}^{(2)} \Theta_{0wi}^{(2)} \right\}, \tag{2.106}$$

$$\begin{aligned}
\Theta_1 \alpha_3 = \frac{2}{15kT} & \left\{ \alpha_{ij}^{(1)} T_{jk} \alpha_{kl}^{(2)} T_{lm} \alpha_{mw}^{(1)} \Theta_{0wi}^{(1)} \right. \\
& \left. + \alpha_{ij}^{(1)} T_{jk} \alpha_{kl}^{(2)} T_{lm} \alpha_{mw}^{(1)} \Theta_{0wi}^{(2)} \right\},
\end{aligned} \tag{2.107}$$

$$\begin{aligned}
\Theta_1 \alpha_4 = \frac{2}{15kT} & \left\{ \alpha_{ij}^{(1)} T_{jk} \alpha_{kl}^{(2)} T_{lm} \alpha_{mn}^{(1)} T_{np} \alpha_{pw}^{(2)} \Theta_{0wi}^{(1)} \right. \\
& \left. + \alpha_{ij}^{(1)} T_{jk} \alpha_{kl}^{(2)} T_{lm} \alpha_{mn}^{(1)} T_{np} \alpha_{pw}^{(2)} \Theta_{0wi}^{(2)} \right\},
\end{aligned} \tag{2.108}$$

$$\Theta_1\alpha_5 = \frac{2}{15kT} \left\{ \alpha_{ij}^{(1)} T_{jk} \alpha_{kl}^{(2)} T_{lm} \alpha_{mn}^{(1)} T_{np} \alpha_{pq}^{(2)} T_{qr} \alpha_{rw}^{(1)} \Theta_{0wi}^{(1)} \right. \\ \left. + \alpha_{ij}^{(1)} T_{jk} \alpha_{kl}^{(2)} T_{lm} \alpha_{mn}^{(1)} T_{np} \alpha_{pq}^{(2)} T_{qr} \alpha_{rw}^{(1)} \Theta_{0wi}^{(2)} \right\}, \quad (2.109)$$

$$\Theta_1\alpha_6 = \frac{2}{15kT} \left\{ \alpha_{ij}^{(1)} T_{jk} \alpha_{kl}^{(2)} T_{lm} \alpha_{mn}^{(1)} T_{np} \alpha_{pq}^{(2)} T_{qr} \alpha_{rs}^{(1)} T_{st} \alpha_{tw}^{(2)} \Theta_{0wi}^{(1)} \right. \\ \left. + \alpha_{ij}^{(1)} T_{jk} \alpha_{kl}^{(2)} T_{lm} \alpha_{mn}^{(1)} T_{np} \alpha_{pq}^{(2)} T_{qr} \alpha_{rs}^{(1)} T_{st} \alpha_{tw}^{(2)} \Theta_{0wi}^{(2)} \right\}. \quad (2.110)$$

The lowest-symmetry molecule treated in this project is  $C_2H_4$ , which is of  $D_{2h}$  symmetry. For this point group, the dynamic polarizability tensor  $\alpha_{ij}^{(1)}$  has three independent components [1], namely

$$\alpha_{ij}^{(1)} = \alpha_{i'j'}^{(2)} = \begin{bmatrix} \alpha_{11} & 0 & 0 \\ 0 & \alpha_{22} & 0 \\ 0 & 0 & \alpha_{33} \end{bmatrix}. \quad (2.111)$$

$\alpha_{ij}^{(2)}$  is the dynamic polarizability tensor of molecule 2 expressed in the molecule-fixed axes of molecule 1, which is provided by

$$\alpha_{ij}^{(2)} = a_\alpha^i a_\beta^j a_{i'}^\alpha a_{j'}^\beta \alpha_{i'j'}^{(2)}. \quad (2.112)$$

For molecules of  $D_{2h}$  symmetry, the traceless quadrupole moment has two independent components [1], and is given by

$$\Theta_{0ij}^{(1)} = \Theta_{0i'j'}^{(2)} = \begin{bmatrix} \Theta_1 & 0 & 0 \\ 0 & \Theta_2 & 0 \\ 0 & 0 & -\Theta_1 - \Theta_2 \end{bmatrix}. \quad (2.113)$$

Similarly,

$$\Theta_{0ij}^{(2)} = a_{\alpha}^i a_{\beta}^j a_{i'}^{\alpha} a_{j'}^{\beta} \Theta_{0i'j'}^{(2)} . \quad (2.114)$$

For axially-symmetric molecules, the polarizability tensor has two independent components ( $\alpha_{11} = \alpha_{22}$  in equation (2.111)), while the quadrupole moment tensor has only one independent component ( $\Theta_1 = \Theta_2$  in equation (2.113)). The second-rank  $T$ -tensor in space-fixed axes is [1]

$$T_{\alpha\beta} = \frac{1}{4\pi\epsilon_0} \nabla_{\alpha} \nabla_{\beta} R^{-1} = \frac{1}{4\pi\epsilon_0} (3R_{\alpha}R_{\beta} - R^2\delta_{\alpha\beta}) R^{-5} . \quad (2.115)$$

In the molecule-fixed axes of molecule 1,  $T_{ij} = a_{\alpha}^i a_{\beta}^j T_{\alpha\beta}$ .

The tensor manipulation facilities of the Macsyma algebraic manipulation package are indispensable in evaluating the expressions for the terms in equations (2.105) to (2.110), particularly as the expressions increase in complexity. Since these expressions become extremely large, often taking several pages to express, they are not explicitly reproduced here. These expressions are integrated (*i.e.* averaged) over the pair-interaction coordinates using equation (2.60), thereby establishing the contribution of each of the  $\Theta_1\alpha_1$ ,  $\Theta_1\alpha_2$ ,  $\dots$  terms to  $B_Q$ .

The integral in equation (2.60) requires an intermolecular potential  $U_{12}(\tau)$ . As previously [47, 48], use is made of the classical potential

$$U_{12}(\tau) = U_{LJ} + U_{\Theta,\Theta} + U_{\Theta, \text{ind } \mu} + U_{\text{shape}} \quad (2.116)$$

where  $U_{LJ}$  is the Lennard-Jones 6:12 potential,  $U_{\Theta,\Theta}$  is the electrostatic quadrupole-quadrupole interaction energy of the two molecules, and  $U_{\Theta, \text{ind } \mu}$  is the quadrupole-induced dipole interaction energy.  $U_{\text{shape}}$  accounts for the angular dependence of

short range repulsive forces for non-spherical molecules. Explicit expressions for each of these contributions to  $U_{12}(\tau)$  for molecules of  $D_{2h}$  symmetry and higher have already been provided [47, 48]. It should be noted that evaluation of the induction energy  $U_{\Theta, \text{ind } \mu}$  requires knowledge of the static molecular polarizability tensor  $\alpha_{ij}^{(0)}$ .

The integrals were evaluated by numerical integration using Gaussian quadrature, with the ranges of the orientation angles being divided into 16 intervals each, while the intermolecular separation  $R$  was given the range of 0.1 to 3.0 nm divided into 64 intervals. The technique of Gaussian quadrature has been used previously in evaluation of second light-scattering virial coefficients and second Kerr-effect virial coefficients, where the convergence of the integrals has been carefully tested to establish the necessary intervals for the angles and the range [47, 48]. Appendix A.1 provides an example Fortran program (for evaluation of the  $\Theta_1\alpha_3$  contribution to  $B_Q$ ). The programs were run in double precision on a personal computer with a dual-core processor using the Salford F90 compiler. Program run-times were typically of the order of 20 minutes each.

Chapter 3 presents the results for the computation of  $B_Q$  for the molecules  $\text{CO}_2$ ,  $\text{C}_2\text{H}_4$  and  $\text{C}_2\text{H}_6$ . These molecules were chosen since their static and dynamic molecular polarizabilities and molecular quadrupole moments have been well characterized in the literature, and the quadrupoles of  $\text{CO}_2$  and  $\text{C}_2\text{H}_4$  are relatively large, so that the contribution to  ${}_mQ$  arising from  $B_Q$  for these species could also be expected to be relatively large. For example, the quadrupole moment of  $\text{CO}_2$  is  $\Theta = -14.27 \times 10^{-40} \text{ C m}^2$  [27], while the  $\text{N}_2$  molecule has  $\Theta = -4.97 \times 10^{-40} \text{ C m}^2$  [26], and the  $\text{O}_2$  molecule  $\Theta = -1.03 \times 10^{-40} \text{ C m}^2$  [30]. The temperature-dependence of the second Kerr-effect virial coefficients  $B_K$  of these molecules have recently been calculated and found to be in good agreement with the available measured data [55], as

have the second light-scattering virial coefficients at room temperature [47, 49, 56].

# Chapter 3

## Results

### 3.1 Carbon Dioxide

The molecular data required to calculate  $B_Q$  for the axially-symmetric  $\text{CO}_2$  molecule are presented in Table 3.1. As for the other molecules considered in this chapter, optimized values for the Lennard-Jones force constants  $R_0$  and  $\varepsilon/k$  and the shape parameter  $D$  are obtained by fitting values of the second pressure virial coefficient  $B(T)$  calculated according to

$$B(T) = \frac{N_A}{2\Omega} \int_{\tau} \left[ 1 - e^{-U_{12}(\tau)/kT} \right] d\tau \quad (3.1)$$

to the experimental data [57] over a range of temperature.

For axially-symmetric molecules, the two independent polarizability tensor components can be extracted from knowledge of the mean polarizability  $\alpha = \frac{1}{3}\alpha_{ii} = (2\alpha_{\perp} + \alpha_{\parallel})$  and the polarizability anisotropy  $\Delta\alpha = (\alpha_{\parallel} - \alpha_{\perp})$ , where in equation (2.111),  $\alpha_{33} = \alpha_{\parallel}$  and  $\alpha_{11} = \alpha_{22} = \alpha_{\perp}$ . All optical-frequency polarizabilities in this chapter are quoted for the Helium-Neon laser wavelength of  $\lambda = 632.8$  nm. Tables 3.2 to 3.5 provide the relative magnitudes of the various contributions to  $B_Q$  calculated over the temperature span 250 K to 500 K.

Table 3.1: The molecular properties of CO<sub>2</sub> used in the calculation of  $B_Q$ .

Property	Value	Reference
$R_0$ (nm)	0.400	[58]
$\varepsilon/k$ (K)	190.0	[58]
$D_1$	0.250 <sup>a</sup>	[56]
$D_2$	0.000	
$10^{40}\Theta_{11}$ (C m <sup>2</sup> )	$7.13_5 \pm 0.17$	[27, 56]
$10^{40}\Theta_{22}$ (C m <sup>2</sup> )	$7.13_5 \pm 0.17$	
$10^{40}\Theta_{33}$ (C m <sup>2</sup> )	$-14.27 \pm 0.33$	
$10^{40}\alpha$ (C <sup>2</sup> m <sup>2</sup> J <sup>-1</sup> )	$2.93141 \pm 0.00021$	[59]
$10^{40}\Delta\alpha$ (C <sup>2</sup> m <sup>2</sup> J <sup>-1</sup> )	$2.356 \pm 0.003$	[56]
$10^{40}\alpha_{11}$ (C <sup>2</sup> m <sup>2</sup> J <sup>-1</sup> )	$2.1461 \pm 0.0012$	
$10^{40}\alpha_{22}$ (C <sup>2</sup> m <sup>2</sup> J <sup>-1</sup> )	$2.1461 \pm 0.0012$	
$10^{40}\alpha_{33}$ (C <sup>2</sup> m <sup>2</sup> J <sup>-1</sup> )	$4.5021 \pm 0.0012$	
$10^{40}\alpha^{(0)}$ (C <sup>2</sup> m <sup>2</sup> J <sup>-1</sup> )	$3.2402 \pm 0.0004$	[60, 61]
$10^{40}\Delta\alpha^{(0)}$ (C <sup>2</sup> m <sup>2</sup> J <sup>-1</sup> )	$2.530 \pm 0.009$	[56, 62]
$10^{40}\alpha_{11}^{(0)}$ (C <sup>2</sup> m <sup>2</sup> J <sup>-1</sup> )	$2.3969 \pm 0.0034$	
$10^{40}\alpha_{22}^{(0)}$ (C <sup>2</sup> m <sup>2</sup> J <sup>-1</sup> )	$2.3969 \pm 0.0034$	
$10^{40}\alpha_{33}^{(0)}$ (C <sup>2</sup> m <sup>2</sup> J <sup>-1</sup> )	$4.9269 \pm 0.0064$	

<sup>a</sup>Obtained by fitting to pressure virial coefficients reported in Ref. 57

Table 3.2: The relative magnitudes of the contributions to  $B_Q$  for  $\text{CO}_2$  at  $T = 250\text{K}$ 

Contributing Term	$10^{30} \times \text{value}$ ( $\text{C m}^8 \text{J}^{-1} \text{mol}^{-2}$ )	% contribution to $B_Q$
$\Theta_1 \alpha_1$	-1.55008	3311.43
$\Theta_1 \alpha_2$	2.12903	-4548.23
$\Theta_1 \alpha_3$	-0.62074	1326.08
$\Theta_1 \alpha_4$	-0.00326	6.96
$\Theta_1 \alpha_5$	-0.00172	3.67
$\Theta_1 \alpha_6$	-0.00004	0.09
$B_Q$	-0.04681	

Table 3.3: The relative magnitudes of the contributions to  $B_Q$  for  $\text{CO}_2$  at  $T = 300\text{K}$ 

Contributing Term	$10^{30} \times \text{value}$ ( $\text{C m}^8 \text{J}^{-1} \text{mol}^{-2}$ )	% contribution to $B_Q$
$\Theta_1 \alpha_1$	-0.93291	-726.11
$\Theta_1 \alpha_2$	1.54221	1200.34
$\Theta_1 \alpha_3$	-0.47679	-371.10
$\Theta_1 \alpha_4$	-0.00265	-2.06
$\Theta_1 \alpha_5$	-0.00135	-1.05
$\Theta_1 \alpha_6$	-0.00003	-0.02
$B_Q$	0.12848	



Table 3.4: The relative magnitudes of the contributions to  $B_Q$  for  $\text{CO}_2$  at  $T = 400\text{K}$ 

Contributing Term	$10^{30} \times \text{value}$ ( $\text{C m}^8 \text{J}^{-1} \text{mol}^{-2}$ )	% contribution to $B_Q$
$\Theta_1 \alpha_1$	-0.45183	-258.54
$\Theta_1 \alpha_2$	0.95879	548.63
$\Theta_1 \alpha_3$	-0.32911	-188.32
$\Theta_1 \alpha_4$	-0.00209	-1.20
$\Theta_1 \alpha_5$	-0.00098	-0.56
$\Theta_1 \alpha_6$	-0.00002	-0.01
$B_Q$	0.17476	

Table 3.5: The relative magnitudes of the contributions to  $B_Q$  for  $\text{CO}_2$  at  $T = 500\text{K}$ 

Contributing Term	$10^{30} \times \text{value}$ ( $\text{C m}^8 \text{J}^{-1} \text{mol}^{-2}$ )	% contribution to $B_Q$
$\Theta_1 \alpha_1$	-0.26916	-178.32
$\Theta_1 \alpha_2$	0.67652	448.20
$\Theta_1 \alpha_3$	-0.25379	-168.14
$\Theta_1 \alpha_4$	-0.00182	-1.21
$\Theta_1 \alpha_5$	-0.00079	-0.52
$\Theta_1 \alpha_6$	-0.00002	-0.01
$B_Q$	0.15094	

Table 3.6: A summary of the calculated  $B_Q$  values for  $\text{CO}_2$ 

$T$ (K)	$10^{30} \times B_Q$ ( $\text{C m}^8 \text{J}^{-1} \text{mol}^{-2}$ )
250	-0.04681
300	0.12848
400	0.17476
500	0.15094

Table 3.6 summarizes the calculated  $B_Q$  temperature dependence. The usual range of experimental temperature for EFGIB measurements in the literature is 300 K to 500 K.  $\text{CO}_2$  displays an unusual trend in that  $B_Q$  reaches a maximum value around 400 K, and diminishes both for higher temperatures and lower temperatures. The reason for this unusual behaviour arises from the  $\Theta_1\alpha_1$  term, which makes a negative contribution to  $B_Q$ , and which rapidly becomes large in magnitude as the temperature diminishes. At 250 K,  $B_Q$  has become negative. Whether this behaviour accurately describes the dependence of  $B_Q$  on temperature, or whether it is an artifact of the limitations of the long-range model, particularly at lower temperatures, could be investigated by experimental measurement of  $B_Q$  over an appropriate range of temperature. Such experimental investigation would only be feasible provided  $B_Q$  is large enough to be discernible by an EFGIB apparatus, which would have its particular limiting resolution for the measured optical retardance  $\delta$  in equation (2.42). While the  $\Theta_1\alpha_2$  term is large and positive, the combined contribution to  $B_Q$  arising from the negative  $\Theta_1\alpha_1$  and  $\Theta_1\alpha_3$  terms is comparatively nearly as large in magnitude (indeed, for 250 K it is a little larger), so that no contribution substantially dominates the overall  $B_Q$ , these large contributions of opposite sign tending to cancel, yielding a relatively small net  $B_Q$ . The  $\Theta_1\alpha_4$  and higher-order terms rapidly

diminish as the series converges, contributing around 3% or less to  $B_Q$  for  $\text{CO}_2$ .

At 300 K,  $\text{CO}_2$  has a measured  ${}_mQ = (-25.33 \pm 0.37) \times 10^{-26} \text{ C m}^5 \text{ J}^{-1} \text{ mol}^{-1}$  [27], which was obtained for an experimental pressure of  $P = 2.635 \text{ MPa}$  at a temperature of  $T = 299.4 \text{ K}$ . Recalling equation (2.54), namely

$${}_mQ = A_Q + \frac{B_Q}{V_m} + \frac{C_Q}{V_m^2} + \dots, \quad (3.2)$$

it is now possible to calculate the  $B_Q/V_m$  pair-interaction contribution to  ${}_mQ$ . The molar volume is obtained by solving the equation

$$V_m = \frac{RT}{P} \left( 1 + \frac{B(T)}{V_m} + \frac{C(T)}{V_m^2} \right), \quad (3.3)$$

using the appropriate second and third pressure virial coefficients from the tabulations of Dymond *et al.* [57]. For the experimental  $P = 2.635 \text{ MPa}$  and  $T = 299.4 \text{ K}$ , this yields  $V_m = 8.087 \times 10^{-4} \text{ m}^3 \text{ mol}^{-1}$ , which coupled with the calculated  $B_Q = 0.12848 \times 10^{-30} \text{ C m}^8 \text{ J}^{-1} \text{ mol}^{-2}$  yields  $B_Q/V_m = 0.016 \times 10^{-26} \text{ C m}^5 \text{ J}^{-1} \text{ mol}^{-1}$ . This is a contribution of only 0.063% to  ${}_mQ$ , and since  ${}_mQ$  has a reported experimental uncertainty of 1.5%, this  $B_Q/V_m$  value is around two orders of magnitude too small to be measurable. While it is possible to measure  ${}_mQ$  with greater precision by averaging a large number of measurements, this route is somewhat impractical since each measurement takes several hours to perform.

$\text{CO}_2$  has a critical temperature and pressure of  $T_c = 304.1 \text{ K}$  and  $P_c = 7.4 \text{ MPa}$ , respectively. For temperatures and pressures exceeding  $T_c$  and  $P_c$ , the  $\text{CO}_2$  becomes a supercritical fluid, the phase behaviour of which becomes ambiguous, being neither a well-defined gas nor liquid. Under these conditions, the virial equation of state can become unreliable in calculating the the molar volume, and experimentally measured isotherms of the compressibility factor  $Z = PV_m/RT$  are used to obtain

reliable values for  $V_m$ , such as the CO<sub>2</sub> data of Holste *et al.* [63], Duschek *et al.* [64], Mantilla *et al.* [65] and Gomez-Osorio *et al.* [66]. Depending on the temperature and pressure, the supercritical fluid can tend to behave more like a gas or more like a liquid.

The relative contribution made to  ${}_mQ$  by interacting pairs of molecules in CO<sub>2</sub> is now assessed over the temperature range 250 to 500 K and the pressure range 1.7 to 10 MPa. Typical EFGIB measurements in the literature have been performed for pressures up to 4 MPa in the temperature range 300 to 500 K, though pressures up to 10 MPa should be accessible to our existing EFGIB apparatus, while temperatures down to 250 K could be achieved with suitable experimental modifications. Table 3.7 contains the CO<sub>2</sub> inverse molar volumes (or densities)  $V_m^{-1}$  for the temperatures 250 K, 300 K, 400 K and 500 K at the pressures 1.7 MPa, 4 MPa and 10 MPa. These  $V_m^{-1}$  data, combined with the  $B_Q$  data in Table 3.6, yield the calculated  $B_Q/V_m$  estimates listed in Table 3.8. For comparative purposes, Table 3.8 also contains the  ${}_mQ$  values interpolated from the EFGIB measurements of Chetty and Couling [27], together with their expected uncertainties. The largest value for  $B_Q/V_m$  of  $0.062 \times 10^{-26} \text{ C m}^5 \text{ J}^{-1} \text{ mol}^{-1}$  (obtained at  $P = 10 \text{ MPa}$  and  $T = 400 \text{ K}$ ) is 0.32% of  ${}_mQ$ , which is almost an order of magnitude smaller than the experimental uncertainty limits and so is well below the presently available experimental limits of detection. Accumulating a large number of  ${}_mQ$  measurements at this temperature and pressure could reduce the experimental uncertainty by up to an order of magnitude, bringing  $B_Q$  contributions to the threshold of detectability. Unfortunately, at this temperature and pressure the supercritical CO<sub>2</sub> is probably behaving more like a liquid than a gas, so that triplet and higher-order interactions are probably making considerable contributions to  ${}_mQ$ , thereby severely complicating the picture.

At  $T = 400 \text{ K}$  and  $P = 100 \text{ MPa}$ ,  $V_m^{-1} = 21\,196 \text{ mol m}^{-3}$ , so that  $B_Q/V_m =$

Table 3.7: Densities (inverse molar volumes) for gaseous CO<sub>2</sub> at relevant temperatures and pressures

$T$ (K)	at $P = 1.7$ MPa, $V_m^{-1}$ (mol m <sup>-3</sup> )	at $P = 4$ MPa, $V_m^{-1}$ (mol m <sup>-3</sup> )	at $P = 10$ MPa, $V_m^{-1}$ (mol m <sup>-3</sup> )
250	995.6 <sup>a</sup>	– <sup>b</sup>	–
300	747.6	2095.8	–
400	527.2	1293.2	3563.2
500	413.8	987.4	2526.2

<sup>a</sup>At  $T = 250$  K,  $P = 1.7$  MPa is just under the saturation vapour pressure of 1.784 MPa

<sup>b</sup>The dash – indicates temperatures and pressures for which the CO<sub>2</sub> is in the liquid phase

Table 3.8: Calculated  $B_Q/V_m$  contributions to  ${}_mQ$  for CO<sub>2</sub> at the temperatures and pressures in Table 3.7

$T$ (K)	$10^{26} {}_mQ^a$ (C m <sup>5</sup> J <sup>-1</sup> mol <sup>-1</sup> )	at $P = 1.7$ MPa, $10^{26} B_Q/V_m$ (C m <sup>5</sup> J <sup>-1</sup> mol <sup>-1</sup> )	at $P = 4$ MPa, $10^{26} B_Q/V_m$ (C m <sup>5</sup> J <sup>-1</sup> mol <sup>-1</sup> )	at $P = 10$ MPa, $10^{26} B_Q/V_m$ (C m <sup>5</sup> J <sup>-1</sup> mol <sup>-1</sup> )
250	$-30.22 \pm 0.40$	-0.005	–	–
300	$-25.31 \pm 0.40$	0.010	0.027	–
400	$-19.18 \pm 0.40$	0.009	0.023	0.062
500	$-15.50 \pm 0.40$	0.006	0.015	0.038

<sup>a</sup>These  ${}_mQ$  values have been interpolated from the measured data in Ref. 27. The uncertainties are indicative of the experimental uncertainties in Ref. 27.

$0.37 \times 10^{-26}$  C m<sup>5</sup>J<sup>-1</sup>mol<sup>-1</sup>. While at first glance this indicates a  $B_Q$  which should in principle be measurable (provided a large number of measurements are averaged

so as to reduce the uncertainty), at such a high pressure the supercritical CO<sub>2</sub> is clearly behaving more like a liquid, which explains the relatively high fluid density, so that each CO<sub>2</sub> molecule will have several closely-neighbouring molecules.

Some general conclusions can be drawn from the foregoing analysis. Our molecular-tensor theory of  $B_Q$  indicates that the measured EFGIB data for CO<sub>2</sub> reported in the literature have been obtained at pressures and temperatures for which molecular pair-interaction contributions are negligible, being an order of magnitude or more below the present limits of detectability. This is reassuring, since experimentalists have up to now been uncertain as to whether their EFGIB measurements have been contaminated by  $B_Q$  contributions, especially for higher pressures. The theory of  $B_Q$  also suggests that it will be very difficult to achieve measurements of  $B_Q$  for CO<sub>2</sub> since the contribution to  ${}_mQ$  is below the threshold of detectability for the existing EFGIB apparatus for those temperatures and pressures where the CO<sub>2</sub> fluid behaves as a gas.

## 3.2 Ethene

The molecular data required in the calculations of  $B_Q$  for  $C_2H_4$  are presented in Table 3.9. Ethene is of  $D_{2h}$  symmetry, and as has been previously demonstrated, approximating the molecule to be of axial symmetry has led to poor agreement of calculated and measured second light-scattering virial coefficients  $B_\rho$  [67, 68] and second Kerr-effect virial coefficients  $B_K$  [69] of up to 40%. Taking the full symmetry of the molecule into account in the description of the molecular properties, which required extensive development of the molecular-tensor theories, brought the calculated  $B_\rho$  to within 3% of the measured value [47], and yielded good agreement between the measured and calculated  $B_K$  values over the full experimental temperature range of 202.4 K to 363.7 K [55].

Tables 3.10 to 3.13 provide the relative magnitudes of the contributing terms to  $B_Q$  calculated at intervals of temperature spanning 250 to 500 K, while Table 3.14 summarizes the calculated  $B_Q$  temperature dependence.  $C_2H_4$  has a critical temperature of  $T_c = 282.4$  K and a critical pressure of  $P_c = 5.06$  MPa. The molar volume of  $C_2H_4$  has been accurately determined as a function of temperature and pressure through experimentally measured isotherms of the compressibility factor  $Z$  [70, 71]. Table 3.15 contains the  $C_2H_4$  inverse molar volumes  $V_m^{-1}$  for the temperatures 250 K, 300 K, 400 K and 500 K at the pressures 2 MPa, 4 MPa and 10 MPa. These  $V_m^{-1}$  data, combined with the  $B_Q$  data in Table 3.14, yield the calculated  $B_Q/V_m$  estimates listed in Table 3.16. For comparative purposes, Table 3.16 also contains the  ${}_mQ$  values calculated via equation (2.46) using the measured room-temperature datum of  $\alpha_{ij}\Theta_{ij}^{(0)} = (15.59 \pm 0.08) \times 10^{-80} \text{ C}^3\text{m}^4\text{J}^{-1}$  obtained by Imrie [5], the electronic distortion term  $b$  in equation (2.46) having been assumed to be zero.

Table 3.9: The molecular properties of  $C_2H_4$  used in the calculation of  $B_Q$ .

Property	Value	Reference
$R_0(\text{nm})$	0.4232	[47, 72]
$\varepsilon/k(\text{K})$	190.0	[47, 72]
$D_1$	0.229650 <sup>a</sup>	[47]
$D_2$	0.213830 <sup>a</sup>	
$10^{40}\Theta_{11}(\text{C m}^2)$	$5.57 \pm 0.63$	[73]
$10^{40}\Theta_{22}(\text{C m}^2)$	$-10.54 \pm 0.63$	
$10^{40}\Theta_{33}(\text{C m}^2)$	$4.94 \pm 0.33$	
$10^{40}\alpha(\text{C}^2 \text{ m}^2 \text{ J}^{-1})$	$4.71 \pm 0.03$	[69]
$10^{40}\Delta\alpha(\text{C}^2 \text{ m}^2 \text{ J}^{-1})$	$1.92 \pm 0.04$	[69]
$10^{40}\alpha_{11}(\text{C}^2 \text{ m}^2 \text{ J}^{-1})$	$4.41 \pm 0.04$	[69]
$10^{40}\alpha_{22}(\text{C}^2 \text{ m}^2 \text{ J}^{-1})$	$3.79 \pm 0.03$	
$10^{40}\alpha_{33}(\text{C}^2 \text{ m}^2 \text{ J}^{-1})$	$5.94 \pm 0.02$	
$10^{40}\alpha^{(0)}(\text{C}^2 \text{ m}^2 \text{ J}^{-1})$	$4.73 \pm 0.03$	[69]
$10^{40}\Delta\alpha^{(0)}(\text{C}^2 \text{ m}^2 \text{ J}^{-1})$	$1.63 \pm 0.05$	[69]
$10^{40}\alpha_{11}^{(0)}(\text{C}^2 \text{ m}^2 \text{ J}^{-1})$	$4.30 \pm 0.04$	[69]
$10^{40}\alpha_{11}^{(0)}(\text{C}^2 \text{ m}^2 \text{ J}^{-1})$	$4.09 \pm 0.03$	
$10^{40}\alpha_{11}^{(0)}(\text{C}^2 \text{ m}^2 \text{ J}^{-1})$	$5.81 \pm 0.02$	

<sup>a</sup>Obtained by fitting to pressure virial coefficients reported in Ref. 57



Table 3.10: The relative magnitudes of the contributions to  $B_Q$  for  $C_2H_4$  at  $T = 250K$ 

Contributing Term	$10^{30} \times$ value ( $C\ m^8\ J^{-1}\ mol^{-2}$ )	% contribution to $B_Q$
$\Theta_1\alpha_1$	3.55966	-1381.16
$\Theta_1\alpha_2$	-4.38384	1700.94
$\Theta_1\alpha_3$	0.60739	-235.67
$\Theta_1\alpha_4$	-0.04288	16.64
$\Theta_1\alpha_5$	0.00289	-1.12
$\Theta_1\alpha_6$	-0.00095	0.37
$B_Q$	-0.25773	

Table 3.11: The relative magnitudes of the contributions to  $B_Q$  for  $C_2H_4$  at  $T = 300K$ 

Contributing Term	$10^{30} \times$ value ( $C\ m^8\ J^{-1}\ mol^{-2}$ )	% contribution to $B_Q$
$\Theta_1\alpha_1$	1.56875	-674.24
$\Theta_1\alpha_2$	-2.22151	954.79
$\Theta_1\alpha_3$	0.43171	-185.54
$\Theta_1\alpha_4$	-0.01347	5.79
$\Theta_1\alpha_5$	0.00214	-0.92
$\Theta_1\alpha_6$	-0.00029	0.12
$B_Q$	-0.23267	

Table 3.12: The relative magnitudes of the contributions to  $B_Q$  for  $C_2H_4$  at  $T = 400K$ 

Contributing Term	$10^{30} \times \text{value}$ ( $C\ m^8J^{-1}mol^{-2}$ )	% contribution to $B_Q$
$\Theta_1\alpha_1$	0.54615	-404.50
$\Theta_1\alpha_2$	-0.96629	715.66
$\Theta_1\alpha_3$	0.28485	-210.96
$\Theta_1\alpha_4$	-0.00119	0.88
$\Theta_1\alpha_5$	0.00149	-1.10
$\Theta_1\alpha_6$	-0.00003	0.02
$B_Q$	-0.13502	

Table 3.13: The relative magnitudes of the contributions to  $B_Q$  for  $C_2H_4$  at  $T = 500K$ 

Contributing Term	$10^{30} \times \text{value}$ ( $C\ m^8J^{-1}mol^{-2}$ )	% contribution to $B_Q$
$\Theta_1\alpha_1$	0.27513	-361.44
$\Theta_1\alpha_2$	-0.57028	749.19
$\Theta_1\alpha_3$	0.21662	-284.58
$\Theta_1\alpha_4$	0.00120	-1.58
$\Theta_1\alpha_5$	0.00119	-1.56
$\Theta_1\alpha_6$	0.00002	-0.03
$B_Q$	-0.07612	

Table 3.14: A summary of the calculated  $B_Q$  values for  $C_2H_4$ 

$T$ (K)	$10^{30} \times B_Q$ ( $C\ m^8\ J^{-1}\ mol^{-2}$ )
200	-0.25773
300	-0.23267
400	-0.13502
500	-0.07612

Table 3.15: Densities (inverse molar volumes) for gaseous  $C_2H_4$  at relevant temperatures and pressures

$T$ (K)	at $P = 2$ MPa, $V_m^{-1}$ ( $mol\ m^{-3}$ )	at $P = 4$ MPa, $V_m^{-1}$ ( $mol\ m^{-3}$ )	at $P = 10$ MPa, $V_m^{-1}$ ( $mol\ m^{-3}$ )
250	1268.8	— <sup>a</sup>	—
300	911.1	2187.2	11511.2 <sup>b</sup>
400	628.4	1315.3	3755.1
500	489.2	993.2	2565.7

<sup>a</sup>The dash — indicates temperatures and pressures for which the  $C_2H_4$  is in the liquid phase

<sup>b</sup>For this temperature and pressure, the supercritical phase closely resembles the liquid phase, having a high density

In Table 3.16, the second-largest value for  $B_Q/V_m$  of  $-0.051 \times 10^{-26}\ C\ m^5\ J^{-1}\ mol^{-1}$  (obtained at  $P = 10$  MPa and  $T = 400$  K, as well as at  $P = 4$  MPa and  $T = 300$  K) is of the same order as the experimental uncertainty limits, and if a large number of  ${}_mQ$  measurements were accumulated and averaged so as to reduce the statisti-

Table 3.16: Calculated  $B_Q/V_m$  contributions to  ${}_mQ$  for  $C_2H_4$  at the temperatures and pressures in Table 3.15

$T$ (K)	$10^{26} {}_mQ^a$ ( $C m^5 J^{-1} mol^{-1}$ )	at $P = 2$ MPa, $10^{26} B_Q/V_m$ ( $C m^5 J^{-1} mol^{-1}$ )	at $P = 4$ MPa, $10^{26} B_Q/V_m$ ( $C m^5 J^{-1} mol^{-1}$ )	at $P = 10$ MPa, $10^{26} B_Q/V_m$ ( $C m^5 J^{-1} mol^{-1}$ )
250	$13.65 \pm 0.07$	-0.032	—	—
300	$11.38 \pm 0.06$	-0.021	-0.051	-0.27
400	$8.53 \pm 0.05$	-0.009	-0.018	-0.051
500	$6.83 \pm 0.04$	-0.007	-0.013	-0.035

<sup>a</sup>These  ${}_mQ$  values have been calculated from equation (2.46) using the measured room-temperature datum of  $\alpha_{ij}\Theta_{ij}^{(0)} = (15.59 \pm 0.08) \times 10^{-80} C^3 m^4 J^{-1}$  in Ref. 5, and assuming  $b = 0$

cal uncertainty, it would become possible in principle to resolve a measured value for  $B_Q$ . The largest value of  $B_Q/V_m = -0.27 \times 10^{-26} C m^5 J^{-1} mol^{-1}$  is obtained at  $P = 10$  MPa and  $T = 300$  K, where the supercritical phase is behaving much more like a liquid, higher-order molecular interactions having become significant, explaining the relatively high fluid density.

As was found in the case of the  $CO_2$  molecule, our molecular-tensor theory of  $B_Q$  indicates that the EFGIB data for  $C_2H_4$  measured by Imrie [5] at ambient temperature in the range  $T = 294.8$  to  $298.4$  K, and for pressures in the range  $P = 2.284$  MPa to  $4.095$  MPa, have been obtained at a temperature and pressures for which molecular pair-interaction contributions are negligible, being at or below the threshold of the present limits of detectability. This result clarifies that Imrie's EFGIB measurements have not been contaminated by  $B_Q$  contributions, especially for the higher experimental pressures around 4 MPa. The theory of  $B_Q$  also suggests that it will in

principle be possible to measure  $B_Q$  for  $C_2H_4$  provided a large number of measurements are accumulated and averaged to reduce the statistical uncertainty in  ${}_mQ$ .

### 3.3 Ethane

Table 3.17 contains the molecular data required in the calculation of  $B_Q$  for the axially-symmetric  $C_2H_6$  molecule. Both the quadrupole moment and the polarizability anisotropy of  $C_2H_6$  are several times smaller than those of either  $CO_2$  or  $C_2H_4$ , which might intuitively suggest that  $B_Q$  for  $C_2H_6$  should be relatively small. Tables 3.18 to 3.21 provide the relative magnitudes of the contributing terms to  $B_Q$  calculated at intervals of temperature spanning 250 to 500 K, while Table 3.22 summarizes the calculated  $B_Q$  temperature dependence. What emerges is a  $B_Q$  that is in fact *larger* in magnitude than those for  $CO_2$  and  $C_2H_4$ . The reason for this is the small and negative  $\Theta_1\alpha_1$  and  $\Theta_1\alpha_3$  term contributions, which do little to attenuate the relatively large and positive  $\Theta_1\alpha_2$  term, this collision-induced contribution making by far the dominant contribution to  $B_Q$ .

The  $C_2H_6$  fluid has a critical temperature of  $T_c = 305.3$  K, and a critical pressure of  $P_c = 4.87$  MPa. The molar volume of  $C_2H_6$  has been accurately determined as a function of temperature and pressure through experimentally measured isotherms of the compressibility factor  $Z$  [70, 74]. Table 3.23 contains the  $C_2H_6$  inverse molar volumes  $V_m^{-1}$  for the temperatures 250 K, 300 K, 400 K and 500 K at the pressures 1 MPa, 4 MPa and 10 MPa. These  $V_m^{-1}$  data, combined with the  $B_Q$  data in Table 3.22, yield the calculated  $B_Q/V_m$  estimates listed in Table 3.24. For comparative purposes, Table 3.24 also contains the  ${}_mQ$  values interpolated from the measured data of Watson [45].

Table 3.17: The molecular properties of  $C_2H_6$  used in the calculation of  $B_Q$ .

Property	Value	Reference
$R_0(\text{nm})$	0.4418	[58]
$\varepsilon/k(\text{K})$	230.0	[58]
$D_1$	0.200 <sup>a</sup>	
$D_2$	0.000	
$10^{40}\Theta_{11}(\text{C m}^2)$	$1.25 \pm 0.13$	[45, 75]
$10^{40}\Theta_{22}(\text{C m}^2)$	$1.25 \pm 0.13$	
$10^{40}\Theta_{33}(\text{C m}^2)$	$-2.50 \pm 0.26$	
$10^{40}\alpha(\text{C}^2 \text{ m}^2 \text{ J}^{-1})$	$4.96798 \pm 0.00035$	[59, 76]
$10^{40}\Delta\alpha(\text{C}^2 \text{ m}^2 \text{ J}^{-1})$	$0.698 \pm 0.056$	[75]
$10^{40}\alpha_{11}(\text{C}^2 \text{ m}^2 \text{ J}^{-1})$	$4.735 \pm 0.019$	
$10^{40}\alpha_{22}(\text{C}^2 \text{ m}^2 \text{ J}^{-1})$	$4.735 \pm 0.019$	
$10^{40}\alpha_{33}(\text{C}^2 \text{ m}^2 \text{ J}^{-1})$	$5.433 \pm 0.038$	
$10^{40}\alpha^{(0)}(\text{C}^2 \text{ m}^2 \text{ J}^{-1})$	$4.9216 \pm 0.0033$	[60, 61]
$10^{40}\Delta\alpha^{(0)}(\text{C}^2 \text{ m}^2 \text{ J}^{-1})$	$0.60_5 \pm 0.10$	[75]
$10^{40}\alpha_{11}^{(0)}(\text{C}^2 \text{ m}^2 \text{ J}^{-1})$	$4.72 \pm 0.04$	
$10^{40}\alpha_{11}^{(0)}(\text{C}^2 \text{ m}^2 \text{ J}^{-1})$	$4.72 \pm 0.04$	
$10^{40}\alpha_{11}^{(0)}(\text{C}^2 \text{ m}^2 \text{ J}^{-1})$	$5.32 \pm 0.07$	

<sup>a</sup>Obtained by fitting to pressure virial coefficients reported in Ref. 57

Table 3.18: The relative magnitudes of the contributions to  $B_Q$  for  $C_2H_6$  at  $T = 250K$ 

Contributing Term	$10^{30} \times$ value ( $C\ m^8\ J^{-1}\ mol^{-2}$ )	% contribution to $B_Q$
$\Theta_1\alpha_1$	-0.10203	-7.68
$\Theta_1\alpha_2$	1.43597	108.22
$\Theta_1\alpha_3$	-0.01421	-1.07
$\Theta_1\alpha_4$	0.00674	0.51
$\Theta_1\alpha_5$	0.00033	0.02
$\Theta_1\alpha_6$	0.00006	0.00
$B_Q$	1.32686	

Table 3.19: The relative magnitudes of the contributions to  $B_Q$  for  $C_2H_6$  at  $T = 300K$ 

Contributing Term	$10^{30} \times$ value ( $C\ m^8\ J^{-1}\ mol^{-2}$ )	% contribution to $B_Q$
$\Theta_1\alpha_1$	-0.06119	-7.07
$\Theta_1\alpha_2$	0.93717	108.36
$\Theta_1\alpha_3$	-0.01595	-1.84
$\Theta_1\alpha_4$	0.00448	0.52
$\Theta_1\alpha_5$	0.00022	0.03
$\Theta_1\alpha_6$	0.00004	0.00
$B_Q$	0.86477	

Table 3.20: The relative magnitudes of the contributions to  $B_Q$  for  $C_2H_6$  at  $T = 400K$ 

Contributing Term	$10^{30} \times$ value ( $C m^8 J^{-1} mol^{-2}$ )	% contribution to $B_Q$
$\Theta_1\alpha_1$	-0.02936	-6.27
$\Theta_1\alpha_2$	0.50984	108.92
$\Theta_1\alpha_3$	-0.01499	-3.20
$\Theta_1\alpha_4$	0.00250	0.53
$\Theta_1\alpha_5$	0.00011	0.02
$\Theta_1\alpha_6$	0.00002	0.00
$B_Q$	0.46812	

Table 3.21: The relative magnitudes of the contributions to  $B_Q$  for  $C_2H_6$  at  $T = 500K$ 

Contributing Term	$10^{30} \times$ value ( $C m^8 J^{-1} mol^{-2}$ )	% contribution to $B_Q$
$\Theta_1\alpha_1$	-0.01727	-5.71
$\Theta_1\alpha_2$	0.3314	109.53
$\Theta_1\alpha_3$	-0.01330	-4.40
$\Theta_1\alpha_4$	0.00165	0.55
$\Theta_1\alpha_5$	0.00007	0.02
$\Theta_1\alpha_6$	0.00002	0.01
$B_Q$	0.30257	



Table 3.22: A summary of the calculated  $B_Q$  values for  $C_2H_6$ 

$T$ (K)	$10^{30} \times B_Q$ ( $C\ m^8\ J^{-1}\ mol^{-2}$ )
250	1.32686
300	0.86477
400	0.46812
500	0.30257

Table 3.23: Densities (inverse molar volumes) for gaseous  $C_2H_6$  at relevant temperatures and pressures

$T$ (K)	at $P = 1$ MPa, $V_m^{-1}$ ( $mol\ m^{-3}$ )	at $P = 4$ MPa, $V_m^{-1}$ ( $mol\ m^{-3}$ )	at $P = 10$ MPa, $V_m^{-1}$ ( $mol\ m^{-3}$ )
250	563.6	— <sup>a</sup>	—
300	434.6	2819.2 <sup>b</sup>	—
400	309.7	1364.2	4197.5 <sup>b</sup>
500	243.5	1009.9	2679.3

<sup>a</sup>The dash — indicates temperatures and pressures for which the  $C_2H_6$  is in the liquid phase

<sup>b</sup>For these temperatures and pressures, the supercritical phase closely resembles the liquid phase, having a high density

As seen in Table 3.24, the largest and second-largest values for  $B_Q/V_m$  of  $0.24 \times 10^{-26}\ C\ m^5\ J^{-1}\ mol^{-1}$  (obtained at  $P = 4$  MPa and  $T = 300$  K) and of  $0.20 \times 10^{-26}\ C\ m^5\ J^{-1}\ mol^{-1}$  (obtained at  $P = 10$  MPa and  $T = 400$  K), are under conditions of pressure and temperature where the supercritical phase is behaving much

Table 3.24: Calculated  $B_Q/V_m$  contributions to  ${}_mQ$  for  $C_2H_6$  at the temperatures and pressures in Table 3.23

$T$ (K)	$10^{26} {}_mQ^a$ ( $C m^5 J^{-1} mol^{-1}$ )	at $P = 1$ MPa, $10^{26} B_Q/V_m$ ( $C m^5 J^{-1} mol^{-1}$ )	at $P = 4$ MPa, $10^{26} B_Q/V_m$ ( $C m^5 J^{-1} mol^{-1}$ )	at $P = 10$ MPa, $10^{26} B_Q/V_m$ ( $C m^5 J^{-1} mol^{-1}$ )
250	$-2.26 \pm 0.09$	0.075	—	—
300	$-2.01 \pm 0.09$	0.038	0.24	—
400	$-1.69 \pm 0.08$	0.015	0.064	0.20
500	$-1.50 \pm 0.08$	0.007	0.031	0.081

<sup>a</sup>These  ${}_mQ$  values have been interpolated from the measured data in Ref. 45. The uncertainties are indicative of the experimental uncertainties in Ref. 45.

more like a liquid, with higher-order molecular interactions having become significant, hence accounting for the relatively high fluid densities.

The next largest values are  $B_Q/V_m = 0.081 \times 10^{-26} C m^5 J^{-1} mol^{-1}$  (obtained at  $P = 10$  MPa and  $T = 500$  K) and  $B_Q/V_m = 0.075 \times 10^{-26} C m^5 J^{-1} mol^{-1}$  (obtained at  $P = 1$  MPa and  $T = 250$  K), and are at pressures and temperatures where the supercritical phase is behaving much more like a gas. Here, the  $B_Q$  contributions are, respectively, the same as and just smaller than the experimental uncertainties, suggesting that if a large number of  ${}_mQ$  measurements were to be undertaken, it would be possible to resolve measured values for  $B_Q$ .

What emerges from the analysis is that, as found for both  $CO_2$  and  $C_2H_4$ , the molecular-tensor theory of  $B_Q$  indicates that the measured EFGIB data for  $C_2H_6$  have been obtained at temperatures and pressures for which molecular pair interaction contributions are negligible, being at or below the threshold of the present limits of detectability. The theory of  $B_Q$  also suggests that it will in principle be

possible to measure  $B_Q$  for  $C_2H_6$  provided a large-enough number of measurements are accumulated.

### 3.4 Concluding Remarks

A molecular-tensor theory has been developed to account for collision-induced contributions to EFGIB arising from molecular pair-interactions in the gas phase. The second EFGIB virial coefficient  $B_Q$  has been calculated for a range of temperature and pressure for the molecules  $CO_2$ ,  $C_2H_4$  and  $C_2H_6$ . These molecules have been chosen since there exist precise experimental measurements of  ${}_mQ$ , and the molecular properties required in the computation of  $B_Q$  are precisely known. In addition, previously developed molecular-tensor theories of the second light-scattering virial coefficient  $B_\rho$  and the second Kerr-effect virial coefficient  $B_K$  have yielded calculated values for  $CO_2$ ,  $C_2H_4$  and  $C_2H_6$  which are in close agreement with the measured data.

The main conclusions to emerge from this project are firstly that the calculated  $B_Q$  values for  $CO_2$ ,  $C_2H_4$  and  $C_2H_6$  indicate that collision-induced contributions to  ${}_mQ$  are at or below the level of the experimental uncertainties, so that the measured  ${}_mQ$  values reported in the literature have not been compromised by the presence of pair-interaction effects. Hence, the extracted molecular quadrupole moments are sound. Secondly, if the precision of measured  ${}_mQ$  data can be increased by around an order of magnitude, it should begin to become possible to resolve  $B_Q$  contributions, particularly for higher gas densities, especially for  $C_2H_4$  and  $C_2H_6$ . The calculated  $B_Q$  data can serve to guide experimentalists in their quest to measure  $B_Q$ , since the necessary experimental conditions and required limits of resolution are now made clear.

A future refinement to the theory will be the inclusion of the interaction-induced contributions to  $B_Q$  arising from the electronic distortion tensors  $B_{ijkl}$ ,  $\mathcal{B}_{ijkl}$  and  $J'_{ijk}$ . While we have assumed that these contributions will be of the order of 10% or smaller, this needs to be definitively established. Mr Ntombela, in his PhD project, is presently investigating these contributions in the BLH formalism of the EFGIB theory.

# Appendix A

## A.1 Fortran Program to calculate the $\Theta_1\alpha_3$ contribution to $B_Q$ .

```
PROGRAM EFGIB_Q1A3

C PROGRAM TO CALCULATE TERM Q1A3 FOR CO2 USING GAUSSIAN INTEGRATION WITH
C 64 INTERVALS FOR THE RANGE, AND 10 INTERVALS FOR ALL ANGULAR VARIABLES
C (I.E. ALPHA1, BETA1, GAMMA1, ALPHA2, BETA2 AND GAMMA2).
C DOUBLE PRECISION IS USED THROUGHOUT.
C

C -----
C SYSTEM INITIALIZATION:
C -----

      IMPLICIT DOUBLE PRECISION (A-H,O-Z)
      COMMON COEF1,DCTC
      DIMENSION COEF2(64,2),COEF1(16,2),SEP(64),AL1(16),BE1(16),GA1(16)
+ ,AL2(16),BE2(16),GA2(16),DCTC(9,16,16,16),FI(16,16,16,16,16),D1(6
+ 4),E1(16,16,16,16,16),F1(16,16,16,16,16),SE3(64),SE4(64),SE5(64),
+ SE6(64),SE8(64),SE12(64),G1(16,16,16),DDP(16,16,16,16,16),DQP(16,
+ 16,16,16,16),DIDP(16,16,16,16,16)
      INTEGER X1,X2,X3,X4,X5,X6,X7

C
C MOLECULAR DATA FOR CO2 (632.8 nm):
C

      SS1=0.000000
      SS2=0.000000
      SS3=0.000000
      SS4=0.000000
      SS5=0.000000
      SS6=0.000000
      SS7=0.000000
```

```

DIP=0.000
A11=2.1461
A22=2.1461
A33=4.5021
ALDYN=(A11+A22+A33)/3
V11=2.3969
V22=2.3969
V33=4.9269
ALSTAT=(V11+V22+V33)/3
Q1=7.135
Q2=7.135
AMIN1=0.1000
AMAX1=3.0000

```

```

C
C READ THE GAUSSIAN COEFFICIENTS FROM THE DATAFILE GAUSS64.DAT:
C

```

```

      OPEN(UNIT=10,FILE='GAUSS64.DAT')
      DO 10 ICTR1=1,64
      DO 20 ICTR2=1,2
      READ(10,1010,END=11)COEF2(ICTR1,ICTR2)
1010      FORMAT(F18.15)
20      CONTINUE
10      CONTINUE
11      CLOSE(UNIT=10)

```

```

C
C CALCULATE THE INTEGRATION POINTS FOR THE RANGE:
C

```

```

      SEP1=(AMAX1-AMIN1)/2
      SEP2=(AMAX1+AMIN1)/2
      DO 30 INDX=1,64
      SEP(INDX)=SEP1*COEF2(INDX,1)+SEP2
30      CONTINUE

```

```

C
C READ THE GAUSSIAN COEFFICIENTS FROM THE DATAFILE GAUSS16.DAT:
C

```

```

      OPEN(UNIT=11,FILE='GAUSS16.DAT')
      DO 100 ICTR1=1,16
      DO 110 ICTR2=1,2
      READ(11,6000,END=12)COEF1(ICTR1,ICTR2)
6000      FORMAT(F18.15)
110      CONTINUE
100      CONTINUE
12      CLOSE(UNIT=11)

```

```

C

```

A.1. FORTRAN PROGRAM TO CALCULATE THE  $\Theta_1\alpha_3$  CONTRIBUTION TO  $B_Q.75$

C CALCULATE THE INTEGRATION POINTS FOR ALPHA1:

C

```
AMIN=0.0
AMAX=2.*3.14159265358979323846
```

```
AL11=(AMAX-AMIN)/2.
AL12=(AMAX+AMIN)/2.
DO 120 INDX=1,16
  AL1(INDX)=AL11*COEF1(INDX,1)+AL12
```

120 CONTINUE

C

C CALCULATE THE INTEGRATION POINTS FOR BETA1:

C

```
AMIN=0.0
AMAX=3.14159265358979323846
```

```
BE11=(AMAX-AMIN)/2.
BE12=(AMAX+AMIN)/2.
DO 121 INDX=1,16
  BE1(INDX)=BE11*COEF1(INDX,1)+BE12
```

121 CONTINUE

C

C CALCULATE THE INTEGRATION POINTS FOR GAMMA1:

C

```
AMIN=0.0
AMAX=2.*3.14159265358979323846
```

```
GA11=(AMAX-AMIN)/2.
GA12=(AMAX+AMIN)/2.
DO 122 INDX=1,16
  GA1(INDX)=GA11*COEF1(INDX,1)+GA12
```

122 CONTINUE

C

C CALCULATE THE INTEGRATION POINTS FOR ALPHA2:

C

```
AMIN=0.0
AMAX=2.*3.14159265358979323846
```

```
AL21=(AMAX-AMIN)/2.
AL22=(AMAX+AMIN)/2.
DO 123 INDX=1,16
  AL2(INDX)=AL21*COEF1(INDX,1)+AL22
```

123 CONTINUE

C

C CALCULATE THE INTEGRATION POINTS FOR BETA2:

```
C
  AMIN=0.0
  AMAX=3.14159265358979323846

  BE21=(AMAX-AMIN)/2.
  BE22=(AMAX+AMIN)/2.
  DO 124 INDX=1,16
    BE2(INDX)=BE21*COEF1(INDX,1)+BE22
124  CONTINUE

C
C CALCULATE THE INTEGRATION POINTS FOR GAMMA2:
C
  AMIN=0.0
  AMAX=2.*3.14159265358979323846

  GA21=(AMAX-AMIN)/2.
  GA22=(AMAX+AMIN)/2.
  DO 125 INDX=1,16
    GA2(INDX)=GA21*COEF1(INDX,1)+GA22
125  CONTINUE

C -----
C MAIN PROGRAM:
C -----

      OPEN(UNIT=4,FILE='BQ_q1a3_250K')

C
C INPUT MOLECULAR PARAMETERS FROM THE KEYBOARD:
C
C      WRITE(6,470)
C470  FORMAT(1X,'INPUT THE TEMPERATURE (IN KELVIN)')
C      READ(5,471)TEMP
C471  FORMAT(F10.5)
      TEMP=250.0
      TEMPK=TEMP*1.380622E-23

C      WRITE(6,472)
C472  FORMAT(1X,'INPUT R(0) (IN nm)')
C      READ(5,473)R
C473  FORMAT(F10.5)
      R=0.40

C      WRITE(6,474)
C474  FORMAT(1X,'E/K (IN K)')
C      READ(5,475)PARAM2
C475  FORMAT(F10.5)
```



A.1. FORTRAN PROGRAM TO CALCULATE THE  $\Theta_1\alpha_3$  CONTRIBUTION TO  $B_Q.77$

```
PARAM2=190.0

C      WRITE(6,476)
C476   FORMAT(1X,'SHAPE1 ')
C      READ(5,477)SHAPE1
C477   FORMAT(F10.5)
      SHAPE1=0.250

C      WRITE(6,478)
C478   FORMAT(1X,'SHAPE2 ')
C      READ(5,479)SHAPE2
C479   FORMAT(F10.5)
      SHAPE2=0.0

C
C CALCULATION OF THE LENNARD-JONES 6:12 POTENTIAL & STORAGE OF THE
C VALUES IN AN ARRAY:
C
      DO 61 X1=1,64

      D1(X1)=4.*PARAM2*1.380622E-23*((R/SEP(X1))**12-(R/SEP(X1))**6)
      SE12(X1)=SEP(X1)**12
      SE5(X1)=SEP(X1)**5
      SE8(X1)=SEP(X1)**8
      SE3(X1)=SEP(X1)**3
      SE4(X1)=SEP(X1)**4
      SE6(X1)=SEP(X1)**6

61     CONTINUE

C
C THE DIRECTION COSINE TENSOR COMPONENTS ARE STORED IN AN ARRAY:
C
      DO 66 X4=1,16
        DO 77 X3=1,16
          DO 88 X2=1,16

C
C DIRECTION COSINE TENSOR COMPONENTS:
C
      A1=COS(AL1(X2))*COS(BE1(X3))*COS(GA1(X4))-1.*SIN(AL1(X2))*SIN(GA1
+ (X4))
      A2=SIN(AL1(X2))*COS(BE1(X3))*COS(GA1(X4))+COS(AL1(X2))*SIN(GA1(X4
```

```

+ ))
A3=-1.*SIN(BE1(X3))*COS(GA1(X4))
A4=-1.*COS(AL1(X2))*COS(BE1(X3))*SIN(GA1(X4))-1.*SIN(AL1(X2))*COS
+ (GA1(X4))
A5=-1.*SIN(AL1(X2))*COS(BE1(X3))*SIN(GA1(X4))+COS(AL1(X2))*COS(GA
+ 1(X4))
A6=SIN(BE1(X3))*SIN(GA1(X4))
A7=COS(AL1(X2))*SIN(BE1(X3))
A8=SIN(AL1(X2))*SIN(BE1(X3))
A9=COS(BE1(X3))

DCTC(1,X2,X3,X4)=A1
DCTC(2,X2,X3,X4)=A2
DCTC(3,X2,X3,X4)=A3
DCTC(4,X2,X3,X4)=A4
DCTC(5,X2,X3,X4)=A5
DCTC(6,X2,X3,X4)=A6
DCTC(7,X2,X3,X4)=A7
DCTC(8,X2,X3,X4)=A8
DCTC(9,X2,X3,X4)=A9

88      CONTINUE
77      CONTINUE
66      CONTINUE

```

```

C
C THE MULTIPOLE INTERACTION ENERGIES ARE CALCULATED AND STORED
C IN ARRAYS:
C

```

```

      DO 939 X7=1,16
      WRITE(4,1000)X7
1000  FORMAT (1X, 'INDEX (IN RANGE 1 TO 16) IS CURRENTLY ',I2 )
      WRITE(6,1111)X7
1111  FORMAT (1X, 'Index (in range 1 to 16) is currently ',I2 )
      DO 40 X6=1,16

      DO 50 X5=1,16

```

```

C
C MOLECULE 2'S DIRECTION COSINE TENSOR COMPONENTS:
C

```

```

B1=DCTC(1,X5,X6,X7)
B2=DCTC(2,X5,X6,X7)
B3=DCTC(3,X5,X6,X7)
B4=DCTC(4,X5,X6,X7)
B5=DCTC(5,X5,X6,X7)

```

A.1. FORTRAN PROGRAM TO CALCULATE THE  $\Theta_1\alpha_3$  CONTRIBUTION TO  $B_Q$ .79

```
B6=DCTC(6,X5,X6,X7)
B7=DCTC(7,X5,X6,X7)
B8=DCTC(8,X5,X6,X7)
B9=DCTC(9,X5,X6,X7)
```

```
DO 60 X4=1,16
  DO 70 X3=1,16
    DO 80 X2=1,16
```

```
C
C MOLECULE 1'S DIRECTION COSINE TENSOR COMPONENTS:
C
```

```
A1=DCTC(1,X2,X3,X4)
A2=DCTC(2,X2,X3,X4)
A3=DCTC(3,X2,X3,X4)
A4=DCTC(4,X2,X3,X4)
A5=DCTC(5,X2,X3,X4)
A6=DCTC(6,X2,X3,X4)
A7=DCTC(7,X2,X3,X4)
A8=DCTC(8,X2,X3,X4)
A9=DCTC(9,X2,X3,X4)
```

```
C
C CALCULATION OF THE DIPOLE-DIPOLE POTENTIAL:
C
```

```
DDP(X2,X3,X4,X5,X6)=8.98758E-24*DIP**2*(-2*A9*B9+A6*B6+A3*B3)
```

```
C
C CALCULATION OF THE DIPOLE-QUADRUPOLE POTENTIAL:
C
```

```
DQP(X2,X3,X4,X5,X6)=8.98758E-25*DIP*(Q2*(-2*A9*B9**2+(2*A6*B6+2*A
+ 3*B3+2*A9**2-2*A8**2-A6**2+A5**2-A3**2+A2**2)*B9+2*A9*B8**2+(-2*A
+ 6*B5-2*A3*B2)*B8+A9*B6**2+(2*A5*A8-2*A6*A9)*B6-A9*B5**2+A9*B3**2+
+ (2*A2*A8-2*A3*A9)*B3-A9*B2**2)+Q1*(-2*A9*B9**2+(2*A6*B6+2*A3*B3+2
+ *A9**2-2*A7**2-A6**2+A4**2-A3**2+A1**2)*B9+2*A9*B7**2+(-2*A6*B4-2
+ *A3*B1)*B7+A9*B6**2+(2*A4*A7-2*A6*A9)*B6-A9*B4**2+A9*B3**2+(2*A1*
+ A7-2*A3*A9)*B3-A9*B1**2))
```

```
C
C CALCULATION OF THE DIPOLE-INDUCED DIPOLE POTENTIAL:
C
```

```
DIDP(X2,X3,X4,X5,X6)=-0.50*ALSTAT*8.07765E-27*DIP**2*(3*B9**2
+ +3*A9**2-2)
```

```
C
C CALCULATION OF THE QUADRUPOLE-QUADRUPOLE POTENTIAL:
```

C

$$\begin{aligned} \text{quad1} = & -16. * (a6*a9 - a5*a8) * (b6*b9 - b5*b8) - 16. * (a3*a9 - a2*a8) * (b3*b9 - b \\ & + 2*b8) + 4. * (2. * a9**2 - 2. * a8**2 - a6**2 + a5**2 - a3**2 + a2**2) * (b9 - b8) * (b9 + \\ & + b8) + (-4. * a9**2 + 4. * a8**2 + 3. * a6**2 - 3. * a5**2 + a3**2 - a2**2) * (b6**2 - b5** \\ & + *2) + 4. * (a3*a6 - a2*a5) * (b3*b6 - b2*b5) + (-4. * a9**2 + 4. * a8**2 + a6**2 - a5** \\ & + 2 + 3. * a3**2 - 3. * a2**2) * (b3**2 - b2**2) \end{aligned}$$

$$\begin{aligned} \text{quad2} = & -16. * (a6*a9 - a4*a7) * (b6*b9 - b4*b7) - 16. * (a3*a9 - a1*a7) * (b3*b9 - b \\ & + 1*b7) + 4. * (2. * a9**2 - 2. * a7**2 - a6**2 + a4**2 - a3**2 + a1**2) * (b9 - b7) * (b9 + \\ & + b7) + (-4. * a9**2 + 4. * a7**2 + 3. * a6**2 - 3. * a4**2 + a3**2 - a1**2) * (b6**2 - b4** \\ & + *2) + 4. * (a3*a6 - a1*a4) * (b3*b6 - b1*b4) + (-4. * a9**2 + 4. * a7**2 + a6**2 - a4** \\ & + 2 + 3. * a3**2 - 3. * a1**2) * (b3**2 - b1**2) \end{aligned}$$

$$\begin{aligned} \text{quad3} = & 4. * (4. * A9**2 - 2. * (A8**2 + A7**2 + A6**2 + A3**2) + A5**2 + A4**2 + A2**2 \\ & + A1**2) * B9**2 - 16. * (2. * A6*A9 - A5*A8 - A4*A7) * B6*B9 - 16 * (2. * A3*A9 - A2*A8 \\ & + -A1*A7) * B3*B9 - 4. * (2. * A9**2 - 2. * A7**2 - A6**2 + A4**2 - A3**2 + A1**2) * B8** \\ & + 2 + 16. * (A6*A9 - A4*A7) * B5*B8 + 16. * (A3*A9 - A1*A7) * B2*B8 - 4. * (2. * A9**2 - 2. \\ & + *A8**2 - A6**2 + A5**2 - A3**2 + A2**2) * B7**2 + 16. * (A6*A9 - A5*A8) * B4*B7 + 16. \\ & + * (A3*A9 - A2*A8) * B1*B7 + (-8. * A9**2 + 4. * (A8**2 + A7**2) + 6. * A6**2 - 3. * (A5* \\ & + *2 + A4**2) + 2 * A3**2 - A2**2 - A1**2) * B6**2 + 4. * (2. * A3*A6 - A2*A5 - A1*A4) * B3 \\ & + * B6 + (4. * A9**2 - 4. * A7**2 - 3. * A6**2 + 3. * A4**2 - A3**2 + A1**2) * B5**2 - 4. * (A \\ & + 3*A6 - A1*A4) * B2*B5 + (4. * A9**2 - 4. * A8**2 - 3. * A6**2 + 3. * A5**2 - A3**2 + A2** \\ & + 2) * B4**2 - 4. * (A3*A6 - A2*A5) * B1*B4 + (-8. * A9**2 + 4. * (A8**2 + A7**2) + 2. * A6 \\ & + **2 - A5**2 - A4**2 + 6. * A3**2 - 3. * (A2**2 + A1**2)) * B3**2 + (4. * A9**2 - 4. * A7* \\ & + *2 - A6**2 + A4**2 - 3. * A3**2 + 3. * A1**2) * B2**2 + (4. * A9**2 - 4. * A8**2 - A6**2 + \\ & + A5**2 - 3. * A3**2 + 3. * A2**2) * B1**2 \end{aligned}$$

$$\begin{aligned} E1(X2, X3, X4, X5, X6) = & 8.98758E-26 * (1./3.) * (Q2**2 * QUAD1 + Q1**2 * QUAD \\ & + 2 + Q1 * Q2 * QUAD3) \end{aligned}$$

C

C CALCULATION OF THE QUADRUPOLE-INDUCED DIPOLE POTENTIAL:

C

$$\begin{aligned} \text{QID1} = & Q2**2 * (4. * A9**4 + (-8. * A8**2 + 4. * A5**2 + 4. * A2**2) * A9**2 + (-8. * A5* \\ & + A6 - 8. * A2*A3) * A8*A9 + 4. * A8**4 + (4. * A6**2 + 4. * A3**2) * A8**2 + A6**4 + (-2. * \\ & + A5**2 + 2. * A3**2 - 2. * A2**2) * A6**2 + A5**4 + (2. * A2**2 - 2. * A3**2) * A5**2 + A3 \\ & + **4 - 2. * A2**2 * A3**2 + A2**4) + Q1**2 * (4. * A9**4 + (-8. * A7**2 + 4. * A4**2 + 4. * \\ & + A1**2) * A9**2 + (-8. * A4*A6 - 8. * A1*A3) * A7*A9 + 4. * A7**4 + (4. * A6**2 + 4. * A3* \\ & + *2) * A7**2 + A6**4 + (-2. * A4**2 + 2. * A3**2 - 2. * A1**2) * A6**2 + A4**4 + (2. * A1* \\ & + *2 - 2. * A3**2) * A4**2 + A3**4 - 2. * A1**2 * A3**2 + A1**4) + Q1*Q2 * (8. * A9**4 + (- \\ & + 8. * A8**2 - 8. * A7**2 + 4. * A5**2 + 4. * A4**2 + 4. * A2**2 + 4. * A1**2) * A9**2 + ((-8 \\ & + . * A5*A6 - 8. * A2*A3) * A8 + (-8. * A4*A6 - 8. * A1*A3) * A7) * A9 + (8. * A7**2 + 4. * A6* \\ & + *2 - 4. * A4**2 + 4. * A3**2 - 4. * A1**2) * A8**2 + (8. * A4*A5 + 8. * A1*A2) * A7*A8 + (4 \\ & + . * A6**2 - 4. * A5**2 + 4. * A3**2 - 4. * A2**2) * A7**2 + 2. * A6**4 + (-2. * A5**2 - 2. * \\ & + A4**2 + 4. * A3**2 - 2. * A2**2 - 2. * A1**2) * A6**2 + (2. * A4**2 - 2. * A3**2 + 2. * A1* \\ & + *2) * A5**2 + (2. * A2**2 - 2. * A3**2) * A4**2 + 2. * A3**4 + (-2. * A2**2 - 2. * A1**2) \\ & + * A3**2 + 2. * A1**2 * A2**2) \end{aligned}$$

A.1. FORTRAN PROGRAM TO CALCULATE THE  $\Theta_1\alpha_3$  CONTRIBUTION TO  $B_Q$ .81

```

QID2=Q2**2*(4.*B9**4+(-8.*B8**2+4.*B5**2+4.*B2**2)*B9**2+(-8.*B5*
+ B6-8.*B2*B3)*B8*B9+4.*B8**4+(4.*B6**2+4.*B3**2)*B8**2+B6**4+(-2.*
+ B5**2+2.*B3**2-2.*B2**2)*B6**2+B5**4+(2.*B2**2-2.*B3**2)*B5**2+B3
+ **4-2.*B2**2*B3**2+B2**4)+Q1**2*(4.*B9**4+(-8.*B7**2+4.*B4**2+4.*
+ B1**2)*B9**2+(-8.*B4*B6-8.*B1*B3)*B7*B9+4.*B7**4+(4.*B6**2+4.*B3*
+ *2)*B7**2+B6**4+(-2.*B4**2+2.*B3**2-2.*B1**2)*B6**2+B4**4+(2.*B1*
+ *2-2.*B3**2)*B4**2+B3**4-2.*B1**2*B3**2+B1**4)+Q1*Q2*(8.*B9**4+(-
+ 8.*B8**2-8.*B7**2+4.*B5**2+4.*B4**2+4.*B2**2+4.*B1**2)*B9**2+((-8
+ .*B5*B6-8.*B2*B3)*B8+(-8.*B4*B6-8.*B1*B3)*B7)*B9+(8.*B7**2+4.*B6*
+ *2-4.*B4**2+4.*B3**2-4.*B1**2)*B8**2+(8.*B4*B5+8.*B1*B2)*B7*B8+(4
+ .*B6**2-4.*B5**2+4.*B3**2-4.*B2**2)*B7**2+2.*B6**4+(-2.*B5**2-2.*
+ B4**2+4.*B3**2-2.*B2**2-2.*B1**2)*B6**2+(2.*B4**2-2.*B3**2+2.*B1*
+ *2)*B5**2+(2.*B2**2-2.*B3**2)*B4**2+2.*B3**4+(-2.*B2**2-2.*B1**2)
+ *B3**2+2.*B1**2*B2**2)

```

```

F1(X2,X3,X4,X5,X6)=-0.5*8.07765E-29*ALSTAT*(QID1+QID2)

```

C

C CALCULATION OF THE INTEGRATION ARGUMENT:

C

```

T11=2.*A7**2-A4**2-A1**2
T22=2.*A8**2-A5**2-A2**2
T33=2.*A9**2-A6**2-A3**2
T12=2.*A7*A8-A4*A5-A1*A2
T13=2.*A7*A9-A4*A6-A1*A3
T23=2.*A8*A9-A5*A6-A2*A3

```

```

T111=2*A7**3-3*A4**2*A7-3*A1**2*A7
T222=2*A8**3-3*A5**2*A8-3*A2**2*A8
T333=2*A9**3-3*A6**2*A9-3*A3**2*A9
T112=2*A7**2*A8-A4**2*A8-A1**2*A8-2*A4*A5*A7-2*A1*A2*A7
T122=2*A7*A8**2-2*A4*A5*A8-2*A1*A2*A8-A5**2*A7-A2**2*A7
T133=2*A7*A9**2-2*A4*A6*A9-2*A1*A3*A9-A6**2*A7-A3**2*A7
T233=2*A8*A9**2-2*A5*A6*A9-2*A2*A3*A9-A6**2*A8-A3**2*A8
T113=2*A7**2*A9-A4**2*A9-A1**2*A9-2*A4*A6*A7-2*A1*A3*A7
T223=2*A8**2*A9-A5**2*A9-A2**2*A9-2*A5*A6*A8-2*A2*A3*A8
T123=2*A7*A8*A9-A4*A5*A9-A1*A2*A9-A4*A6*A8-A1*A3*A8-A5*A6*A7-A2*A
+ 3*A7

```

```

Z11 = A33*(A7**2*B9**2+(2*A4*A7*B6+2*A1*A7*B3)*B9+A4**2*B6**2+2*A
+ 1*A4*B3*B6+A1**2*B3**2)+A22*(A7**2*B8**2+(2*A4*A7*B5+2*A1*A7*B2
+ )*B8+A4**2*B5**2+2*A1*A4*B2*B5+A1**2*B2**2)+A11*(A7**2*B7**2+(2
+ *A4*A7*B4+2*A1*A7*B1)*B7+A4**2*B4**2+2*A1*A4*B1*B4+A1**2*B1**2)

```

```

Z22 = A33*(A8**2*B9**2+(2*A5*A8*B6+2*A2*A8*B3)*B9+A5**2*B6**2+2*A

```

$$\begin{aligned}
& + 2*A5*B3*B6+A2**2*B3**2)+A22*(A8**2*B8**2+(2*A5*A8*B5+2*A2*A8*B2 \\
& + )*B8+A5**2*B5**2+2*A2*A5*B2*B5+A2**2*B2**2)+A11*(A8**2*B7**2+(2 \\
& + *A5*A8*B4+2*A2*A8*B1)*B7+A5**2*B4**2+2*A2*A5*B1*B4+A2**2*B1**2)
\end{aligned}$$

$$\begin{aligned}
Z33 = & A33*(A9**2*B9**2+(2*A6*A9*B6+2*A3*A9*B3)*B9+A6**2*B6**2+2*A \\
& + 3*A6*B3*B6+A3**2*B3**2)+A22*(A9**2*B8**2+(2*A6*A9*B5+2*A3*A9*B2 \\
& + )*B8+A6**2*B5**2+2*A3*A6*B2*B5+A3**2*B2**2)+A11*(A9**2*B7**2+(2 \\
& + *A6*A9*B4+2*A3*A9*B1)*B7+A6**2*B4**2+2*A3*A6*B1*B4+A3**2*B1**2)
\end{aligned}$$

$$\begin{aligned}
Z12 = & A33*(A7*A8*B9**2+((A4*A8+A5*A7)*B6+(A1*A8+A2*A7)*B3)*B9+A4* \\
& + A5*B6**2+(A1*A5+A2*A4)*B3*B6+A1*A2*B3**2)+A22*(A7*A8*B8**2+((A4 \\
& + *A8+A5*A7)*B5+(A1*A8+A2*A7)*B2)*B8+A4*A5*B5**2+(A1*A5+A2*A4)*B2 \\
& + *B5+A1*A2*B2**2)+A11*(A7*A8*B7**2+((A4*A8+A5*A7)*B4+(A1*A8+A2*A \\
& + 7)*B1)*B7+A4*A5*B4**2+(A1*A5+A2*A4)*B1*B4+A1*A2*B1**2)
\end{aligned}$$

$$\begin{aligned}
Z13 = & A33*(A7*A9*B9**2+((A4*A9+A6*A7)*B6+(A1*A9+A3*A7)*B3)*B9+A4* \\
& + A6*B6**2+(A1*A6+A3*A4)*B3*B6+A1*A3*B3**2)+A22*(A7*A9*B8**2+((A4 \\
& + *A9+A6*A7)*B5+(A1*A9+A3*A7)*B2)*B8+A4*A6*B5**2+(A1*A6+A3*A4)*B2 \\
& + *B5+A1*A3*B2**2)+A11*(A7*A9*B7**2+((A4*A9+A6*A7)*B4+(A1*A9+A3*A \\
& + 7)*B1)*B7+A4*A6*B4**2+(A1*A6+A3*A4)*B1*B4+A1*A3*B1**2)
\end{aligned}$$

$$\begin{aligned}
Z23 = & A33*(A8*A9*B9**2+((A5*A9+A6*A8)*B6+(A2*A9+A3*A8)*B3)*B9+A5* \\
& + A6*B6**2+(A2*A6+A3*A5)*B3*B6+A2*A3*B3**2)+A22*(A8*A9*B8**2+((A5 \\
& + *A9+A6*A8)*B5+(A2*A9+A3*A8)*B2)*B8+A5*A6*B5**2+(A2*A6+A3*A5)*B2 \\
& + *B5+A2*A3*B2**2)+A11*(A8*A9*B7**2+((A5*A9+A6*A8)*B4+(A2*A9+A3*A \\
& + 8)*B1)*B7+A5*A6*B4**2+(A2*A6+A3*A5)*B1*B4+A2*A3*B1**2)
\end{aligned}$$

$$\begin{aligned}
W11 = & V33*(A7**2*B9**2+(2*A4*A7*B6+2*A1*A7*B3)*B9+A4**2*B6**2+2*A \\
& + 1*A4*B3*B6+A1**2*B3**2)+V22*(A7**2*B8**2+(2*A4*A7*B5+2*A1*A7*B2 \\
& + )*B8+A4**2*B5**2+2*A1*A4*B2*B5+A1**2*B2**2)+V11*(A7**2*B7**2+(2 \\
& + *A4*A7*B4+2*A1*A7*B1)*B7+A4**2*B4**2+2*A1*A4*B1*B4+A1**2*B1**2)
\end{aligned}$$

$$\begin{aligned}
W22 = & V33*(A8**2*B9**2+(2*A5*A8*B6+2*A2*A8*B3)*B9+A5**2*B6**2+2*A \\
& + 2*A5*B3*B6+A2**2*B3**2)+V22*(A8**2*B8**2+(2*A5*A8*B5+2*A2*A8*B2 \\
& + )*B8+A5**2*B5**2+2*A2*A5*B2*B5+A2**2*B2**2)+V11*(A8**2*B7**2+(2 \\
& + *A5*A8*B4+2*A2*A8*B1)*B7+A5**2*B4**2+2*A2*A5*B1*B4+A2**2*B1**2)
\end{aligned}$$

$$\begin{aligned}
W33 = & V33*(A9**2*B9**2+(2*A6*A9*B6+2*A3*A9*B3)*B9+A6**2*B6**2+2*A \\
& + 3*A6*B3*B6+A3**2*B3**2)+V22*(A9**2*B8**2+(2*A6*A9*B5+2*A3*A9*B2 \\
& + )*B8+A6**2*B5**2+2*A3*A6*B2*B5+A3**2*B2**2)+V11*(A9**2*B7**2+(2 \\
& + *A6*A9*B4+2*A3*A9*B1)*B7+A6**2*B4**2+2*A3*A6*B1*B4+A3**2*B1**2)
\end{aligned}$$

$$\begin{aligned}
W12 = & V33*(A7*A8*B9**2+((A4*A8+A5*A7)*B6+(A1*A8+A2*A7)*B3)*B9+A4* \\
& + A5*B6**2+(A1*A5+A2*A4)*B3*B6+A1*A2*B3**2)+V22*(A7*A8*B8**2+((A4 \\
& + *A8+A5*A7)*B5+(A1*A8+A2*A7)*B2)*B8+A4*A5*B5**2+(A1*A5+A2*A4)*B2 \\
& + *B5+A1*A2*B2**2)+V11*(A7*A8*B7**2+((A4*A8+A5*A7)*B4+(A1*A8+A2*A \\
& + 7)*B1)*B7+A4*A5*B4**2+(A1*A5+A2*A4)*B1*B4+A1*A2*B1**2)
\end{aligned}$$

$$W13 = V33*(A7*A9*B9**2+((A4*A9+A6*A7)*B6+(A1*A9+A3*A7)*B3)*B9+A4*$$

A.1. FORTRAN PROGRAM TO CALCULATE THE  $\Theta_1\alpha_3$  CONTRIBUTION TO  $B_Q$ .83

```

+   A6*B6**2+(A1*A6+A3*A4)*B3*B6+A1*A3*B3**2)+V22*(A7*A9*B8**2+((A4
+   *A9+A6*A7)*B5+(A1*A9+A3*A7)*B2)*B8+A4*A6*B5**2+(A1*A6+A3*A4)*B2
+   *B5+A1*A3*B2**2)+V11*(A7*A9*B7**2+((A4*A9+A6*A7)*B4+(A1*A9+A3*A
+   7)*B1)*B7+A4*A6*B4**2+(A1*A6+A3*A4)*B1*B4+A1*A3*B1**2)

```

```

W23 = V33*(A8*A9*B9**2+((A5*A9+A6*A8)*B6+(A2*A9+A3*A8)*B3)*B9+A5*
+   A6*B6**2+(A2*A6+A3*A5)*B3*B6+A2*A3*B3**2)+V22*(A8*A9*B8**2+((A5
+   *A9+A6*A8)*B5+(A2*A9+A3*A8)*B2)*B8+A5*A6*B5**2+(A2*A6+A3*A5)*B2
+   *B5+A2*A3*B2**2)+V11*(A8*A9*B7**2+((A5*A9+A6*A8)*B4+(A2*A9+A3*A
+   8)*B1)*B7+A5*A6*B4**2+(A2*A6+A3*A5)*B1*B4+A2*A3*B1**2)

```

```

Q11 = A7**2*B8**2*Q2+2*A4*A7*B5*B8*Q2+2*A1*A7*B2*B8*Q2+A4**2*B5
1   **2*Q2+2*A1*A4*B2*B5*Q2+A1**2*B2**2*Q2+A7**2*B9**2*(-Q2-Q1)+2
2   *A4*A7*B6*B9*(-Q2-Q1)+2*A1*A7*B3*B9*(-Q2-Q1)+A4**2*B6**2*(-Q2
3   -Q1)+2*A1*A4*B3*B6*(-Q2-Q1)+A1**2*B3**2*(-Q2-Q1)+A7**2*B7**2*
4   Q1+2*A4*A7*B4*B7*Q1+2*A1*A7*B1*B7*Q1+A4**2*B4**2*Q1+2*A1*A4*B
5   1*B4*Q1+A1**2*B1**2*Q1

```

```

Q22 = A8**2*B8**2*Q2+2*A5*A8*B5*B8*Q2+2*A2*A8*B2*B8*Q2+A5**2*B5
1   **2*Q2+2*A2*A5*B2*B5*Q2+A2**2*B2**2*Q2+A8**2*B9**2*(-Q2-Q1)+2
2   *A5*A8*B6*B9*(-Q2-Q1)+2*A2*A8*B3*B9*(-Q2-Q1)+A5**2*B6**2*(-Q2
3   -Q1)+2*A2*A5*B3*B6*(-Q2-Q1)+A2**2*B3**2*(-Q2-Q1)+A8**2*B7**2*
4   Q1+2*A5*A8*B4*B7*Q1+2*A2*A8*B1*B7*Q1+A5**2*B4**2*Q1+2*A2*A5*B
5   1*B4*Q1+A2**2*B1**2*Q1

```

```

Q33 = A9**2*B8**2*Q2+2*A6*A9*B5*B8*Q2+2*A3*A9*B2*B8*Q2+A6**2*B5
1   **2*Q2+2*A3*A6*B2*B5*Q2+A3**2*B2**2*Q2+A9**2*B9**2*(-Q2-Q1)+2
2   *A6*A9*B6*B9*(-Q2-Q1)+2*A3*A9*B3*B9*(-Q2-Q1)+A6**2*B6**2*(-Q2
3   -Q1)+2*A3*A6*B3*B6*(-Q2-Q1)+A3**2*B3**2*(-Q2-Q1)+A9**2*B7**2*
4   Q1+2*A6*A9*B4*B7*Q1+2*A3*A9*B1*B7*Q1+A6**2*B4**2*Q1+2*A3*A6*B
5   1*B4*Q1+A3**2*B1**2*Q1

```

```

Q12 = A7*A8*B8**2*Q2+A4*A8*B5*B8*Q2+A5*A7*B5*B8*Q2+A1*A8*B2*B8*
1   Q2+A2*A7*B2*B8*Q2+A4*A5*B5**2*Q2+A1*A5*B2*B5*Q2+A2*A4*B2*B5*Q
2   2+A1*A2*B2**2*Q2+A7*A8*B9**2*(-Q2-Q1)+A4*A8*B6*B9*(-Q2-Q1)+A5
3   *A7*B6*B9*(-Q2-Q1)+A1*A8*B3*B9*(-Q2-Q1)+A2*A7*B3*B9*(-Q2-Q1)+
4   A4*A5*B6**2*(-Q2-Q1)+A1*A5*B3*B6*(-Q2-Q1)+A2*A4*B3*B6*(-Q2-Q1
5   )+A1*A2*B3**2*(-Q2-Q1)+A7*A8*B7**2*Q1+A4*A8*B4*B7*Q1+A5*A7*B4
6   *B7*Q1+A1*A8*B1*B7*Q1+A2*A7*B1*B7*Q1+A4*A5*B4**2*Q1+A1*A5*B1*
7   B4*Q1+A2*A4*B1*B4*Q1+A1*A2*B1**2*Q1

```

```

Q13 = A7*A9*B8**2*Q2+A4*A9*B5*B8*Q2+A6*A7*B5*B8*Q2+A1*A9*B2*B8*
1   Q2+A3*A7*B2*B8*Q2+A4*A6*B5**2*Q2+A1*A6*B2*B5*Q2+A3*A4*B2*B5*Q
2   2+A1*A3*B2**2*Q2+A7*A9*B9**2*(-Q2-Q1)+A4*A9*B6*B9*(-Q2-Q1)+A6
3   *A7*B6*B9*(-Q2-Q1)+A1*A9*B3*B9*(-Q2-Q1)+A3*A7*B3*B9*(-Q2-Q1)+
4   A4*A6*B6**2*(-Q2-Q1)+A1*A6*B3*B6*(-Q2-Q1)+A3*A4*B3*B6*(-Q2-Q1
5   )+A1*A3*B3**2*(-Q2-Q1)+A7*A9*B7**2*Q1+A4*A9*B4*B7*Q1+A6*A7*B4
6   *B7*Q1+A1*A9*B1*B7*Q1+A3*A7*B1*B7*Q1+A4*A6*B4**2*Q1+A1*A6*B1*

```

7 B4\*Q1+A3\*A4\*B1\*B4\*Q1+A1\*A3\*B1\*\*2\*Q1

Q23 = A8\*A9\*B8\*\*2\*Q2+A5\*A9\*B5\*B8\*Q2+A6\*A8\*B5\*B8\*Q2+A2\*A9\*B2\*B8\*  
 1 Q2+A3\*A8\*B2\*B8\*Q2+A5\*A6\*B5\*\*2\*Q2+A2\*A6\*B2\*B5\*Q2+A3\*A5\*B2\*B5\*Q  
 2 2+A2\*A3\*B2\*\*2\*Q2+A8\*A9\*B9\*\*2\*(-Q2-Q1)+A5\*A9\*B6\*B9\*(-Q2-Q1)+A6  
 3 \*A8\*B6\*B9\*(-Q2-Q1)+A2\*A9\*B3\*B9\*(-Q2-Q1)+A3\*A8\*B3\*B9\*(-Q2-Q1)+  
 4 A5\*A6\*B6\*\*2\*(-Q2-Q1)+A2\*A6\*B3\*B6\*(-Q2-Q1)+A3\*A5\*B3\*B6\*(-Q2-Q1  
 5 )+A2\*A3\*B3\*\*2\*(-Q2-Q1)+A8\*A9\*B7\*\*2\*Q1+A5\*A9\*B4\*B7\*Q1+A6\*A8\*B4  
 6 \*B7\*Q1+A2\*A9\*B1\*B7\*Q1+A3\*A8\*B1\*B7\*Q1+A5\*A6\*B4\*\*2\*Q1+A2\*A6\*B1\*  
 7 B4\*Q1+A3\*A5\*B1\*B4\*Q1+A2\*A3\*B1\*\*2\*Q1

term1=A33\*\*2\*(-Q2-Q1)\*T33\*\*2\*Z33+A22\*\*2\*Q2\*T23\*\*2\*Z33+A11\*\*2\*Q1  
 1 \*T13\*\*2\*Z33+2\*A33\*\*2\*(-Q2-Q1)\*T23\*T33\*Z23+2\*A22\*\*2\*Q2\*T22\*T23  
 2 \*Z23+2\*A11\*\*2\*Q1\*T12\*T13\*Z23+A33\*\*2\*(-Q2-Q1)\*T23\*\*2\*Z22+A22\*\*  
 3 2\*Q2\*T22\*\*2\*Z22+A11\*\*2\*Q1\*T12\*\*2\*Z22+2\*A33\*\*2\*(-Q2-Q1)\*T13\*T3  
 4 3\*Z13+2\*A22\*\*2\*Q2\*T12\*T23\*Z13+2\*A11\*\*2\*Q1\*T11\*T13\*Z13+2\*A33\*\*  
 5 2\*(-Q2-Q1)\*T13\*T23\*Z12+2\*A22\*\*2\*Q2\*T12\*T22\*Z12+2\*A11\*\*2\*Q1\*T1  
 6 1\*T12\*Z12+A33\*\*2\*(-Q2-Q1)\*T13\*\*2\*Z11+A22\*\*2\*Q2\*T12\*\*2\*Z11+A11  
 7 \*\*2\*Q1\*T11\*\*2\*Z11

term2=A33\*\*2\*Q33\*T33\*\*2\*Z33+2\*A22\*A33\*Q23\*T23\*T33\*Z33+2\*A11\*A33  
 1 \*Q13\*T13\*T33\*Z33+A22\*\*2\*Q22\*T23\*\*2\*Z33+2\*A11\*A22\*Q12\*T13\*T23\*  
 2 Z33+A11\*\*2\*Q11\*T13\*\*2\*Z33+2\*A33\*\*2\*Q33\*T23\*T33\*Z23+2\*A22\*A33\*  
 3 Q23\*T22\*T33\*Z23+2\*A11\*A33\*Q13\*T12\*T33\*Z23+2\*A22\*A33\*Q23\*T23\*\*  
 4 2\*Z23+2\*A22\*\*2\*Q22\*T22\*T23\*Z23+2\*A11\*A33\*Q13\*T13\*T23\*Z23+2\*A1  
 5 1\*A22\*Q12\*T12\*T23\*Z23+2\*A11\*A22\*Q12\*T13\*T22\*Z23+2\*A11\*\*2\*Q11\*  
 6 T12\*T13\*Z23+A33\*\*2\*Q33\*T23\*\*2\*Z22+2\*A22\*A33\*Q23\*T22\*T23\*Z22+2  
 7 \*A11\*A33\*Q13\*T12\*T23\*Z22+A22\*\*2\*Q22\*T22\*\*2\*Z22+2\*A11\*A22\*Q12\*  
 8 T12\*T22\*Z22+A11\*\*2\*Q11\*T12\*\*2\*Z22+2\*A33\*\*2\*Q33\*T13\*T33\*Z13+2\*  
 9 A22\*A33\*Q23\*T12\*T33\*Z13+2\*A11\*A33\*Q13\*T11\*T33\*Z13+2\*A22\*A33\*Q  
 : 23\*T13\*T23\*Z13+2\*A22\*\*2\*Q22\*T12\*T23\*Z13+2\*A11\*A22\*Q12\*T11\*T23  
 ; \*Z13+2\*A11\*A33\*Q13\*T13\*\*2\*Z13+2\*A11\*A22\*Q12\*T12\*T13\*Z13+2\*A11  
 < \*\*2\*Q11\*T11\*T13\*Z13+2\*A33\*\*2\*Q33\*T13\*T23\*Z12+2\*A22\*A33\*Q23\*T1  
 = 2\*T23\*Z12+2\*A11\*A33\*Q13\*T11\*T23\*Z12+2\*A22\*A33\*Q23\*T13\*T22\*Z12  
 > +2\*A22\*\*2\*Q22\*T12\*T22\*Z12+2\*A11\*A22\*Q12\*T11\*T22\*Z12+2\*A11\*A33  
 ? \*Q13\*T12\*T13\*Z12+2\*A11\*A22\*Q12\*T12\*\*2\*Z12+2\*A11\*\*2\*Q11\*T11\*T1  
 @ 2\*Z12+A33\*\*2\*Q33\*T13\*\*2\*Z11+2\*A22\*A33\*Q23\*T12\*T13\*Z11+2\*A11\*A  
 1 33\*Q13\*T11\*T13\*Z11+A22\*\*2\*Q22\*T12\*\*2\*Z11+2\*A11\*A22\*Q12\*T11\*T1  
 2 2\*Z11+A11\*\*2\*Q11\*T11\*\*2\*Z11

TERM=term1+term2

FI(X2,X3,X4,X5,X6)=(SIN(BE1(X3))\*SIN(BE2(X6)))\*TERM



A.1. FORTRAN PROGRAM TO CALCULATE THE  $\Theta_1\alpha_3$  CONTRIBUTION TO  $B_Q$ .85

```

C
C CALCULATION OF THE SHAPE POTENTIAL:
C
      G1(X3,X4,X6)=4.*PARAM2*1.380622E-23*R**12*(SHAPE1*(3.*COS(BE1(X3)
+ )**2+3.*COS(BE2(X6))**2-2.)+SHAPE2*(3.*COS(GA1(X4))**2*SIN(BE1(X3)
+ )**2+3.*COS(GA2(X7))**2*SIN(BE2(X6))**2-2.))

80          CONTINUE
70          CONTINUE
60          CONTINUE
50          CONTINUE

c          WRITE(4,1444)term
c1444      FORMAT(1X,'term IS',E15.7)

40          CONTINUE

C
C THE INTEGRAL IS CALCULATED:
C
      SS6=0.00
      DO 940 X6=1,16
c          WRITE(6,1911)X6
c1911      FORMAT (1X, 'sub-index (in range 1 to 16) is currently ',I2 )
      SS5=0.00
      DO 950 X5=1,16
      SS4=0.00
      DO 960 X4=1,16
      SS3=0.00
      DO 970 X3=1,16
      SS2=0.00
      DO 980 X2=1,16
      SS1=0.00
      DO 990 X1=1,64

C
C SUMMATION OF THE ENERGY TERMS WITH SUBSEQUENT DIVISION BY (-kT):
C
      G3=-1.*(D1(X1)+E1(X2,X3,X4,X5,X6)/SE5(X1)+F1(X2,X3,X4,X5,X6)/SE8(
+ X1)+G1(X3,X4,X6)/SE12(X1)+DDP(X2,X3,X4,X5,X6)/SE3(X1)+DIDP(X2,X3,
+ X4,X5,X6)/SE6(X1)+DQP(X2,X3,X4,X5,X6)/SE4(X1))/TEMPK

      IF(G3.LT.-85) GO TO 5000
      G4=2.71828**G3

```

```

      GO TO 5010
5000  G4=0
C5010  SS1=SS1+(FI(X2,X3,X4,X5,X6)/(SEP(X1)**6))*G4*COEF2(X1,2)
5010  SS1=SS1+(FI(X2,X3,X4,X5,X6)/(SEP(X1)**4))*G4*COEF2(X1,2)
990    CONTINUE
      SS2=SS2+SS1*COEF1(X2,2)
C
C
980    CONTINUE
      SS3=SS3+SS2*COEF1(X3,2)
C
C
970    CONTINUE
      SS4=SS4+SS3*COEF1(X4,2)
C
C
960    CONTINUE
      SS5=SS5+SS4*COEF1(X5,2)
C
C
950    CONTINUE
      SS6=SS6+SS5*COEF1(X6,2)
C
C
940    CONTINUE
      SS7=SS7+SS6*COEF1(X7,2)
C
C
939    CONTINUE
      ANS=SS7*SEP1*AL11*BE11*GA11*AL21*BE21*GA21*6.022169**2*
+ 8.987552**3*1E-37/(TEMP*1.380622*90*3.14159265358979323846**2)
C
C THE INTEGRAL IS PRINTED TOGETHER WITH MOLECULAR DATA USED
C
      WRITE(4,2266)
2266  FORMAT(1X,'THE Q1A3 TERM CONTRIBUTION TO B_Q FOR CO2:')
      WRITE(4,2267)
2267  FORMAT(1X,'  ')
      WRITE(4,2269)
2269  FORMAT(1X,'  ')
      WRITE(4,1140)ANS
1140  FORMAT(1X,'THE INTEGRAL IS',E15.7)
      WRITE(4,2150)
2150  FORMAT(1X,'INPUT DATA:')
      WRITE(4,2155)TEMP

```

A.1. FORTRAN PROGRAM TO CALCULATE THE  $\Theta_{1\alpha_3}$  CONTRIBUTION TO  $B_Q$ .87

```

2155  FORMAT(1X,'TEMPERATURE:          ',F10.5)
      WRITE(4,9260)ALDYN
9260  FORMAT(1X,'MEAN DYNAMIC ALPHA:',F10.5)
      WRITE(4,9261)A11
9261  FORMAT(1X,'DYNAMIC ALPHA11:    ',F10.5)
      WRITE(4,9262)A22
9262  FORMAT(1X,'DYNAMIC ALPHA22:    ',F10.5)
      WRITE(4,9263)A33
9263  FORMAT(1X,'DYNAMIC ALPHA33:    ',F10.5)
      WRITE(4,9264)ALSTAT
9264  FORMAT(1X,'MEAN STATIC ALPHA:  ',F10.5)
      WRITE(4,9961)V11
9961  FORMAT(1X,'STATIC ALPHA11:     ',F10.5)
      WRITE(4,9962)V22
9962  FORMAT(1X,'STATIC ALPHA22:     ',F10.5)
      WRITE(4,9963)V33
9963  FORMAT(1X,'STATIC ALPHA33:     ',F10.5)
      WRITE(4,2190)Q1
2190  FORMAT(1X,'THETA11:           ',F10.5)
      WRITE(4,2241)Q2
2241  FORMAT(1X,'THETA22:           ',F10.5)
      WRITE(4,2210)R
2210  FORMAT(1X,'R(0):              ',F6.5)
      WRITE(4,2220)SHAPE1
2220  FORMAT(1X,'SHAPE FACTOR 1:    ',F10.5)
      WRITE(4,2221)SHAPE2
2221  FORMAT(1X,'SHAPE FACTOR 2:    ',F10.5)
      WRITE(4,2230)PARAM2
2230  FORMAT(1X,'E/K:              ',F9.5)
      WRITE(4,2235)AMIN1,AMAX1
2235  FORMAT(1X,'MIN AND MAX POINTS OF RANGE (64 INTERVALS):',2(F10.5,3
+ X))
      WRITE(4,2240)
2240  FORMAT(1X,'END BT')
      WRITE(4,2261)
2261  FORMAT(1X,'  ')
      WRITE(4,2262)
2262  FORMAT(1X,'  ')
      WRITE(4,2263)
2263  FORMAT(1X,'  ')
      WRITE(4,2264)
2264  FORMAT(1X,'  ')
      WRITE(4,2265)
2265  FORMAT(1X,'  ')
      CLOSE(UNIT=4)
      END

```

# Bibliography

1. A D Buckingham. Permanent and induced molecular moments and long-range intermolecular forces. *Adv. Chem. Phys.*, 12:107–142, 1967.
2. L D Barron. *Molecular Light Scattering and Optical Activity*. Cambridge University Press, Cambridge, 2004.
3. R E Raab and O L de Lange. *Multipole Theory in Electromagnetism*. Clarendon Press, Oxford, 2005.
4. A D Buckingham. Molecular quadrupole moments. *Quart. Rev.*, 13:183–214, 1959.
5. D A Imrie. *The Measurement of Electric Quadrupole Moments of Gas Molecules by Induced Birefringence*. PhD thesis, University of Natal, 1993.
6. A D Buckingham. Direct method of measuring molecular quadrupole moments. *J. Chem. Phys.*, 30:1580–1585, 1959.
7. A D Buckingham and R L Disch. The quadrupole moment of the carbon dioxide molecule. *Proc. R. Soc. London A*, 273:275–289, 1963.
8. G L D Ritchie. In *Optical, Electric and Magnetic Properties of Molecules*. Elsevier, Amsterdam, 1997.
9. A Rizzo and S Coriani. Birefringences: a challenge for both theory and experiment. *Adv. Quantum Chem.*, 50:143–184, 2005.

10. A D Buckingham and H C Longuet-Higgins. The quadrupole moments of dipolar molecules. *Mol. Phys.*, 14:63–72, 1968.
11. D A Imrie and R E Raab. A new molecular theory of field gradient induced birefringence used for measuring electric quadrupole moments. *Mol. Phys.*, 74: 833–842, 1991.
12. A Rizzo, S Coriani, A Halkier, and C Hättig. Ab initio study of the electric-field-gradient-induced birefringence of a polar molecule: CO. *J. Chem. Phys.*, 113:3077–3087, 2000.
13. S Coriani, A Halkier, D Jonsson, J Gauss, A Rizzo, and O Christiansen. On the electric field gradient induced birefringence and electric quadrupole moment of CO, N<sub>2</sub>O, and OCS. *J. Chem. Phys.*, 118:7329–7339, 2003.
14. R E Raab and O L de Lange. Forward scattering theory of electric-field-gradient-induced birefringence. *Mol. Phys.*, 101:3467–3475, 2003.
15. O L de Lange and R E Raab. Reconciliation of the forward scattering and wave theories of electric-field-gradient-induced birefringence. *Mol. Phys.*, 102: 125–130, 2004.
16. A D Buckingham, R L Disch, and D A Dunmur. The quadrupole moments of some simple molecules. *J. Am. Chem. Soc.*, 90:3104–3107, 1968.
17. R J Emrich and W Steele. The quadrupole moment of chlorine. *Mol. Phys.*, 40: 469–475, 1980.
18. A D Buckingham, C Graham, and J H Williams. Electric field-gradient-induced birefringence in N<sub>2</sub>, C<sub>2</sub>H<sub>6</sub>, C<sub>3</sub>H<sub>6</sub>, Cl<sub>2</sub>, N<sub>2</sub>O and CH<sub>3</sub>F. *Mol. Phys.*, 49:703–710, 1983.
19. M R Battaglia, A D Buckingham, D Neumark, R K Pierens, and J H Williams.

- The quadrupole moments of carbon dioxide and carbon disulphide. *Mol. Phys.*, 43:1015–1020, 1983.
20. M R Battaglia, A D Buckingham, and J H Williams. The electric quadrupole moments of benzene and hexafluorobenzene. *Chem. Phys. Lett.*, 78:421–423, 1983.
21. C Graham, J Pierrus, and R E Raab. Measurement of the electric quadrupole moments of CO<sub>2</sub>, CO and N<sub>2</sub>. *Mol. Phys.*, 67:939–955, 1989.
22. J N Watson, I E Craven, and G L D Ritchie. The quadrupole moments of carbon dioxide and carbon disulphide. *Chem. Phys. Lett.*, 274:1–6, 1997.
23. R I Keir, D W Lamb, G L D Ritchie, and J N Watson. Polarizability anisotropies, magnetizability anisotropies and molecular quadrupole moments of acetylene, methylacetylene and dimethylacetylene. *Chem. Phys. Lett.*, 279:22–28, 1997.
24. C Graham, D A Imrie, and R E Raab. Measurement of the electric quadrupole moments of CO<sub>2</sub>, CO, N<sub>2</sub>, Cl<sub>2</sub> and BF<sub>3</sub>. *Mol. Phys.*, 93:49–56, 1998.
25. G L D Ritchie and J N Watson. Temperature dependence of electric field-gradient induced birefringence (the Buckingham effect) in C<sub>6</sub>H<sub>6</sub> and C<sub>6</sub>F<sub>6</sub>: Comparison of electric and magnetic properties of C<sub>6</sub>H<sub>6</sub> and C<sub>6</sub>F<sub>6</sub>. *Chem. Phys. Lett.*, 322:143–148, 2000.
26. G L D Ritchie, J N Watson, and R I Keir. Temperature dependence of electric field-gradient induced birefringence (Buckingham effect) and molecular quadrupole moment of N<sub>2</sub>. Comparison of experiment and theory. *Chem. Phys. Lett.*, 370:376–380, 2003.
27. N Chetty and V W Couling. Measurement of the electric quadrupole moments of CO<sub>2</sub> and OCS. *Mol. Phys.*, 109:655–666, 2011.

28. N Chetty and V W Couling. Measurement of the electric quadrupole moment of N<sub>2</sub>O. *J. Chem. Phys.*, 134:144307, 2011.
29. N Chetty and V W Couling. Measurement of the electric quadrupole moment of CO. *J. Chem. Phys.*, 134:164307, 2011.
30. V W Couling and S S Ntombela. The electric quadrupole moment of O<sub>2</sub>. *Chem. Phys. Lett.*, 614:41–44, 2014.
31. T Helgaker, S Coriani, P Jørgensen, K Kristensen, J Olsen, and K Ruud. Recent advances in wave function-based methods of molecular-property calculations. *Chem. Rev.*, 112:543–631, 2012.
32. A D Buckingham and J A Pople. Electromagnetic properties of compressed gases. *Disc. Faraday Soc.*, 22:17–21, 1956.
33. D Marchesan, S Coriani, and A Rizzo. Density dependence of the electric-field-gradient induced birefringence of the helium, neon and argon gases. *Mol. Phys.*, 101:1851–1865, 2003.
34. A Samanta, A Zhao, G K H Shimizu, P Sarkar, and R Gupta. Post-combustion CO<sub>2</sub> capture using solid sorbents: A review. *Ind. Eng. Chem. Res.*, 51:1438–1463, 2012.
35. N Hedin, L Andersson, L Bergström, and J Yan. Adsorbents for the post-combustion capture of CO<sub>2</sub> using rapid temperature swing or vacuum swing adsorption. *Appl. Energ.*, 104:418–433, 2013.
36. J Shang, G Li, R Singh, P Xiao, D Danaci, J Z Liu, and P A Webley. Adsorption of CO<sub>2</sub>, N<sub>2</sub>, and CH<sub>4</sub> in Cs-exchanged chabazite: A combination of van der Waals density functional theory calculations and experiment study. *J. Chem. Phys.*, 140:084705, 2014.

37. T Du, X Fang, L Liu, J Shang, B Zhang, Y Wei, H Gong, S Rahman, E F May, P A Webley, and G Li. An optimal trapdoor zeolite for exclusive admission of CO<sub>2</sub> at industrial carbon capture operating temperatures. *Chem. Commun.*, 54: 3134–3137, 2018.
38. M J Purdue and Z W Qiao. Molecular simulation study of wet flue gas adsorption on zeolite 13X. *Micropor. Mesopor. Mat.*, 261:181–197, 2018.
39. R Wordsworth, Y Kalugina, S Lokshtanov, A Vigasin, B Ehlmann, J Head, C Sanders, and H Wang. Transient reducing greenhouse warming on early Mars. *Geophys. Res. Lett.*, 44:665–671, 2017.
40. F Xiao, B Gamiz, and J J Pignatello. Adsorption and desorption of nitrous oxide by raw and thermally air-oxidized chars. *Sci. Total Environ.*, 643:1436–1445, 2018.
41. D R Nutt and M Meuwly. Migration in native and mutant myoglobin: Atomistic simulations for the understanding of protein function. *Proc. Natl. Acad. Sci. U.S.A.*, 101:5998–6002, 2004.
42. L Zamirri, S Casassa, A Rimola, M Segado-Centellas, C Ceccarelli, and P Ugliengo. IR spectral fingerprint of carbon monoxide in interstellar water-ice models. *Mon. Not. R. Astron. Soc.*, 480:1427–1444, 2018.
43. A D Buckingham and J A Pople. Theoretical studies of the Kerr effect I: Deviations from a linear polarization law. *Proc. Phys. Soc. A*, 68:905–909, 1955.
44. A D Buckingham and J A Pople. A theory of magnetic double refraction. *Proc. Phys. Soc. B*, 69:1133–1138, 1956.
45. J N Watson. *The Measurement of Field Gradient Induced Birefringence in Gases*. PhD thesis, University of New England, 1994.



46. J Vrbancich and G L D Ritchie. Quadrupole moments of benzene, hexafluorobenzene and other non-dipolar aromatic molecules. *J. Chem. Soc., Faraday Trans. II*, 76:648–659, 1980.
47. V W Couling and C Graham. Calculation and measurement of the second light-scattering virial coefficients of nonlinear molecules: a study of ethene. *Mol. Phys.*, 87:779–799, 1996.
48. V W Couling and C Graham. Second Kerr effect virial coefficients of polar molecules with linear and lower symmetry. *Mol. Phys.*, 93:31–47, 1998.
49. V W Couling and C Graham. Measurement and interpretation of the second light-scattering virial coefficients of linear and quasi-linear molecules. *Mol. Phys.*, 82:235–244, 1994.
50. V W Couling and C Graham. Depolarized interaction-induced Rayleigh light scattering in gaseous  $\text{SO}_2$ . *Mol. Phys.*, 96:921–925, 1999.
51. V W Couling and R V Nhlebela. Calculation and measurement of the second light-scattering virial coefficient of  $(\text{CH}_3)_2\text{O}$ . *Phys. Chem. Chem. Phys.*, 3:4551–4554, 2001.
52. A D Buckingham, P A Galwas, and L Fan-Chen. Polarizabilities of interacting polar molecules. *J. Mol. Struct.*, 100:3–12, 1983.
53. V W Couling and C Graham. Calculation of second Kerr effect virial coefficients of  $\text{H}_2\text{S}$ . *Mol. Phys.*, 98:135–138, 2000.
54. V W Couling, B W Halliburton, R I Keir, and G L D Ritchie. Anisotropic molecular polarizabilities of  $\text{HCHO}$ ,  $\text{CH}_3\text{CHO}$ , and  $\text{CH}_3\text{COCH}_3$ . Rayleigh depolarization ratios of  $\text{HCHO}$  and  $\text{CH}_3\text{CHO}$  and first and second Kerr virial coefficients of  $\text{CH}_3\text{COCH}_3$ . *J. Phys. Chem. A*, 105:4365–4370, 2001.

55. P Naidoo. Second Kerr-effect Virial Coefficients of Non-dipolar Molecules with Axial and Lower Symmetry. Master's thesis, University of Kwa-Zulu Natal, 2017.
56. P C Balachandran Pillai and V W Couling. Dispersion of the Rayleigh light-scattering virial coefficients and polarisability anisotropy of CO<sub>2</sub>. *Mol. Phys.*, 117:289–297, 2019.
57. J H Dymond, K N Marsh, R C Wilhoit, and K C Wong. *The Virial Coefficients of Pure Gases and Mixtures*. Springer-Verlag, Berlin, 2002.
58. J O Hirschfelder, C F Curtiss, and R B Bird. *Molecular Theory of Gases and Liquids*. Wiley, New York, 1954.
59. U Hohm. Frequency-dependence of second refractivity virial coefficients of small molecules between 325 nm and 633 nm. *Mol. Phys.*, 81:157–168, 1994.
60. J W Schmidt and M R Moldover. Dielectric permittivity of eight gases measured with cross capacitors. *Int. J. Thermophys.*, 24:375–403, 2003.
61. U Hohm. Experimental static dipole-dipole polarizabilities of molecules. *J. Mol. Struct.*, 1054–1055:282–292, 2013.
62. A Chrissanthopoulos, U Hohm, and U Wachsmuth. Frequency-dependence of the polarizability anisotropy of CO<sub>2</sub> revisited. *J. Mol. Struct.*, 526:323–328, 2000.
63. J C Holste, K R Hall, P T Eubank, G Esper, M Q Watson, W Warowny, D M Bailey, J G Young, and M T J Bellomy. Experimental ( $P, V_m, T$ ) for pure CO<sub>2</sub> between 220 and 450 K. *J. Chem. Thermodyn.*, 19:1233–1250, 1987.
64. W Duschek, R Kleinrahm, and W Wagner. Measurement and correlation of the (pressure, density, temperature) relation of carbon dioxide I. The homogeneous

- gas and liquid regions in the temperature range from 217 K to 340 K at pressures up to 9 MPa. *J. Chem. Thermodyn.*, 22:827–840, 1990.
65. I D Mantilla, D E Cristancho, S Ejaz, and K R Hall.  $P - \rho - T$  data for carbon dioxide from (310 to 450) K up to 160 MPa. *J. Chem. Eng. Data.*, 55:4611–4613, 2010.
66. M A Gomez-Osorio, R A Browne, K R Carvajal Diaz, M Hall, and J C Holste. Density measurements for ethane, carbon dioxide, and methane + nitrogen mixtures from 300 to 470 K up to 137 MPa using a vibrating tube densimeter. *J. Chem. Eng. Data.*, 61:2791–2798, 2016.
67. C Graham. Calculations of second light-scattering virial coefficients of linear and quasi-linear molecules. *Mol. Phys.*, 77:291–309, 1992.
68. V W Couling and C Graham. Higher-order dipole-dipole, dipole-quadrupole and field gradient contributions to the second light-scattering virial coefficient. *Mol. Phys.*, 79:859–867, 1993.
69. R Tammer and W Hüttner. Kerr effect and polarizability tensor of gaseous ethene. *Mol. Phys.*, 83:579–590, 1994.
70. P Claus, R Kleinrahm, and W Wagner. Measurements of the  $(p, \rho, T)$  relation of ethylene, ethane, and sulphur hexafluoride in the temperature range from 235 K to 520 K at pressures up to 30 MPa using an accurate single-sinker densimeter. *J. Chem. Thermodyn.*, 35:159–175, 2003.
71. J Smukala, R Span, and W Wagner. New equation of state for ethylene covering the fluid region for temperatures from the melting line to 450 K at pressures up to 300 MPa. *J. Phys. Chem. Ref. Data*, 29:1053–1121, 2000.
72. Y Das Gupta, Y Singh, and S Singh. Effect of shape of molecules on transport

- and equilibrium properties of nonpolar polyatomic gases. *J. Chem. Phys.*, 59:1999–2006, 1973.
73. W Majer, P Lutzmann, and W Hüttner. The molecular electric quadrupole tensor of ethene from the rotational Zeeman effect of  $\text{CH}_2=\text{CD}_2$ . *Mol. Phys.*, 83:567–578, 1994.
74. D Bückner and W Wagner. A reference equation of state for the thermodynamic properties of ethane for temperatures from the melting line to 675 K and pressures up to 900 MPa. *J. Phys. Chem. Ref. Data*, 35:205–266, 2006.
75. M H Coonan. *Temperature Dependence of the Cotton-Mouton Effect in Gases*. PhD thesis, University of New England, 1995.
76. U Hohm. Experimental determination of the dispersion in the mean linear dipole polarizability  $\alpha(\omega)$  of small hydrocarbons and evaluation of Cauchy moments between 325 nm and 633 nm. *Mol. Phys.*, 78:929–941, 1993.